

+ + lin



PhD thesis, draft 1  
Dynamic Electrochemical Impedance  
Spectroscopy for Energy Storage Applications:  
from Electrode to Cell

Federico Scarpioni

August 28, 2025



# Contents

|   |           |
|---|-----------|
| <b>1 Introduction</b>   | <b>1</b>  |
| <br>  |           |
| <b>I Theoretical framework</b>  | <b>3</b>  |
| <br>  |           |
| <b>2 Electrochemistry</b>   | <b>5</b>  |
| Thermodynamics . . . . .  | 5         |
| The origin of the chemical potential . . . . .  | 5         |
| The electrochemical potential as a function of concentration<br>and temperature . . . . . | 6         |
| Measuring the electrochemical potential . . . . .   | 6         |
| The effect of the pH and temperature (the Pourbaix diagram)                               | 7         |
| Kinetics . . . . .  | 7         |
| Double layer structure . . . . .  | 8         |
| Electrochemical methods . . . . .   | 9         |
| Three electrode cells . . . . .   | 10        |
| Electrochemical impedance spectroscopy . . . . .  | 10        |
| Resistance and impedance . . . . .  | 11        |
| Passive elements . . . . .  | 11        |
| Impedance of simple circuits . . . . .  | 12        |
| Graphic representation of the impedance . . . . .   | 12        |
| <br>  |           |
| <b>3 Batteries</b>  | <b>13</b> |
| Non-rechargeable batteries . . . . .  | 13        |
| A brief historical overview . . . . .   | 14        |
| Performance of batteries . . . . .  | 14        |
| Secondary batteries . . . . .   | 14        |
| The choice of metallic ion for shuttling . . . . .  | 15        |
| Electrolytes . . . . .  | 16        |
| State of the art of Li-ion batteries . . . . .  | 16        |
| Positive electrodes . . . . .   | 16        |
| Graphite as negative electrode . . . . .  | 17        |
| The solid-electrolyte interface . . . . .   | 17        |
| Solid electrolytes . . . . .  | 18        |
| On the nomenclature . . . . .   | 18        |
| Manufacturing of batteries . . . . .  | 19        |
| Battery degradation . . . . .   | 20        |
| Electrochemical characterization of batteries . . . . .                                   | 20        |
| Fast charging . . . . .   | 21        |

|   |           |
|---|-----------|
| <b>4 Identification of dynamical systems</b>                                  | <b>23</b> |
| Definition of system and properties . . . . .                                 | 23        |
| Modeling with differential equations . . . . .                                | 24        |
| Transfer function . . . . .   | 25        |
| Kramers-Kroning relationship . . . . .  | 26        |
| Time-domain response . . . . .  | 26        |
| Frequency-domain response . . . . .   | 27        |
| State-space formulation . . . . .   | 28        |
| Model parameters and order . . . . .  | 29        |
| Non-linear systems . . . . .  | 31        |
| Non-stationary systems . . . . .  | 31        |
| System identification in the frequency domain . . . . .                       | 32        |
| Definition . . . . .  | 32        |
| Excitation signals . . . . .  | 33        |
| Parameters estimation . . . . .   | 34        |
| Model selection and validation . . . . .                                      | 35        |
| Model selection criteria . . . . .  | 36        |
| Identification in non-stationary case . . . . .                               | 38        |
| Digital signal processing . . . . .   | 38        |
| Digital sampling . . . . .  | 38        |
| Discrete Fourier Transform . . . . .  | 39        |
| Noise . . . . .   | 41        |
| Wavelets method . . . . .   | 42        |
| Filters . . . . .   | 42        |
| Removal of trends . . . . .   | 43        |
| Signal synthesis . . . . .  | 43        |
| Further resources . . . . .   | 44        |
| <b>5 Dynamic Electrochemical Impedance spectroscopy:<br/>state of the art</b> | <b>45</b> |
| <b>II Methodologies</b>   | <b>47</b> |
| <b>6 Acquisition of non-stationary impedance</b>                              | <b>49</b> |
| Multi-frequency data acquisition . . . . .                                    | 49        |
| Description of the set-up . . . . .   | 50        |
| Automation of the acquisition for batteries . . . . .                         | 50        |
| Problem statement . . . . .   | 50        |
| Software solution . . . . .   | 52        |
| Design principle . . . . .  | 52        |
| Automatic calculation of the impedance . . . . .                              | 53        |
| DEIStools: a Python application for dynamic impedance . . . . .               | 54        |
| Software limits . . . . .   | 54        |
| Multi-sine design . . . . .   | 55        |
| Frequencies selection . . . . .   | 55        |
| Amplitude optimization . . . . .  | 55        |
| Phase optimization . . . . .  | 56        |
| Multi-sine splitting . . . . .  | 57        |
| Software . . . . .  | 58        |
| Impedance estimation . . . . .  | 59        |
| Old part . . . . .  | 60        |

|   |           |
|---|-----------|
| Arbitrary waveform generator . . . . .                                      | 60        |
| Multi-sine design . . . . .   | 61        |
| Running the multi-sine in the waveform generator . . . . .                  | 61        |
| Digital acquisition device . . . . .  | 61        |
| Connecting cells in three-electrode configuration . . . . .                 | 63        |
| Electrochemical devices . . . . .   | 63        |
| Connecting the device and acquiring the signals: set-up version 1 . . . . . | 64        |
| Automatic cycling with . . . . .  | 64        |
| <b>7 Analysis of impedance</b>  | <b>65</b> |
| Parametric models . . . . .   | 65        |
| Physical model . . . . .  | 66        |
| Transfer function model . . . . .   | 66        |
| Simultaneous fitting . . . . .  | 66        |
| Fitting error . . . . .   | 67        |
| Determination of the system degrees of freedom . . . . .                    | 67        |
| Determining transfer function structure . . . . .                           | 67        |
| <b>III Results and discussions</b>  | <b>69</b> |
| <b>8 Coin cells</b>   | <b>71</b> |
| Method . . . . .  | 72        |
| Cycling test . . . . .  | 72        |
| Operando acquisition of static impedance . . . . .                          | 72        |
| Real time acquisition of dynamic impedance . . . . .                        | 72        |
| Analysis of impedance data . . . . .  | 73        |
| Results . . . . .   | 73        |
| Discussion . . . . .  | 73        |
| Choice of the cell . . . . .  | 74        |
| Performance test of the cell . . . . .                                      | 75        |
| Static impedance evaluation . . . . .                                       | 75        |
| Time-varying impedance acquisition . . . . .                                | 75        |
| regression of rational polynomial . . . . .                                 | 79        |
| Associating measurement values with battery state . . . . .                 | 82        |
| <b>9 Identify lithium plating on graphite</b>                               | <b>83</b> |
| Cell assembling . . . . .   | 83        |
| Time-varying impedance measurements . . . . .                               | 84        |
| <b>10 Discriminating sodium storage mechanisms</b>                          | <b>87</b> |
| Silicon carbonitride . . . . .  | 87        |
| Storage mechanisms . . . . .  | 88        |
| Cell housing for three electrodes and optimization . . . . .                | 89        |
| Microscopic reference electrode of sodium . . . . .                         | 90        |
| Time-varying impedance . . . . .  | 91        |
| Sodium electrodeposition on sodium substrate . . . . .                      | 92        |
| Time-Varying impedance during SEI formation . . . . .                       | 92        |

|   |            |
|---|------------|
| <b>11 Studying intercalation</b>                          | <b>99</b>  |
| Materials and cell assembly . . . . .                     | 99         |
| Measurement set-up . . . . .                              | 99         |
| Physical model for intercalation . . . . .                | 100        |
| Results and discussions . . . . .                         | 100        |
| Comment . . . . .   | 101        |
| <b>12 Studying non-Faradic reaction in symmetric cell</b> | <b>103</b> |
| Materials and cell assembling . . . . .                   | 103        |
| Reference electrode and position in the stack . . . . .   | 104        |
| Physical model . . . . .                                  | 104        |
| Results and discussions . . . . .                         | 104        |
| Quantitative interpretation of the impedance . . . . .    | 105        |
| Remarks . . . . .   | 105        |

# 1

## Introduction

Here it goes a general introduction to the thesis explaning the need for an interdisciplinar background.



## Part I

# Theoretical framework



# 2

## Electrochemistry

### Contents

---

|  |    |
|--|----|
| Thermodynamics . . . . .                         | 5  |
| Kinetics . . . . .                               | 7  |
| Electrochemical methods . . . . .                | 9  |
| Electrochemical impedance spectroscopy . . . . . | 10 |

---

### Thermodynamics

Electrochemistry is the transformation of chemical energy into electrical energy. The process happens at the electrode. The electrode is considered an interphase between two phases (solid-solid) or (solid-liquid) in which the electrical current carried by ions is converted to electrons current after a redox reaction.

This principle was first discovered by the chemists XXX and defines empirically the relationship between electrical charge and mass of electroactive material dissolved in solution (during oxidation) or deposited from solution to the electrode (during reduction).

<put the math here>

### The origin of the chemical potential

It is then important to understand the origin of the chemical potential from a fundamental perspective. This is particularly useful when describing the electrochemical potential of battery materials. From a materials science or inorganic chemistry perspective, the chemical potential at room temperature correspond to the fermi level of the electrons in the solid, hence the distance from the latest occupied atomic orbit and the void state (where the electron is not bounded). The Fermi level depends on the class of material. For metals, the situation is quite simple because the electrons can occupy any energy from a continuous band. For semiconductors and insulators this is not true. A gap of unaccesible energy levels is found, known as band gap. Depending on the material composition and strucutre, the band gap can be different leading to a different chemical potential and hence the electrochemical potential of the electrochemical cell were said material is used. When designing useful electrochemical device, the scientist

put a lot of effort on the design of materials with certain properties. The description of the electronic structure, also known as density of states, is an hard task and require to solve big system of equations. The Density Functional Theory allow to semplify the calculation under certain conditions and led to a new reserach field of computation material science discovery, altough it is not matter of this thesis to dive deeper into it.

Electrochemistry first developed studying redox reaction of metals in aqueous electrolytic solutions. While today there is a lot of focus on insulating materials for their properties described later in the text. It is important to remember the distinction, especially for the case of energy storage device that might have materials from both types in the same cell, as well as elecgtrlyzers and fuell cells.

It is not the topic of this work, but rather interesting to mention, that the redox reaction can be also of the type of biologic reactions in living organisms.

## The electrochemical potential as a function of concnetration and temperature

We saw that the parts that compose the electrochemical potential but we have not yet considered two important aspect of the thermodynamic: the temperature of the system and the number of particle, or better, the concentration.

The effect of these quantities on the electrochemical potential was firstly deduce by XXX Nerst in XXXX. The Nernst equation is still quite important and has the form of

<put the math here>

## Measuring the electrochemical potential

It is clear already how improtant is the direct measurement of the electrochemical potential for a specific electrode. Unfortunatly it is impossible to get this value from direct measurement. In fact, the simplest electrochemical cells is made of two electrodes and ehnce we can only get a voltage difference. One can get the electrochemical potential of an electrode under study if the second electrode in the cell has a known electrochemical potential. For this task has been developed specific electrode that can deliver such properties called "reference electrodes". The most known reference is the standard hydrogen electrodes made of a platinum electrode immersed in a sulforic acid solution at the temperature of 25 degrees in which pure hydrogen is bubbled at the pressure of 1 atm giving a solution of unitary fugacity. This set-up is reproducible which lead to the decision of using it as a reference point. The electrochemical potential of all the metals are measured in respect to this value and it is referred to "standard reduction potential" (standard beacause standard conditions) and it is the value used in the nerst equation.

The standard hydrogen electrode, unfortunalty precents some practical shortcoming mostly due to the handling and storage of the flammable hydrogen gas. For the everyday labowork, simpler and safer electrodes are used. Exemples are the calomel electrode and the silver/silver chloride. The latter being the standard in every lab. These electrodes are not as stable

and reproducible as the standard hydrogen electrode but they are easily to prepare and handle and present a quasi-stable electrochemical potential when well maintained.

It is interesting to consider the case of silver/silver chloride because offer an example of a quasi-reference electrode. Silver is completely surrounded by silver chloride between which an equilibrium redox reaction is present. Such electrode is immersed in a superconcentrated solution of KCl (3M) in order to have enough Cl ions to not change the composition of the AgCl. The whole semi-cell is encapsulate into a glass container which terminates with a glass frit to allow the passage of ion.

It is sometimes forgotten that to measure any voltage a small quantity of current has to flow, in fact the electrochemical potential is the measure of work needed to move the electrode from its orbital. This leads to some redox reaction to happen, altering the surface morphology of the electrode as well as concentrations of the solution which alters the electrochemical potential.

One can even think of putting silver directly in contact with a solution containing silver ions, even in direct contact with the electrode of which measuring one is interested of measuring the potential. In principle, this type of configuration can be used as reference electrode, but it has to be granted a constant concentration of silver ion and absence of other ions that might alter the silver redox. This type of reference electrodes are called pseudo-reference electrode and although much more prone to drift, they might be the only possible solution for certain cell configuration, especially when introducing them in real working devices.

Other issues of secondary reference electrodes might be the interference of the redox reaction at the reference electrode of ions coming from the other electrodes (known as poisoning) or the other way around, where the components of the reference electrode are interfering with the other part of the cell.

Note: in general the cell is considered to be divided in two semi-cell. Each semi-cell is in ionic contact and have their own electrode. A salt bridge help to keep separated the electrolyte of the two.

## The effect of the pH and temperature (the Paurbaix diagram)

The pH of the solution, or the diffusive layer (important remark), effect also the chemical equilibrium of the redox species. Some reactions become thermodynamically favorable under certain combination of these factors, altering the electrochemical reaction and hence the electrochemical potential of the electrode. See Paurbaix diagram about this.

## Kinetics

Up to this moment, I only covered the case of systems at the equilibrium which represent an interesting case for study the principles of electrode potential and electromotive force but lacks the description of the effect of the current on the double layer. These aspects are particularly important in applications as for example corrosion of metals, anodization, energy storage in batteries and electrocatalysis.

When a current flows through the poles of a cell, the double layer at each electrodes is altered because of the change of concentration of ions. What happens is an increase (oxidation) or depletion (reduction) of ions at the interface which alters the double layer capacitance. A change in the latter modifies the electrical field which is reduced or increased in respect to the equilibrium value. This difference is referred to as over-potential or under-potential (potential can be swapped with voltage when there is no reference electrode in the cell). The over- or under-potential is stronger the higher is the current, because the faster is the chemical kinetics of the reaction and hence the amount of ion produced or depleted at the interface. The amount of over- under- potential depends on how fast new ions are brought towardes the surface when depleted or moved out the surface when generated, a behaviour that depends on the diffusivity and mobility of the charged species. This effect can be easily noticed when sweeping the voltage applied to an electrochemical cell from the equilibrium value to above. There is a zone where the current is small enough that only the redox reaction is the limiting factor while the ions are moved in or out the surface fast enough to not change the concentration. On the end of the curve the diffusivity of the ions become the rate determining step. In the middle there is a gray zone. The first part, that depends only on the transfer of electrons between the redox active species and the external circuit, was firstly described empirically by Tafel in XXX and later formalized in the Butler-Volmer equation derived from the Fick's laws of diffusion.

<Tafel equation> [put plot and linearization] <B-V equation> [plot]

## Double layer structure

Since the electrode is a conductor, it can in first principles be considered to behave like an ideal resistor. In fact, early experiments showed that imposing a direct current through two electrode (that makes up an electrochemical cell) produces a certain voltage difference between the poles. It follows that the voltage measured is produced by the electrochemical work or Gibb's free energy of the chemical reaction. To be precise, the voltage difference between the electrode correspond to the different in free energy between the redox reaction of the two electrodes, which means that no voltage difference is produced when the two electrodes are of the same chemical nature. One of the first historical examples of electrochemical cell is the pile of Alessandro Volta made of zinc and copper put immersed in an electrolyte solution.

This leads to the second empirical quantity of early electrochemistry which is the electromotive force of a cell. The electromotive force integrated in time gives the electrochemical work of the cell.

This simple model though falls short when imposing an alternate current at the cell terminal. In fact, using the language of electrotechnics, the phase of the current gets shifted that means there is a behaviour similar to an ideal capacitor present in the circuit. To be precise, the capacitor has been demonstrated to be in parallel with the resistor, making up the so called RC circuit; more on this later. The presence of a capacitor in the model means that there is a separation of charge at the interface between the redox active material and the electrolyte phase. Different models were proposed to represent the properties of such capacitive interphase: - the Stern model

- Helmholtz-Perrin - the Guy-Chapman model The most recent model describes the interphase as composed by different layers (from here the name electrical Double-layer): - adsorbed ions - gradient of concentration made of two parts – the diffused where the electric field is not zero (then the bulk starts) and migration takes place – the diffusion layer where the gradient of ion concentration cause diffusion from the bulk to the surface of the electro-active material. The most important take on the existence of a capacity double layer is that the voltage difference across the interphase is not anymore just the Gibbs free energy of reaction but there is also a component of electrostatic interaction between charges and the electrical field. In other words, the voltage difference between the two terminals is the difference between the electrochemical potential. A quantity made of the sum of chemical potential and electrical potential acting to the species. A note on terminology: the word electrode is often vague and used to describe the electro-active material only or the current collector but here is used to indicate the threedimensional region of space in which the electrochemical reaction takes place, as for IUPAC convention.

## Electrochemical methods

This chapter described the fundamental principles behind electrochemistry and about battery technology. The electrochemical methods are divided in two big families, direct current method and alternate current method. The first family deals with applying a voltage or a current and observing the other with time. Also in this case we can make a distinction between constant perturbation method or sweeping methods. In the first case the control is kept constant in time, this methods are known as galvanostatic and potentiostatic. The constant perturbation can be also stepped from zero to the value to zero again (pulsed) or continuous to increase in constant increments as a staircase. In the latter falls the method of polarization experiment used in certain fields. This class of experiment is used in corrosion, electrodeposition and battery characterization, more on this later. The other type of method instead involves the sweep of the control quantity, which means a constant increase in time with fixed ratio. This is a very typical experiment done from early days of electrochemistry to explore windows of potential and find the electrochemical potential value for an analytes. It is common to sweep the voltage in both directions and this is known as cyclic voltammetry. Voltammetry is used for characterizing HOMO and LUMO of molecules as well as sensing and qualitative analysis of chemicals in solution.

The second family of methods is based on alternating current. As mentioned before, the method is crucial to characterize capacitive behaviour in the electrode. The most common technique under this family is the Electrochemical Impedance Spectroscopy. The peculiarity of it is to apply an alternating voltage or current (sinus wave) at different frequency to the electrochemical cell and measure the output. The output will have a change in amplitude, following Ohm's Law, as well as phase. The change in amplitude and phase is a characteristic of the electrode and can be thought as a unique fingerprint. Using alternate methods at different frequencies allows to capture the kinetics of different processes and to quantify the resistance. This topic is divulged in the next section of the chapter.

## Three electrode cells

Taking back the concept of reference electrodes introduced before, it is now important a precisation for the case of measurement outside the thermodynamical equilibrium. In fact, reference electrodes should stay at equilibrium and they accept only small current through them (order of pA) for the sake of probing the voltage. If one is interested of measuring the potential of an electrode when a bigger current is flown, an auxiliary electrode is needed. This electrode has the role of closing the electrical circuit between the electrode under study, called working electrode) for the flow of current. At the same time a second high-impedance circuit is used to measure the voltage difference between the working electrode and the reference electrode. This gives also experimental access to the over-potential generated by the current.

The position of the reference electrode in a three-electrode set-up is quite important. Consider that between working and auxiliary electrodes current is flowing in the form of flux of ions. The movement of charged particles generate an electromagnetic field which alters the local electric field. This means that the double layer of the reference electrode might be altered and shift the electrochemical potential of the electrode. It is then recommended to place the reference electrode far from the current lines. Furthermore, it is not wise to put the reference electrode too far because of the longer path for the ionic current between working and reference electrode. A longer path produces an ohmic drop in the measured voltage difference which also alters read out voltage. The voltage drop due to the placement of the reference electrode is called "I-R drop", and can be corrected through alternate current methods. Modern electrochemistry devices have the feature to perform an I-R drop compensation automatically, but it is generally better to place the reference electrode as close as possible to the working electrode, still not in the middle of current lines.

## Electrochemical impedance spectroscopy

This technique is complex and interesting enough to deserve its own section. It is also the main experimental technique explored during this work, so it is necessary to delve into the details.

The full power of the technique is achieved when the impedance spectrum of the same electrode is obtained under different conditions. The first is temperature because one can extract the activation energy of the process via Arrhenius law. Or otherwise one can change the voltage at which the impedance is measured to activate thermodynamically or not specific reactions.

In the study of electrochemistry it is advantageous to be familiar with basic electrotechnic concepts for both simplify electrochemical processes as their equivalent circuit, for the analysis of data, or understand the electrochemical instrumentation to confidently design the experiment, understand the output and troubleshooting. This section deals with the basic passive elements, basic circuits, operational amplifiers and the concept of noise.

## Resistance and impedance

Electrical circuits have at least two poles at different voltage, usually one put to ground that is considered the reference point for zero. Inside the circuit flows the current. The flow can be continuous and we call it direct current or oscillating and we call it alternating current. This distinction is important because defines two similar quantities: electrical resistance and electrical impedance. Both are defined as the ratio of voltage and current for the cases of direct and alternate current. When describing the passive elements in the following, it is highlighted the impedance that later will become important for characterizing the properties of electrochemical systems. The main difference between the two signals is that voltage and current are not only related by a different in amplitude but also a shift in phase. For two oscillating signal, the phase or phase shift is the time difference between the same reference point in the two signals, for example the crest of a sinusoidal wave.

## Passive elements

### Resistor

The resistor is the simplest ideal element. The voltage applied to it is linearly related to the current and no phase shift is happening. The linear relationship is defined with the Ohm's law

$$V = RI$$

with the resistance  $R$  as proportionality factor, measured in Ohm. When an alternating current is applied, the same relationship holds so the impedance  $Z$  is equal to the  $R$ .

### Capacitor

The ideal capacitor is a device constituted by two parallel conductive plates separated by an insulator. When current flows in the circuit, the charges accumulate on the plates until the voltage between them is equal but opposite to the voltage applied to the circuit. The behaviour of a capacitor under constant current is then dynamic. The plates charge for a certain characteristic time that depends on the current applied and then no more current flows, behaving like an open circuit.

When an alternating current is applied to a capacitor, the voltage produced has a phase shift of  $90^\circ$  and no current flowing. The mathematical expression of the impedance for an ideal capacitor is then:

$$Z = -\frac{1}{j\omega C}$$

Where  $C$  is the capacitance.

### Inductor

The ideal inductor is a device that opposes to the change ???

[I don't know]

The mathematical expression of its impedance is:

$$Z = \frac{1}{j\omega L}$$

Where  $L$  is the inductance.

### Impedance of simple circuits

The impedance of a circuit of simple element is quite straightforward to calculate when considering the Thevenin and Norton laws. They state that in a branch of circuit the voltage drops of each electrical element adds up so at each node only one value of the voltage is present and the currents for each branch are equal on each electronic element that compose it and at a node all the currents sum up. It follows that the impedance of element in the same branch, i.e. connected in series, is also additive while the impedance of a circuit made of branches connected to the same nodes, i.e. connected in parallel, are inversely additive. For the scope of this work is interesting to consider the case of circuits of resistance, capacitors and inductors connect in various configuration. The most interesting will be the series and parallel connection of capacitors and resistor as well as the integration of an inductor to them.

#### The R-C circuit

When a circuit if formed by the series connection of a resistor and a capacitor

#### Graphic representation of the impedance

The impedance is a complex-valued number collected over a range of frequencies. Its analysis consist on evaluating how the module and phase change with the frequency.

$$\text{Module} = \sqrt{Z_{real}^2 + Z_{imag}^2}$$

$$\text{Phase} = \arctan(Z)$$

A visual evaluation allows to understand at a glance the behavior of the impedance.

# 3

## Batteries

### Contents

---

|   |    |
|---|----|
| Non-rechargeable batteries . . . . .                    | 13 |
| A brief historical overview . . . . .                   | 14 |
| Performance of batteries . . . . .                      | 14 |
| Secondary batteries . . . . .                           | 14 |
| The choice of metallic ion for shuttling . . . . .      | 15 |
| Electrolytes . . . . .                                  | 16 |
| State of the art of Li-ion batteries . . . . .          | 16 |
| On the nomenclature . . . . .                           | 18 |
| Manufacturing of batteries . . . . .                    | 19 |
| Battery degradation . . . . .                           | 20 |
| Electrochemical characterization of batteries . . . . . | 20 |
| Fast charging . . . . .                                 | 21 |

---

This thesis deals with the use of electrochemical methods to study redox active materials for the storage of electrical energy in the form of batteries (with a short excursus on double-layer electrochemical capacitors at the very end). In batteries, the electrodes are not called working and auxiliary (aka counter) as for analytical electrochemistry, but rather positive and negative electrode (IUPAC convention).

Batteries are classified based on the reversibility of the redox reactions into primary and secondary battery, which means in a more intuitive way: non rechargeable and rechargeable.

### Non-rechargeable batteries

Non-rechargeable batteries are the first type of batteries to reach commercialization and low prices. A primary battery uses inexpensive material that spontaneously react when the external circuit is close. This means the voltage of the cell is always positive. Upon time, the material of the electrodes are consumed during the electrochemical reaction until the reaction cannot anymore proceed. The electromotive force of the cell goes to zero as well as the voltage difference between the poles.

Non-rechargeable batteries allowed for the diffusion of portable electronic device, from the TV remotes, wrist watches and the Walkman to earing implants. For such they need to deliver a voltage difference of a few Volt to

power the circuit boards, enough "energy" to keep the device on for enough time to be useful. A third requirement for their diffusion is the low price, for being easily replaced in consumer electronics.

## A brief historical overview

If we take again the first example of battery made of zinc and copper, the voltage is quite low. Later metallic positive electrodes were substituted with oxides.

## Performance of batteries

The performance of energy storage system is assessed following two parameters: power and energy. Power is the electric work that an energy storage system can produce while energy is the amount of charge that the cell can deliver. Here, I am speaking of energy storage systems because power and energy can be calculated for any (electro-) chemical system. It is in fact quite interesting to compare different technologies to find the most suited for a specific application. To compare technologies or different chemistries for the same type of storage systems, power and energy are computed per unit of mass or volume; we then speak of power density and energy density. As an example we can think of an electric power tool to need a high power output but not much energy is required, while a pace maker doesn't require much power but rather high energy. For some applications the space is a constraint and there high energy density is of highest importance. For example, in transportation high energy density, both per unit of mass and volume) are a deciding factor.

Achieving high energy density or high power density (or both) can be technically challenging or economically expensive. To make another example, to store electrical energy from solar panels on the roof of public houses, energy density is not as important quite rather the absolute energy per unit of cost.

[ragone plot]

## Secondary batteries

The redox reaction at the electrode is an equilibrium reaction that can always be reverted when applying external energy from the outside. In common words we say charging. The sign of the current between the positive and negative terminal of the battery is positive (opposite), the electromotive force, hence Gibbs free energy of reaction, is also positive (which means work is made from the environment to the system) and, ideally, the redox active material is brought back to its original state. This type of operation is called electrochemical cell while for spontaneous reaction (electromotive force negative) it is referred in electrochemistry as galvanic cell.

In real cases, reverting the reaction might be inefficient. In fact, many side products can be formed, such as metal oxides, metal hydroxides or gas evolution due to electrolyte (or electrode material) decomposition. Common materials used in primary batteries can actually be recharged but the

process produces hydrogen from the split of water electrolyte and upon discharge cycling metal like zinc convert into oxide, passivating the surface of the negative electrode.

Efficiency is then the key to have a functioning secondary batteries. One can calculate the number of charge-discharge cycles that a battery can undergo based on the cycle efficiency. For commercial application the efficiency should be as close as possible to 100%, from 99.95% above.

The key for high efficiency is reversibility of the redox reactions. This is achieved using material that can intercalate ions; which means the ions are not converted to other chemical forms (metallic, oxide, etc.) but rather stored as ions. Materials with ordered structures (ionic or covalent) are the candidate for this mechanisms. Pairing of them and ions can shuttle from one electrode to the other. Typical examples of such materials are transition metals oxide, phosphates, sulfates and graphite.

The redox active metal is part of the crystal, upon reduction, a cation is hosted in the free spaces of the structure maintaining electroneutrality. The opposite happen when inverting the current. The mechanisms is also known as "rocking-chair" because of the back and forth of the ions. Transition metals have also high reduction potential producing cells with high voltage difference and hence high power density.

This concept, paired with organic electrolytes, allowed to obtain lithium ion-batteries with astonishing efficiency that now power all our electronic devices and electric vehicles.

## The choice of metallic ion for shuttling

The lithium-ion battery is known by anyone nowadays, regardless the scientific background. Lithium is such a good candidate because it is the smallest ion (in ionic radius) with single charge. This make it suitable for intercalating in many structures. In principle any metal can be used but the intercalation become more difficult increasing the radius and number of charges. The next logical candidate is sodium which indeed is seeing first commercialization in the latest few years (first li-ion battery based on organic electrolyte was commercialized in XXX with a energy density of ?? while the first na-ion batteries was commercialized in XXXX with an energy density of XXX; at the same year li-ion energy density reached XXX).

In principle any metal from earth to transition can be used for such a purpose. As an example, zinc is already used in primary batteries for its abundance. It all come to a matter of finding the right "host" for the ion would that be through intercalation or conversion. When the ionic radius is larger, though, it is more difficult to find a suitable crystal structure and when the charge per ion is two or three (Al), more than one electron transfer step is needed for the reduction.

On the other hand, having a less reactive cation allows to use aqueous electrolyte which, despite a smaller operational voltage window, is cheaper and safer (not flammable, not toxic).

The research is exploring the use of potassium, calcium, zinc in both aqueous and organic electrolyte.

## Electrolytes

Electrolytes are evaluated based on two properties: the voltage stability window and conductivity. Ideally one wants to obtain high values of both. The stability windows allows to use electrodes with a voltage difference high, while conductivity reduces the resistance to the ionic transport and the diffusivity of species in the diffuse layer of the interphase that affect the over-potential. Both characteristics ensure high power density. Note that the conductivity has a secondary effect because with high conductivity and small concentration over-potential, the same electrode can be used in its full capacity (suppose it has more plateau) inside the stability windows of the electrolyte. Experimentally, the stability window is estimated sweeping the voltage from very low to very high values, the electrolyte is stable when the current that flows in the region is negligible. The most simple example is the one of water. The stability window of water is 1.2V vs SHE. In fact, from 1.2V the oxygen in water oxidizes to produce pure oxygen gas while below 0V vs SHE, hydrogen gas is evolved. Of course this is a thermodynamic evaluation, kinetics of such reaction must be much lower than the redox at the electrode material. The window of aqueous solution can be extended working with the solute. In highly concentrated solution the windows can be kinetically extended increasing the reaction over-potential. In fact when water molecules are solvating an ion, they are blocked in the position by the electrostatic local field. In this case it is commonly used the name water in salt with electrolyte solution of 5 to 20 M. The extended voltage window comes with the price in conductivity because the high concentration reduces the mobility of the species. For battery application it is still a good trade-off facilitating the use of certain electrodes and increasing the final cell operating voltage.

### Deep eutectic point solvents?

The opposite case is the one of organic solvents that usually present wider stability window but lower conductivity. Organic solvents allow also to have in the electrochemical cell metals in the reduced form while the absence of oxygen ions to react with. The most used organic compound in batteries are cyclic carbonates which have wide voltage windows of 4 to 5 V but high viscosity at room temperature. To obtain sufficient conductivity the viscosity is reduced by mixing them and balance their properties.

These compounds are unfortunately flammable and toxic which present a problem for the safety of the user as well as the environment in case of leakage and during the disposal of exhausted batteries. This is a topic of great discussion in the community and for this reason aqueous electrolytes (and electrodes for them) as well as solid-electrolyte (see later for more) are actively researched with great investments in the public and private sector.

## State of the art of Li-ion batteries

### Positive electrodes

To achieve high power density, the positive electrode should have a high electrochemical potential. Looking at the standard reduction potentials of the metals in the periodic table is clear that the best choice are

transition metals. As mentioned before, it is convenient for achieving high reversibility to shuttle a small cation inside a crystalline structure so the best candidates as redox active materials are oxides and The state of the art for Li-ion batteries is NMC622 as positive electrode and graphite as negative electrode.

## Graphite as negative electrode

Graphite can reach 0V vs Li (-3 vs SHE) making it the lowest electrochemical potential from the periodic table. It is tempting to think of substituting graphite with metallic lithium which has a nominal energy density XX time larger, but its drawback is the morphology of electrodeposition because lithium, especially at higher current densities, doesn't electrodeposit uniformly but rather form dendritic structures that easily lead to short-circuit.

[describe plateau of graphite]

## The solid-electrolyte interface

Organic electrolytes start to reduce around 100mV vs Li forming various short chained organic compounds. At the same time, the potential is near to the formation of lithium fluorides catalyzed by the release of fluorine from the decomposition of the electrolyte as well as Lithium oxide and other inorganic compounds. All of these new phases tend to grow at the surface of the negative electrode where the electrochemical potential of the electrons is around 0V vs Li. A solid layer is then formed around the particles of the graphite (or lithium) at the negative electrode. This layer happens to be ionic conductive and doesn't impede the operation of the cell. This layer called solid-electrolyte interface forms as soon from the reduction of the negative electrode but stops growing soon. This creates a stable situation where no more electrolyte is decomposed while the lithium ion can pass through it. The growth of the layer is important for stabilizing it early. A uniform layer will stop growing sooner, while a porous layer will continue to grow for many cycles of the cell. A uniform layer is catalyzed by slow current density on the negative electrode so after a battery cell is assembled, the first one or two cycles are carried out at very small currents. This time-consuming step is referred to as "formation" and it is a critical step of battery production. Because of its complexity it is difficult to control or predict. It is also difficult to evaluate experimentally because the layer is thin, soft and has the same composition of the rest of the cell. Many strategies have been proposed to get a uniform and short-growing SEI but the research is still highly active, but from the perspective of experimental characterization and modelling. It is important to remark the importance of a SEI that stops growing soon. Despite being ionic conductive and not impeding the cell behaviour itself, its formation is a sign of electrolyte decomposition and reaction with lithium. When lithium reacts it is not capable anymore to be shuttled because the total energy of the cell drops. This mechanism of lithium loss is called "loss of lithium inventory" and it is one of the three major causes of battery degradation (also called "aging") together with the degradation of electroactive materials at the positive and negative electrodes.

## Solid electrolytes

Once the li-ion batteries started to plateau in energy and power density with the advent of NMC622, the research interest moved to high energy cathode which have the problem of structure instability and lack of stable organic electrolyte at voltage above 4.5V and on the other hand solid-state electrolytes to unlock the potentiality of metallic lithium.

Solid electrolytes are interesting because the absence of liquid reduce the safety risk concerned to toxicity, gas evolution and leakage in the environment when damaged. A solid electrolyte can be also thinner than the usual polymeric separator that holds the liquid, increasing the power and energy density while keeping the same redox active materials. Furthermore, the hope of the scientific community is to facilitate the safe use of metallic negative electrodes (Li, Na, K,...) because a solid electrolyte might suppress the growth of dendrites. Unfortunately introduces other problems like the loss of surface contact between the metallic electrode and the solid electrolyte during reduction and oxidation as well as promoting the metal growth in the free spaces of the solid electrolytes. Nonetheless it is one of the hottest topic of research at the moment from both universities and private companies. Latest results show a cyclability of 500 cycles in pouch cell format. The scaling up of the production of such materials is also a matter of research.

## On the nomenclature

In the battery technology field positive and negative electrode are usually referred to as cathode and anode. These names originate from early time of electrochemistry. The cathode is where oxidation takes place, from Greek, while anode is where the oxidation takes place. For a primary battery that undergoes "spontaneous discharge", the positive electrode behaves as a cathode while the negative electrode behaves like an anode. For secondary battery during charge, i.e. operated as electrochemical cell, the positive electrode undergoes reduction behaving as anode, while the negative electrode as cathode. Despite the change in current sign the positive electrode remains "positive" in the sense of having a higher electrochemical potential compared to the other electrode of the cell.

It is anyway common, especially from scientist coming from the field of chemical synthesis and material science with a limited interest in electroanalytical, to call the electrodes cathode and anode.

Another source of misconception is the equivalence in meaning of the words charge and capacity. The latter comes from the idea of maximum quantity of something that in case of batteries is the electronic charge. It has not to be confused with the term capacitance of the electrical element capacitor. The term capacity is widely used in the sector while the correct one would be total charge (measured in Coulombs or Ah in the battery world). When the charge is integrated in the time of operation of a battery, gives the electrical energy (or work) of the device.

In this text, the IUPAC convention will be followed.

## Manufacturing of batteries

We have covered the chemical aspect of redox active materials and electrolyte but for producing commercial batteries there are many other practical aspects to consider to reduce the volume of the cell. The first thing to consider is the conductivity of the components. Ceramic materials are in fact electric insulator, so, to guarantee an electrical contact with the external circuit, a conductive element is added usually in the form of carbon particles. The redox active materials together with carbon are kept in place using polymer binders. The ratio between the components is usually 90-5-5 but it is a design choice based on the properties of the materials and the needs of the final results. The part of the composition which is not active material is a passive component that doesn't contribute with the reaction but increases weight and volume of the cell reducing the voltage and power density. For this reason the Ragone plot shown before is of such importance, because includes in the full picture all the direct and indirect effect of the choice of the chemicals in the final performance of the device.

To make an electrode one other component is needed: the current collector. It has the scope of transferring the electron from the external circuit to the redox active material and also provides a rigid substrate on which adhere the particles of active material. In practical terms the components stated above (active material, binder and conductor) are first dispersed in a solvent capable of dissolving the polymeric chain, the so called "slurry" (which should be very homogeneous, hard to achieve) is then spread on the foil of a current collector and the solvent evaporated. The drying process is critical in industrial manufacturing because the solvents used for NMC are toxic (PVDF) and the evaporation requires a lot of energy and time. Attempts to produce electrodes via extrusion of the electroactive materials are under research, but, when homogeneity is achieved, they are not trivial to scale up for industrial production.

Immediately come the second consideration which is the thickness of the components. The particles of active material must be in close contact with the electrolyte to allow lithium to get in and out the crystal, so the electrode must be thin highly porous and not too thick. This limits the upper limit of the volume occupied by the active material while it is difficult to shrink too much the volume of the passive component. As state of the art, active materials and additives spread on the substrate have a thickness of around 40 µm while a porous polymer separates the electrodes to avoid short circuit. The porosity of the separator and its morphology is important because the electrolyte is soaked in them and direct diffusion path must be guaranteed. The thickness of separators can arrive down to 12 µm.

As current collectors aluminum and nickel are commonly employed. Aluminum, which is cheaper than nickel cannot be used as negative electrode in lithium ion batteries because aluminum alloys with lithium.

Batteries can also be produced with different form factors, the most known one is the cylindrical cell, but there is also the prismatic cell and the pouch cell. Each one with pros and cons.

## Battery degradation

The maximum charge that a battery can store sets the operation time. Upon usage, the battery loses some of it because of side processes. These losses regards both the amount of lithium and redox active material. Active lithium ions can be lost during further SEI formation on late life time of the cell. Despite the SEI growth stops early in the life of the cell it is still thermodynamically possible and if the morphology of the graphite particle changes, because of cracking for example (discussed later) new SEI can form that include the reaction with lithium ion. Another possibility of losing active lithium is through electrodeposition, especially during charging at high current density (aka fast charging). The third plateau of graphite is a few mV above the thermodynamic reduction potential of lithium. Furthermore, the potential is not equivalent in all the point of the volume of the graphite, some might have higher or lower values, what is measured is an average. Then lithium can electrodeposit at the negative electrode. The electrodeposition, as already introduced, it is not a uniform processes and might lead to cylindrical shapes which can both: re-dissolved, if the critical radius is not reached, leading only to loss of efficiency of the discharge cycle or in the worst case detach from the surface as a metal macroscopic particle and float in the electrolyte. Since no electrical contact is present, oxidation and dissolution back to the electrolyte might not happen and that amount of lithium is loss from the total count.

The other major source of degradation for batteries is the loss of active material (both at positive and negative electrodes) for losing contact with some particles. This is especially true when at high current rates particles are subjected to a change in volume. Upon cycling the mechanical stress can induce cracks.

Other minor sources of degradation are the reaction of the metal current collector with the product of electrolyte degradation. Furthermore, aluminum from the positive electrode might slowly dissolve into solution and travel to the negative electrode to alloy with lithium; reversing the alloying reaction is inefficient.

## Electrochemical characterization of batteries

The characterization of the battery means knowing:

-specific power, -specific energy, -maximum charge.

This information is extracted experimentally from electrochemical tests based on constant current techniques. The idea behind the experiment is to charge and discharge the battery with constant currents and observe the degradation over time measure in loss, or fading, of charge.

The choice of the current to perform the experiment is quite arbitrary and it is based on the concept of "charging-rate", usually called simply C-rate. The C-rate is the inverse of the time (in hours) needed to completely charge the cell up to its maximum theoretical capacity from a state of complete discharge. Hence, the current to achieve it is then

$$I = \text{maximum charge } [Ah] * \text{c-rate } [h^{-1}].$$

For lithium ion batteries, very slow charges are C/20 or C/10 used for example in the formation process. 1C is the stand for a lab test. A battery

is considered at commercial standard when the maximum charge reaches 80% of its original values after 1000 cycles. Fast charge is C/3 and goes to "extremelly fast charge" at C/4 or C/5.

Because of the over-potential, cycling at 1C, will not allow to charge the battery up to the full capacity. A strategy to metigate it is to apply a constant voltage technique after the constant current, with a voltage value equal to the upper voltage limit of the constant current charge. This allow to intercalate some more ions in the strucutre without goign outside the thermodynamic stability of the electrodes. This approach is common in battery cycling and it is referred to as constant-current-costant-voltage (CCCV) protocol.

[How much does it intercalate?]

## Fast charging

For batteries in electrical mobility, especially cars, it became important in the last years the idea of charging them very fast, let's say a time comparable to the stop at the gas station to refill the oil tank of a car based on thermal engine. 20-10 minutes seems the goal for fast charging. It has to be noted that fast charging is always performed in a limited state of charge, usually between 20 and 80%, in fact otherwise the over-potential would be too high and the lithium intercalation too ununiform to damage the particles of active material. Furthermore extremelly fast charge can be achieved only with silicon-graphite alloys with high concentration of silicon which bring in the problem of volume expansion. Furthermore at this power loads the termal dissipation is extremelly important and require fine engineering of the whole battery pack and thermal management system.

Up to this time the record is hold by the private company Store Dot which achieve extremelly fast chargin from 20 to 80% in 8 minutes with good termals.



# 4

## Identification of dynamical systems

### Contents

---

|   |    |
|---|----|
| Definition of system and properties . . . . .           | 23 |
| System identification in the frequency domain . . . . . | 32 |
| Digital signal processing . . . . .                     | 38 |

---

### Definition of system and properties

A dynamic system is a system whose output evolves over time in response to one or more inputs. To describe such a system rigorously, we begin by defining its inputs  $u(t)$  (the signals or forces we apply), its outputs  $y(t)$  (the measurable responses), and its internal state  $x(t)$ , which encodes the minimum set of variables (e.g. concentrations, voltages, positions) that, together with the inputs, fully determine future behavior.

From these definition follow three properties: causality, stationarity and linearity. Causality means that the system cannot “anticipate” the future—its output at time  $t$  depends only on inputs (and states) at times less or equal  $t$ , never on future values. This reflects physical intuition (you cannot react before being stimulated) and is essential when designing real-time controllers or simulators. The next property is system stationarity that means system internal state  $x(t)$  doesn’t change with over time. In other words, when the input has a time delay, the output is delayed by the same amount without change in response shape. A stationary system, also referred as time-invariant, it is easier to analyse because it behaves uniformly across all time, allowing to use frequency-domain techniques for its analysis like the Fourier Transform that rely on shift symmetry as will be discussed later in detail. Many real systems though, are not stationary that means the internal state  $x(t)$  changes over time: it is time-variant. In this case, any delay of the input does not simply delay the output but there is also a memory effect of the previous states of the system. Time-variant and invariant system requires different formalisms that will be discussed in the following of this section. Lastly, the linearity property includes homogeneity and superposition principle: scaling the input by a constant results in the output scaled by the same constant as well as the sum of inputs produces an output that is the sum of the individual inputs response. Linear system admit

algebraic representation that means that the input-output representation can be written as ordinary algebraic equations and represented as matrices which can be manipulated with well-known linear algebra methods. Again, in the real world, many systems respond to input in a non-linear manner and the homogeneity and superposition principles do not hold. The output depends on the amplitude of the input and the state of the system and all behaviours cannot be represented by a constant-coefficient matrix as for the linear case.

## Modeling with differential equations

When we model the physics of a system, we must choose between lumped-parameter and distributed-parameter descriptions. Lumped-parameter models assume that each state variable is uniform over its domain (e.g. the voltage across an ideal capacitor or the temperature of a well-stirred reactor), yielding ordinary differential equations (ODEs) in time only. Distributed-parameter models recognize spatial variation (e.g. diffusion of ions in an electrode, heat conduction in a battery cell) and lead to partial differential equations (PDEs) in both space and time. While lumped models are simpler to analyze and simulate, distributed models capture gradients and wave-like phenomena that can dominate behavior in large or heterogeneous electrochemical systems.

If one can assume each variable (say, ion concentration or electrode potential) to be spatially uniform within its region, then you partition the system into discrete lumps and write ordinary differential equations (ODEs) of the form

$$\frac{dx}{dt} = f(x, u, t),$$

where  $x(t)$  is a vector of state variables,  $u(t)$  the inputs (current, temperature, etc.), and  $f$  encapsulates generation, consumption or storage rates (e.g. reaction kinetics, double-layer charging). This lumped-parameter approach yields a finite set of ODEs requiring only initial conditions  $x(t_0) = x_0$  to specify a unique time-evolution. When spatial gradients cannot be neglected—such as ion diffusion through porous electrodes or potential drops across an electrolyte—you must adopt a distributed-parameter model and derive partial differential equations (PDEs). A canonical example is the diffusion equation for concentration  $c(x, t)$ :

$$\frac{\partial c}{\partial t} = -\nabla J + R(c, \varphi, t),$$

with flux  $J$  often given by Fick's law  $J = -D\nabla c$  and  $R$  representing local reaction or source terms. The solution of such a PDE demands, in addition to an initial concentration profile  $c(x, t_0) = c_0(x)$ , boundary conditions on the domain's edges—Dirichlet (fixed value), Neumann (prescribed flux) or mixed Robin types—so that the problem is well posed.

Formally, ODE- and PDE-based models differ only in whether your independent variables include space; both require clear statements of (1) governing equations from conservation or constitutive relations, (2) initial conditions for all states, and (3) boundary conditions for spatial domains. Analytic solutions exist only for the simplest geometries and linear kinetics; in practice, one discretizes PDEs (via method of lines, finite differences

or finite elements) into a large ODE system and then integrates numerically. This rigorous ODE/PDE formalism ensures that key electrochemical phenomena—time-constant separation between fast surface reactions and slow diffusion, non-uniform current distributions, dynamic adsorption—are faithfully captured, setting the stage for accurate simulation, control design and parameter estimation.

Electrochemical systems are described by a special case of partial differential equation in which the order of the derivatives is not an integer but rather a fraction, hence the physical model must be described with fraction differential equations (FDE).

This type of models based on differential equation are referred to as parameteric models for they contain coefficients, or parameters, that multiply each N-th order temporal derivate variable. System can be also model used non-parametric descriptions, but will not be considered in this work.

## Transfer function

In a linear time-invariant (LTI) system, the transfer function provides an algebraic description of how inputs are mapped to outputs in the complex-frequency domain. For a dynamic system with lumped parameters described by  $dt/dt = f(x, u, t)$  the function  $f$  must be linear and time invariant in this limiting case of LTI. Hence  $f$  can only be described as a linear combination of the states of which the coefficents are time-indipendent parameters, which leads to the ordinary differential equation to take the form

$$a_n y^n(t) + a_{n-1} y^{n-1}(t) + \dots + a_0 y(t) = b_m x^m(t) + b_{m-1} x^{m-1}(t) + \dots + b_0 x(t),$$

where  $n$  is the order of the ODE. Solving the equation for  $a_i$  and  $b_i$  is impossible with algebraic method for the presence of the derivative. This historic mathematical problem was tackled by Pierre-Simon Laplace across the eightteenth and nineteenth centuries. He had the intuition of applying a variable trasnformation to convert derivatives into multiplication, simply identify the coefficients in the new space and then invert the trasnformation to its original variable space for the solution of the equation. The transformation is now known as Laplace transform, an operator denoted as  $\mathcal{L}$  that acts on the function  $f(u,x,t)$

$$\mathcal{L}\{f\}(s) = \int_0^\infty f(t)e^{-st}dt,$$

where  $s$  is a complex number. the resulting functional is usually written with capital letter :  $F(s)$  in the new variable  $s$ . (Note: not to be confused with the Fourier transform. Here I am using F only because of the function  $f(u,x,t)$  defined before) When taking the Laplace transform under zero initial conditions to the constant-coefficient ordinary differential equation it become:

$$Y(s)[a_0 + a_1 s + \dots + a_n s^n] = X(s)[b_0 + b_1 s + \dots + b_m s^m].$$

Here it is introduced the definition of transfer function as the ration

$$H(s) = \frac{Y(s)}{X(s)}$$

or

$$H(s) = \frac{b_0 + b_1 s + \dots + b_m s^m}{a_0 + a_1 s + \dots + a_n s^n}.$$

By evaluating  $H(s)$  on the imaginary axis ( $s=j\omega$ ), one directly obtains the frequency response, much clearer for practical applications. The Laplace transform can be written directly as function of  $j\omega$  and be called Fourier Transform. When plotted in Bode plots, the shape of the magnitude and phase of the transfer function is used to study resonance analysis and controller design. In fact, the transfer function is a rational polynomial function and as such one can calculate the solution for zero, or roots, for the numerator and denominator, usually referred as zeroes and poles for the reason that the transfer function approaches zeroes (i.e. attenuates the input) when the nominator tends to zero and approaches infinite (i.e. system natural modes, where it is stationary; it means that before that value, the system decays exponentially after an impulse while for greater values it grows unstable) when the denominator tends to zero. In discrete-time, an equivalent formulation arises by applying the z-transform to a linear difference equation, yielding  $H(z) = Y(z)/X(z)$ . Thus, the transfer-function formulation transforms differential (or difference) equations into algebraic ratios in  $s$  or  $z$ , enabling powerful tools for analysis, simulation and design entirely within the complex-frequency domain.

In signal processing and control theory, a transfer function is a compact mathematical description of how a linear time-invariant (LTI) system maps an input to an output in the complex-frequency domain. Here, “linear time-invariant” means the system’s output depends linearly on past inputs and its characteristics do not change over time. By applying the Laplace transform to the input signal  $x(t)$  and output signal  $y(t)$ , one obtains  $X(s)$  and  $Y(s)$  as functions of the complex frequency variable  $s$ ; under zero initial conditions, the transfer function is defined as  $H(s) = Y(s) / X(s)$ . In discrete time, the analogous definition uses the z-transform,  $H(z) = Y(z)/X(z)$ . Because  $H(s)$  (or  $H(z)$ ) is typically a ratio of two polynomials, its zeros (numerator roots) create frequency bands of attenuation, while its poles (denominator roots) correspond to the system’s natural modes and govern stability. Evaluating  $H(s)$  along the imaginary axis ( $s = j\omega$ ) yields the frequency response  $H(j\omega)$ , whose magnitude and phase plotted against  $\omega$  (Bode plots) immediately reveal gain, bandwidth, resonances, roll-off rates and phase margins. Transfer functions therefore serve as the foundation for system analysis (predicting step and impulse responses), filter design (pole-zero placement), controller tuning (adjusting crossover frequencies and margins), and system identification from measured input-output data.

## Kramers-Kroning relationship

???

## Time-domain response

Time-domain responses offer an intuitive picture of a system’s dynamics by showing how it reacts over time to simple probes such as an ideal impulse  $\delta(t)$  and a unit step  $u(t)$ . The impulse response  $h(t)$  fully characterizes the

system—any output follows by convolution,

$$y(t) = \int_0^\infty h(\tau)x(t-\tau)d\tau,$$

while the step response

$$y_s(t) = \int_0^\infty h(\tau)d\tau$$

highlights cumulative behaviors such as rise time, overshoot and settling. Each term in  $h(t)$  corresponds to a modal response  $e^{p_i t}$ , where poles  $p_i = \sigma_i \pm j\omega_i$  set decay rates ( $\tau_i = -1/\sigma_i$ ) and oscillation frequencies  $\omega_i$ . In principle, a single time-domain experiment can excite all of a cell's characteristic modes—charging, diffusion, adsorption—in one go, revealing the distinct “humps” or decays associated with each physical process. Another approach for probing the system is using a broadband excitations and Deconvolution such as a chirp, multi-sine or pseudo-random binary sequence (PRBS) that spans the desired frequency range with known amplitude and phase, then compute the impulse response by deconvolving the input from the output (or by cross-correlation for PRBS). Experimentally,  $\delta(t)$  is approximated by a very short voltage or current pulse of duration  $\Delta t \ll \min(\tau_i)$ , yielding a near-flat spectrum across all modes, whereas step tests involve abrupt, sustained input changes. By recording the resulting transients in voltage or current, one observes distinct decays or “humps” that map directly to physical processes (for electrochemical systems double-layer charging, charge-transfer kinetics and mass-transport diffusion) and can extract each time constant and gain from a single measurement. In practice, however, generating an ideal input is challenging: pulses must be short yet energetic enough for a clean signal, and extracting the true impulse response often amplifies noise when one differentiates a measured step. Moreover, overlapping time constants can blur together, making it hard to assign each feature to its underlying mechanism.

### Frequency-domain response

The frequency-domain response is the quantitative measure of the magnitude and phase of the output as a function of input frequency. The frequency response for a linear and time-invariant system (LTI) is the ratio of the Fourier spectra  $X(\omega)$  and  $Y(\omega)$  of the input  $x(t)$  and the output  $y(t)$ :

$$H(\omega) = \frac{Y(\omega)}{X(\omega)}.$$

For electrochemical systems inputs and outputs are generally voltages  $u(t)$  or current  $i(t)$  giving as transfer function the impedance or admittance:

$$Z(\omega) = \frac{u(\omega)}{i(\omega)} \quad \text{or} \quad Y(\omega) = \frac{1}{Z(\omega)} = \frac{i(\omega)}{u(\omega)}.$$

The input can be a waveform with a single frequency components, such as a sine, or a broadband excitation such as chirp, multi-sine or pseudo-random binary sequences. In practice, when stimulating the system with input with different frequencies one obtains the frequency response function

(FRF) over those (angular) frequencies. The frequency response function is the practical realization of the transfer function. Frequency and time -domain characterization methods are looking at the same system from two different perspective so the choice of the method depend on the particular case.

Here are some difference between the two approaches:

#### Excitation

Time-domain: single step or short pulse (broadband in principle)

Frequency-domain: sinusoids (one at a time) or broadband signals (chirps, multi-sine, PRBS)

#### Measurement

Time-domain: record transient  $y(t)$  immediately after input; extract  $h(t)$  or step response  $y_s(t)$  features

Frequency-domain: wait for (or isolate) steady-state sinusoidal output, then measure gain and phase at each  $\omega$  (or compute  $H(\omega) = \frac{Y(\omega)}{X(\omega)}$ )

#### Data Processing

Time-domain: curve-fit exponentials or deconvolve pulses; may differentiate noisy data to obtain  $h(t)$

Frequency-domain: FFT (or cross-spectra) and ratio formation; Bode/Nyquist plotting

#### Advantages

Time-domain: one test captures all modes at once; intuitive identification of time-constants and overshoot

Frequency-domain: high SNR at each  $\omega$ ; clean separation of processes by frequency; easy to apply windowing and averaging

#### Limitations

Time-domain: hard to generate ideal impulses; overlapping decays can be ambiguous; noise amplification in differentiation

Frequency-domain: sequential  $\omega$ -points lengthen total test time (unless using broadband patterns); requires steady-state per tone

#### Typical Use

Time-domain: fast-survey of overall dynamics; educational demonstrations; some controller designs (pulse response)

Frequency-domain: impedance spectroscopy; precision filter or controller tuning; system identification with narrow-band models

## State-space formulation

Beyond single-input/single-output ODEs or transfer functions, the state-space approach offers a compact, general framework—especially powerful for multi-input/multi-output (MIMO) or high-order systems, and a natural bridge from distributed-parameter (PDE) models after spatial discretization. You begin by collecting all the system’s “memory” variables (e.g. surface concentrations, electrode potentials, capacitor voltages) into a state vector  $x(t)$ . The evolution of  $x$  is then governed by a first-order vector differential equation  $\dot{x}(t) = Ax(t) + Bu(t)$  where  $u(t)$  is the input vector (voltage, current, temperature, ecc.),  $A$  is the state-matrix that encodes internal coupling and time-constants, and  $B$  maps inputs into the state dynamics. The output vector  $y(t)$ —the measurable voltages, currents or other signals—follows  $y(t) = Cx(t) + Du(t)$  with  $C$  selecting or combining states

into outputs and D capturing any direct feedthrough from input to output. Why use state-space?

- Universality: any LTI system (of order N) can be cast in this form, whether it started as a set of ODEs, after discretizing a PDE, or even as a higher-order transfer function.
- MIMO handling: A,B,C,D naturally generalize to multiple inputs and outputs without cumbersome transfer-matrix algebra.
- Time-domain clarity: initial conditions  $x(0)$  enter directly, so you can simulate transients under arbitrary start-up states.
- Analytical tools: eigenvalues of A are the system poles (modes), and the resolvent  $(sI - A)^{-1}$  appears in the transfer-function relation

$$H(s) = C(sI - A)^{-1}B + D,$$

linking state-space and frequency-domain descriptions.

- Extension to time-varying or nonlinear dynamics: by allowing A, B, C, D to depend on t or x, u, you move naturally into more advanced modeling without abandoning the same notation. In electrochemical systems, state-space models let you represent coupled reaction kinetics, double-layer capacitance, and diffusion processes in one unified set of matrices—ready for simulation, model reduction or control design.

Compared to the use of transfer function for frequency-domain characterization, state-space representation is used for characterize system in time. Not only state-space has the advantage of handling multiple input systems but also its linear algebra nature make it easy to scale to higher dimensions and use algebraic techniques like validating the internal stability with the Lyapunov method.

## Model parameters and order

In dynamic-systems modeling, the “order” of a model refers to the number of state variables (or energy-storage elements) needed to capture its behavior—in essence, the dimension of the underlying set of differential equations. High-order or distributed-parameter models (e.g. detailed diffusion PDEs) can faithfully describe every subtle spatial and temporal effect but become computationally expensive, hard to identify from data, and unwieldy for control or optimization. Model reduction seeks a lower-order approximation that retains the system’s dominant dynamics over the frequency or time range of interest. Model order—the number of state variables in your model—directly ties to which internal modes actually matter for input–output behavior. Controllability asks “can my inputs excite each state?” and observability asks “can I infer each state from my outputs?” In a full-order model some states may be neither reachable by any input nor visible in any output; those uncontrollable or unobservable modes never influence the signals you care about. By applying the Kalman decomposition (or checking the rank of the controllability and observability Gramians), you identify and remove exactly those redundant

states, yielding a minimal realization whose order equals the dimension of the controllable-and-observable subspace. Thus, controllability and observability are the gatekeepers for model reduction: they tell you which state dynamics you can safely discard without altering the measured transfer behavior, ensuring your reduced-order model remains both compact and faithful. Frequency-domain methods (i.e. electrochemical impedance spectroscopy) have become the gold standard for battery characterization because they deliver a direct, frequency-resolved view of each physical process—charge transfer, double-layer charging, solid-state diffusion—by measuring complex impedance  $Z(\omega) = V(\omega)/I(\omega)$ . Modern potentiostats integrate precision waveform generators (single- or multi-sine, chirp) and phase-sensitive detectors, so although the hardware is more involved than a simple current-pulse setup, you gain much higher signal-to-noise ratio at each frequency and unambiguous separation of overlapping time-constants. By contrast, time-domain techniques apply a step or short pulse and monitor the transient voltage (or current) relaxation. You cannot produce a true Dirac impulse, but methods like GITT (Galvanostatic Intermittent Titration Technique) approximate it by applying small current pulses followed by long rest periods and analyzing the potential versus  $\sqrt{t}$  to extract diffusion coefficients and resistances. GITT is widely used for diffusion quantification and state-of-charge profiling, but it smears together fast and slow processes and typically requires curve-fitting of overlapping exponentials—making interpretation more model-dependent. From a systems-theoretic viewpoint, neither domain changes the underlying controllability or observability of the battery’s modes: as long as your excitation (pulse or broadband waveform) contains energy at a mode’s frequency, that mode is controllable; and as long as you measure the resulting voltage/current, it is observable. The practical advantage of the frequency domain is that you can concentrate excitation energy into narrow bands—boosting SNR where you need it—and directly read off gain and phase without deconvolution or numerical differentiation. Time-domain tests remain valuable for rapid surveys or diffusion-specific studies (via GITT/PITT), but for full dynamic system identification and high-fidelity equivalent-circuit fitting, frequency-domain characterization typically offers superior precision and clarity. Beyond diffusion-limited behavior, a current-step transient actually unfolds in several phases:

1. Instantaneous IR drop: the very first jump in voltage reflects the cell’s ohmic resistance (electrolyte, wiring, contacts).
2. Fast exponential decay(s): immediately after the IR drop, you often see one or more exponentials whose time constants ( $\tau \approx R_{ct} \times C_{dl}$  or adsorption time constants) arise from charge-transfer resistance ( $R_{ct}$ ) and double-layer or adsorbed-species capacitances ( $C_{dl}$ ,  $C_{ads}$ ).
3.  $\sqrt{t}$ -dependent diffusion regime: on longer time scales the voltage relaxes roughly linearly with  $\sqrt{t}$ , characteristic of semi-infinite solid-state or porous-electrode diffusion.

GITT and similar methods typically focus on the third regime—using long enough pulses and rest periods to isolate diffusion and extract  $D$  via the  $\sqrt{t}$  slope. The earlier exponential phases do contain charge-transfer and

adsorption information, but they are short, often buried in noise, and overlap when multiple time constants coexist. Extracting them reliably requires very high time resolution, careful baseline subtraction, and multi-exponential fitting—challenges that make time-domain extraction of  $R_{ct}$  and  $C_{dl}$  less robust than frequency-domain impedance, where each process cleanly appears at its own corner frequency.

## Non-linear systems

Nonlinear systems are those in which the principle of superposition (i.e. the sum of individual responses equals the response to the sum of inputs) no longer holds because one or more elements—reaction rates, transport coefficients or material properties—depend on the current state or input amplitude. Unlike linear systems, whose behavior is fully captured by constant-coefficient ODEs, transfer functions and fixed poles/zeros, non-linear systems can exhibit amplitude-dependent gains, harmonics, limit cycles, multiple equilibria or even chaotic dynamics. An applied sinusoid may generate new frequencies through distortion, and small changes in operating point can dramatically alter time-constants or stability. Analytically, one often resorts to numerical integration, perturbation expansions around an operating point to compensate or remove the non-linearity from the output. In alternative to approximate describing-function techniques to study such behavior. The magnitude and phase of these harmonics can be directly linked to physical nonlinearities—such as the exponential dependence of Faradaic current on overpotential (revealing Tafel slopes), coverage-dependent adsorption pseudocapacitance, or concentration-polarization effects under large polarization. By extracting and modeling these higher-order impedance kernels, one gains insight into reaction orders, adsorption isotherms, and dynamic coupling between charge transfer and mass transport—information that is invisible in conventional, strictly linear EIS. In the classic electrochemical impedance spectroscopy, however, one deliberately keeps perturbations small enough (typically a few millivolts or microamperes) that the cell’s response remains in its nearly linear regime. This “small-signal” assumption ensures that the measured impedance truly reflects the linearized transfer function around the chosen operating point, avoiding the complications of nonlinear dynamics. The simple transfer-function definition  $H(s) = Y(s)/X(s)$  only holds for linear, time-invariant (LTI) systems under zero initial conditions. Time-varying systems – Their impulse response  $h(t,\tau)$  depends on both the observation time  $t$  and the input time  $\tau$ , so you write  $y(t) = \int h(t,\tau)x(\tau)d\tau$  – You cannot collapse this into a single-variable  $H(s)$ ; instead you must work with the two-time-index kernel  $h(t,\tau)$  or its time-varying Fourier/Laplace counterparts. Nonlinear systems – Superposition no longer applies, so  $y(t) \approx h*x$ . – You must resort to Volterra/Wiener series (multi-kernel expansions) or describing-function methods for small-signal, approximate frequency-domain descriptions.

## Non-stationary systems

In contrast to time-invariant systems—whose rules never change—a time-varying (non-stationary) system has dynamics that explicitly depend on the absolute time at which inputs are applied. Formally, its input–output

relation must be written with a two-time kernel  $y(t) = \int_0^t h(t, \tau)x(\tau), d\tau$ , where  $h(t, \tau)$  no longer “slides” with  $t$  but changes shape as  $t$  evolves. Equivalently, in state-space one writes

$$\dot{x}(t) = A(t)x(t) + B(t)u(t), y(t) = C(t)x(t) + D(t)u(t),$$

with  $A, B, C, D$  all functions of  $t$ . Why does this matter? In batteries and electrochemical cells, internal parameters (resistances, diffusivities, capacitances) drift with state-of-charge, temperature or aging. As a result, the same excitation at two different instants produces outputs with different gains, time-constants or phase lags. Special cases and analysis tools include:

- Linear-Parameter-Varying (LPV) models, where  $A, B, C, D$  depend smoothly on measurable “scheduling” variables (e.g. SoC), allowing global non-linearity to be handled via local LTI patches.
- Periodic (Floquet) systems, in which  $h(t+T, \tau+T) = h(t, \tau)$  and one can use harmonic-balance or stroboscopic maps to analyze stability and resonance.
- Slow-variation (quasi-stationary) approximations, applying sliding-window or recursive-least-squares identification to treat the system as locally LTI over short intervals.

## System identification in the frequency domain

### Definition

System identification is the process of choosing statistically a mathematical model appropriate to describe the system under study based on measured input/output data (data-driven). For system identification in the frequency domain, that we are using here, it is finding a mathematical formulation for the transfer function that describes the system given its experimental frequency response function. Its primary goals are:

- Structure selection—choosing a model form that can capture the system’s behavior (e.g. equivalent-circuit, state-space or black-box polynomial models).
- Parameter estimation—determining the numerical values (resistances, capacitances, transfer-function coefficients, etc.) that best fit the data.
- Uncertainty quantification—assessing the confidence or variance in those estimates to support robust simulations and control design.

System identification has a multitude of applications from among which:

- *control* the system input in order to maintain a desired output. It is a dedicated branch of engineering called System control and it is fundamental for industrial automation and the base for the functioning of many electronic devices. I annoverate here the importance of PID controllers;

- *prediction* of the system output outside the testing input values;
- *forecast* of the system output at future time;
- *understand* the system underline physics.

The first big choice is between parametric and non-parametric models. The first step is the choice of the model between three approaches:

- white-box models, where every equation and parameter stems from first-principles physics;
- gray-box models, which embed mechanistic structure (e.g. RC networks for electrochemical cells) but tune some parameters from data;
- black-box models, which use purely data-driven forms

Choosing an appropriate modeling approach for an electrochemical system hinges on the balance between physical insight, computational effort and data availability. At one extreme, white-box models—built from first-principles PDEs of mass transport, charge conservation and reaction kinetics—offer high fidelity but demand detailed material parameters, fine spatial discretization and heavy numerical simulation. At the other, black-box techniques can fit arbitrary I/O behavior from relatively little data, yet yield little chemical or mechanistic interpretation. Grey-box models—most commonly equivalent-circuit representations in EIS—strike a practical compromise: each resistor, capacitor, constant-phase element or Warburg branch carries clear electrochemical meaning, while their numerical values are identified from measured impedance spectra. PDE-based models are used when you need predictive accuracy across wide operating ranges; employ grey-box EIS fitting for rapid characterization, diagnostics and BMS implementation; and reserve black-box methods for purely control-oriented applications where internal physical detail is secondary. For frequency-domain characterization the identification of a black-box model can be non parametric. Compute the cross- and auto-spectra of input  $u(t)$  and output  $y(t)$  (e.g. via Welch's method) or parametric using a rational function with no physical interpretation of poles/zeros. For the estimation of  $a$  and  $b$  is used one of these techniques: Sanathanan–Koerner, vector-fitting or maximum-likelihood algorithms.

## Excitation signals

This work deals with frequency-domain characterization of electrochemical systems. Compared to the step or pulse (rectangular) excitation of the time-domain characterization there are multiple excitation types for the frequency domain. The chosen perturbation signal determines which dynamics components of the system will be excited, hence visible in the identification process, how the frequency response function can be estimated and how long the experiment takes. In practical terms, one must decide the type and frequency of the excitation and the amplitude: large enough to be distinguished from noise but small enough to keep the system in its linear regime. The types of perturbation are:

- sine waves, that stimulate only one frequency at the time; for an identification experiment, sine waves are generated one after the other

generally from high to low in EIS experiments in a process called stepped sine experiment;

- swept-sine signals (or chirps) are signals in which the frequency varies continuously over time.
- multi-sine waves are the superimposition of multiple sinusoidal components of different frequency (and phase), reducing experiment time;
- pseudo-random binary sequences switches (randomly) between two levels producing flat spectral density with low power.

Sine and multi-sine excitation signals are the most used perturbation types because all the power is used to excite a specific frequency leading to higher signal to noise ratio and simplicity of interpretation of amplitude and phase characteristics, but they require more complicated hardware for the generation of pure sinusoidal forms or arbitrary waveforms. For some industrial or high scale application this is not possible and binary sequence, that require more sophisticated analysis, are instead implied.

The frequency response function is estimated from the synchronous records of the input excitation  $u(t)$  and output  $i(t)$  of the system via non-parametric function of its simplest form as:

$$H(\omega) = \frac{U(\omega)}{I(\omega)} = \frac{|U|}{|I|} e^{-j\pi\phi_u - \phi_i},$$

where  $U$  and  $I$  are the Fourier Transform of  $u(t)$  and  $i(t)$ .

## Parameters estimation

In system identification, “parameter estimation” goes beyond ordinary curve-fitting by explicitly accounting for the system’s dynamical structure and the statistical properties of its disturbances. Whereas a typical fit might simply minimize the sum of squared differences between a model’s output and data (assuming independent, identically distributed errors), identification algorithms embed a specific model form—ARX, state-space, transfer function, etc.—and often include an explicit noise model (as in ARMAX or Box–Jenkins). Methods like prediction-error minimization (a weighted least-squares that accounts for colored noise), instrumental-variable estimators (to eliminate bias when regressors correlate with disturbances), and maximum-likelihood or Bayesian approaches (to achieve statistical efficiency and uncertainty bounds) ensure that the estimated parameters are not only the “best fit” in a least-squares sense but also consistent, unbiased and accompanied by confidence measures. Regularization techniques further guard against overfitting by penalizing overly complex models. In short, system-identification parameter estimation rigorously marries the dynamic model structure with noise characterization and statistical theory—whereas normal fitting treats the model as a static curve and typically ignores these subtleties.

For these reasons, typically, parameters estimation in the system identification sense estimates noise or nonlinearities together with the transfer function.

When fitting the chosen model  $G(\omega; \theta)$  to the data, one minimizes a weighted

least-square error:

$$\min_{\theta} \sum_{\omega} w(\omega) |Z(\hat{\omega}) - G(\omega; \theta)|,$$

where  $Z(\hat{\omega})$  is the frequency response function (the hat symbol is used to denote the experimental data). Under Gaussian-noise assumptions this criterion is also the maximum-likelihood estimator. An estimator is simply a rule or formula that takes your measured data—in this case the sampled input  $u(t)$  and output  $y(t)$ —and produces an estimate of some underlying quantity you care about (e.g. a transfer function  $H$ , a parameters, or a noise PSD).

## Model selection and validation

As discussed in the previous section, the choice of the model order reflects on the degrees of freedom of the dynamic model. During the identification processes one must decide the model order, in other words the number of parameters of the transfer function or of the physical model. Too little parameters makes the model simple and fast to fit or ease to implement in control but it might loose the ability to represent certain dynamics. On the other hand a model with high order may fit noise instead of the features of the system, leading to the so-called over-parametrization. In both cases the model would not be able to generalize to new data. When we say order, we mean the actual order of the variables in the differential equations. Another problem in model selection is to verify that all the parameters are uniquely determined from the input-output measurement. In practical cases, an high order model might be needed but some parameters corresponding to lower orders might not be influencing the input-output relationship causing again over-parametrization. To address identifiability one examines the sensitivity matrix  $S$ , i.e. the Hessian of the cost function:

$$S_{ij} = \frac{\delta y(t_i; \theta)}{\delta \theta_j},$$

where  $y$  is the model linearized around the optimal parameters  $\theta_{opt}$ . If none of the columns of  $S$  can be written as combination of the others (full column rank), each parameter produces a unique variation in the output and is locally structurally identifiable. Conversely, if two columns of  $S$  are nearly collinear (scalar multiple of each other), the corresponding parameters can compensate for one another and only their combination is identifiable.

From  $S$  one builds the Fisher information or Hessian approximation  $H \approx S^T W S$  where  $W$  contains your error-weighting), and its eigenvalues indicate how tightly each parameter is constrained by the data. Small eigenvalues (or large diagonal entries in the inverse Hessian) correspond to flat valleys in the cost surface—parameters that the data cannot pin down.

To go beyond this local, linearized picture, one often employs profile-likelihood or profile-cost methods: you fix one parameter at a succession of values, re-optimize all others, and watch how the minimum cost grows. A shallow profile means the parameter is only weakly identifiable (large confidence interval), whereas a steep rise defines precise confidence bounds. Model selection and parameter identifiability check are performed in the same step of fitting, they are two sides of the same coin.

Once a model to test is selected and fitted to the data, it must be validated. The purpose is to verify that the dynamic of the system is captured and is general (valid on unseen data). At the heart of validation lies the analysis of the residuals, which are the differences between the measured outputs and the model's predictions. In a well-specified model, these residuals should behave like random noise—lacking any systematic trends, uncorrelated with past inputs, and exhibiting a flat spectrum when viewed in the frequency domain. Any remaining structure in the residuals—whether a repeating pattern in time, a peak in the spectrum, or significant coherence with the input signal—indicates that the model has failed to capture some aspect of the system's behavior. Beyond residual analysis, one typically divides data into training and validation sets (or employs cross-validation) to ensure the model generalizes to unseen conditions, and computes statistical measures such as the normalized root-mean-square error, R-squared, or information criteria (AIC/BIC) to compare competing models while penalizing excessive complexity. Monte Carlo or bootstrap techniques can further propagate measurement uncertainty through to parameter estimates, yielding robust confidence intervals for each model parameter.

## Model selection criteria

To verify and select a model among multiple options, one needs an arbitrary evaluator based on statistical principles. This section describes some common model selection criteria to identify the most appropriate model for fitting the data avoiding over- or under-parametrization. These methods are based on the concepts of balancing the quality of the fitting with the complexity of the model. The first, also called generally "goodness of fit" reflects how close the parametrized model is to the experimental data. Its value depends on the method use for the fitting. For least-square cost function minimization, the parameter is the sum of squared errors  $\chi^2$ , the coefficient of determination or the normalized root-mean-square error. The natural step is to consider the maximum likelihood estimation, a principle that bridge between fit quality and statistical inference. The maximum likelihood is the principle of choosing the parameter values that would make the observed data most plausible, or probable. Maximizing the likelihood of observing the data is mathematically equivalent to minimizing the  $\chi^2$ . More generally, MLE adapts the goodness-of-fit criterion to whatever error distribution is appropriate—so whether errors are Gaussian, Laplacian or colored, the likelihood function automatically weights residuals in a way that yields statistically efficient parameter estimates. The beauty of MLE is that, under broad conditions, it yields estimates that converge to the true values as you gather more data (consistency) and that attain the smallest possible variance (efficiency) among unbiased estimators.

Concretely, if one has  $N$  independent measurements  $y_1, \dots, y_N$  and a parametric model that predicts their joint probability density  $p(y; \theta)$ , the likelihood is

$$L(\theta) = \prod_{i=1}^N p(y_i; \theta)$$

and the log-likelihood is

$$\ll(\theta) = \log L(\theta) = \prod_{i=1}^N \log p(y_i; \theta).$$

Finally the maximum likelihood

$$\hat{\ll} = \max_{\theta} \ll(\theta).$$

The Akaike Information Criteria (AIC) was invented in 1973 from Hirotugu Akaike as approximately unbiased estimator of the expected relative Kullback–Leibler divergence<sup>1</sup> between the true data–generating distribution and the fitted model. The AIC adds a penalty factor equal to two times the number of parameter k to the negative log-likelihood, hence it favor models that minimize the information loss relative to the "truth".

$$AIC = -2l + 2k$$

The AIC is based on a much broader mathematical framework for quantifying information, uncertainty and the cost of encoding data, developed by Claude Shannon when studying the communication of words through the telegraph accounting the noise of the signal. The central quantity is the entropy of information

$$H(p) = - \sum_x p(x) \log p(x),$$

which measures the average "surprise" of samples drawn from a distribution p(x).

The AICc is a corrected method from the AIC valid when the number of samples N is small relative to the parameters k:

$$AICc = AIC + \frac{2k(k+1)}{n-k-1}$$

Closely related to the AIC there is the Bayesian information criterion (BIC) or Schwarz criterion was introduced by Gideon Schwarz in 1978 from the idea of Bayesian statistics of testing how probable is the hypothesis (in this case, a model) to be correct given the N observations.

$$BIC = -2l + k \log(n).$$

The BIC ensure to estimate a few more parameters without overfitting when more data are available. The  $\log n$  comes in fact from the idea of statistics that with more data points one can justify more parameters but each add "costs" approximately  $\log n$ .

The criterion of Minimum Description Length, developed by Rissanen in 1978 is also rooted in information theory and depending on the assumptions, gives a similar expression than BIC:

$$MDL \approx -l + \frac{k}{2} \log(n).$$

---

<sup>1</sup>In statistics, a divergence is a non-negative measure of how one probability distribution differs from another. The most widely used example is the Kullback–Leibler (KL) divergence. Other divergence families (e.g. Jensen–Shannon, Hellinger) symmetrize or generalize this idea, but in all cases a divergence provides a principled way to quantify "distance" between probability models—central to information theory, model selection and hypothesis testing.

Finally, one can use to a parametric estimator such as the cross-validation (CV) that predicts the quality of the model by repeatedly partitioning the data into "training" and "test" sets, fitting on one and evaluating on the other. It makes no asymptotic assumptions and is widely applicable to any model class. A partition is called a "fold" and the average error is:

$$CV_k = \frac{1}{k} \sum_{i=1}^k E_i,$$

with  $E_i$  any prediction error (e.g. mean squared error) on the fit when excluding the  $i$ -th fold. One can think of this criterion as "predictive" validation. AIC and BIC are usually more robust for small dataset compared to CV and faster to compute (source: Hoornweg, Victor (2018). "Chapter 9". Science: Under Submission. Hoornweg Press. ISBN 978-90-829188-0-9.)

### Identification in non-stationary case

System identification for non-stationary systems extends the classical LTI framework by explicitly accounting for parameters that drift or jump over time—as often occurs in batteries whose resistance, capacitance and diffusion coefficients change with state-of-charge, temperature or aging. Rather than assuming a single static model, one partitions the data into short, quasi-stationary intervals (via sliding-window or STFT methods) or formulates a linear-parameter-varying (LPV) model whose matrices  $A(t), B(t), C(t)$  depend on measurable "scheduling" variables (e.g. SoC). Recursive estimation algorithms—such as recursive least-squares with a forgetting factor or Kalman filters—adapt parameter estimates on the fly, balancing sensitivity to genuine drift against robustness to noise. Alternatively, adaptive subspace methods re-identify a new state-space realization at each time step, tracking evolving modes and time constants without prescribing a rigid model order in advance. These approaches yield time-stamped parameter trajectories that faithfully capture the system's evolving dynamics, enabling real-time monitoring, diagnostics and control of non-stationary electrochemical cells.

## Digital signal processing

### Digital sampling

In real world any quantity changes continuously in time. When performing an experiment, the scientist measures the values of those quantities with instrumentation at a specific point in time. Commonly, the measurement is carried out at constant intervals of time to get a time series. In modern times, measurement are carried out with electronic devices which contains component capable of sampling quantities and save the digitalized data into memory or sending to a personal computer. This processes is sampling and the electronic components that allow that in a device is called analog to digital converter or commonly ADC. The most important parameter to consider in sampling is the time interval or its reciprocal sampling frequency. To analyze the spectral content of a signal, the sampling frequency must be at least two folds the frequency of the highest oscillation components.

This is known as Nyquist-Shannon sampling theorem. Sampling below this threshold causes higher-frequency components to “fold” back into lower frequencies—a phenomenon known as aliasing—which corrupts the true spectral content of the signal. Aliasing can not only be avoided by sampling at high frequency but alternatively using an analog or digital anti-aliasing filter before the sampling stage. This could be important because sampling at high frequencies require more sophisticated and expensive devices and of course the signal will occupy a lot of virtual storage space which might make long term experiment unfeasible.

## Discrete Fourier Transform

The Fourier Transform is used for the spectral analysis of signals, that is the process of decomposing a time-domain signal into its constituent frequencies and quantifying the amplitude and often phase (or power) associated with each. One converts a signal  $x(t)$  or  $x[n]$  into  $X(\omega)$  or  $X[k]$ , revealing how its energy or variance is distributed across frequency. This frequency-domain view makes it easy to identify periodic components, resonances, noise bands and characteristic time-constants that may be hidden in the raw waveform. Since Joseph Fourier’s 1822 breakthrough showed that any periodic function can be expressed as a sum of sinusoids, the Fourier transform (FT) has become a cornerstone of signal analysis: mathematically, the continuous-time FT of a signal  $x(t)$  is defined as

$$F(\omega) = \int_{-\infty}^{\infty} x(t)e^{-j\omega t} dt,$$

and it enjoys key properties such as linearity, time- and frequency-shifting, duality, and the convolution theorem (i.e. convolution in time becomes multiplication in frequency). In practice one works with the discrete Fourier transform (DFT)

$$F(\omega) = \sum_{n=0}^{N-1} x[n]e^{-j2\pi kn/N}.$$

For its properties, the Fourier Transform can be inverted to get back a time-dependent signal from its frequency spectra. The process is called inverse Fourier Transform and it is valid also for the discrete Fourier Transform. Cooley and Tukey developed an algorithm for the efficient computation of the summation called Fast Fourier Transform (FFT). The complexity of the problem is  $O(N \log N)$  compared to the  $O(N^2)$  of the direct summation, although it requires the length of the input signal to be equal to  $2^n$  with  $n$  integer number. In real world applications of signal processing, the spectral information changes with time. A few examples are the real-time processing of music (digital equalization), human voice (speech recognition) or images (object recognition). To analyze these signals, the approach is to perform the Fourier Transform on a small part of the signal at the time, with a process called windowing. The method is called short-time Fourier Transform (STFT) and extends the classic FT to non-stationary signals by sliding a finite window  $w[n]$  along the data and computing a local DFT on each segment. Formally, for a discrete signal  $x[n]$  and window shift  $R$ :

$$X(m, k) = \sum_{n=0}^{N-1} x[n + mR] \cdot w[n] \cdot e^{-j2\pi kn/N},$$

where  $m$  indexes time frames and  $k$  frequency bins. While the short-time Fourier Transform can effectively capture the spectral context of transient processes, the accuracy of the result depends on careful design of the calculation. First, there is a time-frequency resolution trade-off, known also as Gabor uncertainty principle  $\Delta t \cdot \Delta f$  where  $\Delta t$  is the window length and  $\Delta f$  is the inverse of it. Equality is reached only by a Gaussian window, which is therefore "optimal" in the sense of joint time-frequency localization. The window length  $N$  controls the balance: a short window localizes well in time (small  $\Delta t$ ) but its Fourier transform is broad (large  $\Delta f$ ), so fast transients are captured but spectral peaks smear, while a long window gives fine frequency discrimination (small  $\Delta f$ ) at the expense of temporal precision (large  $\Delta t$ ), so you resolve closely spaced frequencies but miss rapid changes. Another important aspect is the window shape and the overlap, the latter derived by the window shift value  $R$  in the STFT definition. To produce smooth progression between following windowing, an overlap is used of 50% or 75%.

These concepts are essential for the discussion on the methods to estimate the non-stationary impedance given later in the text and they must be carefully taken into consideration depending on the characteristic frequency of evolution of the given signal.

Here, I would like to remark that the spectral analysis does not necessarily go through the calculation of the Discrete Fourier Transform. In fact, the DFT calculates amplitudes and phases for all the  $N$  frequencies equally distributed between  $-\Delta f/2$  and  $\Delta f/2$ . When one is interested in analyzing only a specific set of known frequencies can calculate the Fourier Transform of only those frequency points. In system identification, as for the calculation of the impedance when a set of known frequencies are perturbed, it is known as Goertzel filter and it requires much less mathematical operation to be conducted making it ideal for application in limited hardware.

### Spectral leakage

Spectral leakage is the effect typical in the Discrete Fourier Transform of "leaking" or "spilling" of spectral components into neighboring frequency bins, producing spurious components where the spectra baseline should be flat (or to noise level). Multiple causes produce spectral leakage. The most typical is due to a discrete signal  $x[n]$  that does not contain an integer number of periods of the oscillatory components. When the signal contains non-integer cycles, tapered windows shall be employed to mitigate the leakage. Although system identification in electrochemistry for the frequency domain employs cyclic perturbation (i.e. single sine waves or multi-sines), it will be useful in the following discussion in this text to introduce some aspects of window functions. The most known are Hanning, Hamming and Blackman functions characterised by three main properties:

- roll-off and characteristic frequency
- passband flatness
- group delay

The main characteristic is called roll-off which means "how fast" the amplitude of the original signal is attenuated. From the view of the frequency

domain, the part of the filter that attenuates the signal are called sidelobes. The characteristic frequency, also called cut-off, is the frequency at which the attenuation is  $\sqrt{2}$  ( $\approx -3$  dB) of the maximum value. Different windows function have steeper or smoother roll-off and this is important when realizing, for example, a low pass filter using the same function. Passband flatness is how uniform is the magnitude response across the main lobe (the passband) to avoid any distortion of the amplitude. It is also important, especially for the complex signals like the impedance, to evaluate also the phase shift or group delay that must be flat in the frequency region of analysis. Windows have usually a zero or very low attenuation in the middle that translates to a very well analysis of the spectral characteristics of the middle point of the signal. This is somehow translated to an "instantaneous information" even if the windows has finite length. Usually it is impossible to have optimal values for this parameters but a compromise has to be made.

Other causes of spectral leakage derive from practical hardware limitations such or user errors in the choice on the design of the experiment such as:

- asynchronization of ADC and DAC clock
- Instability of the ADC (data acquisition) or DAC (signal generator) clock;
- ADC aperture jitter adn slew-rate;
- Low resolution of the ADC compared to the oscillation amplitude might produce spurious harmonics;
- aliasing due to the choice of sampling frequency or decimation/interpolation wihtou proper filtering;

## Noise

Noise, signal-to-noise ratio (SNR) and averaging are foundational in any measurement or communication system. Noise denotes random, unwanted fluctuations superimposed on the desired signal—originating from physical sources (thermal, shot), instrumentation (quantization, clock jitter) or environment (EM interference). SNR quantifies their relative power, defined as  $\text{SNR} = \text{Psig}/\text{Pnoise}$  (often in dB:  $10 \cdot \log_{10} \text{Psig}/\text{Pnoise}$ ), and dictates how reliably one can detect or process the signal. Averaging is the primary tool for improving SNR: by repeating the same measurement or subdividing a long record into M independent segments, uncorrelated noise averages toward zero while the coherent signal adds constructively. The net SNR gain scales as  $\sqrt{M}$  (a 3 dB increase per doubling of M). In the time domain this is ensemble or block averaging; in the frequency domain it appears as spectral averaging or Welch's method, where overlapping, windowed segments are FFT'd and their periodograms averaged. Care must be taken to ensure segment independence (avoid drift or decorrelation) and choose appropriate windowing and overlap to balance variance reduction, resolution and computational cost. Noise is considered an incoherent source, that is, each noise sample has random phase and amplitude that is uncorrelated from one time frame to the next (random). Any other physical effect (ex.

electrochemical noise) and response to any perturbation is considered a coherent signal. The averaging can be alternatively obtained increasing the acquisition time of the periodic signal or the length of the window. In fact narrowing the spectral bin's bandwidth reduces linearly the noise power in it (i.e. doubling the signal length,  $\Delta f$  halves and so the power in each bin while the coherent signal amplitude in the bin does not change. or simply increasing the perturbation amplitude when possible.

## Wavelets method

Wavelet analysis decomposes a signal into shifted and scaled versions of a short, zero-mean “mother” wavelet, yielding a time-scale (or time-frequency) map that can capture both slow and fast features with variable resolution. Unlike the STFT’s fixed window, wavelets automatically use wide windows at low frequencies (for fine frequency resolution) and narrow windows at high frequencies (for fine time resolution), making them ideal for detecting transients, abrupt changes or multi-scale phenomena. They are widely used in vibration analysis, denoising and feature extraction where signal characteristics evolve over time. For a system driven by a strictly fixed-frequency perturbation, the benefit of wavelets is limited—standard Fourier or narrow-band filtering already isolates the tone most efficiently—though wavelets can still reveal subtle non-stationarities or harmonic distortions around that frequency.

## Filters

A filter in signal processing is a system that selectively modifies an input signal’s amplitude and/or phase as a function of frequency. Fundamentally, one describes a filter by its impulse response  $h(t)$  (continuous-time) or  $h[n]$  (discrete-time), and equivalently by its frequency response  $H(\omega)$  or  $H(e^{j\omega})$ , which shows how each spectral component is scaled and shifted in phase. Filters may be analog—operating continuously on voltages or currents—or digital—processing sampled data—and they can be linear (obeying superposition) or nonlinear (introducing harmonics). Additional key properties include time-invariance, where the filter’s behavior does not change over time, and causality, which requires outputs to depend only on present and past inputs. By their effect on frequency content, filters are classified as low-pass (passing frequencies below a cutoff  $f_c$ ), high-pass (passing frequencies above  $f_c$ ), band-pass (passing a band between two cutoffs), or band-stop/notch (rejecting a specific band). In the analog domain, common design prototypes are Butterworth filters (maximally flat passband), Chebyshev filters (steep transition at the cost of ripple), and elliptic filters (sharpest transition for given ripple). In digital implementations, infinite impulse response (IIR) filters use feedback to achieve steep responses with few coefficients, while finite impulse response (FIR) filters use only feedforward terms and can be designed for exactly linear phase—ensuring constant group delay, which is the derivative of the phase response with respect to frequency and measures how different spectral components are time-aligned. Performance metrics include passband ripple (amplitude variation within the passband), stopband attenuation (suppression of unwanted bands), transition bandwidth (width of the roll-off region), group delay variation, and

computational complexity (operations per sample). Filters are indispensable for noise reduction, anti-aliasing before sampling, channel equalization and signal extraction, enabling precise control over signal fidelity, latency and resource utilization.

## Removal of trends

Baseline or trend removal, often called detrending, is the process of eliminating slow-varying offsets or drifts from a signal so that its remaining fluctuations can be treated as (approximately) zero-mean and stationary. Undesired trends can arise from sensor drift, temperature changes, power-supply fluctuations or low-frequency interference, and if left uncorrected they bias spectral estimates (manifesting as excessive low-frequency power or leakage) and corrupt time-domain analyses. Common detrending techniques include subtracting the signal's long-term mean or a low-order polynomial fit, applying a high-pass filter with a cutoff below the band of interest (using a linear-phase FIR to avoid phase distortion), or employing moving-average/median filters to track and remove slow baseline wander. More advanced methods—such as empirical mode decomposition (EMD) or wavelet-based multiscale filtering—can adaptively separate baseline components from overlapping signal features. In all cases, one must choose parameters (filter cutoff, polynomial order, window length) so that genuine signal dynamics are preserved while the unwanted trend is effectively suppressed.

In the analysis of signals through Fourier Analysis, the removal of trends mitigate an effect called Gibbs phenomenon that is the presence of an infinite series of harmonics produced by sharp transition in the signals caused by its dynamic (drift) as well as experimental, coming from the digitization process (an artifact known as ringing).

## Signal synthesis

To perform certain experiments, a scientist might be interested to perturb the system with non-constant signals like pulses, ramps, sinuses or arbitrary shapes. This requires to design a signal from mathematical functions and usually require a computer to define it. The desired waveform is generated from the instrumentation using an electronic component capable of transforming a user-defined digital waveform to a continuous analog signal. The process is called digital to analog conversion and the electronic component capable of it the digital to analog converter or simply DAC. There are several methods of implementing a digital to analog converter on hardware with different complexity and properties, the most simple is the direct digital synthesis method.

### Direct Digital Synthesis

This method relies on the 'look-up table' method in which the desired waveform is stored as a table of pairs value-time and at constant time interval the value is read from the table and converted to analog value.

### Further resources

The recommended resource for learning about signal processing is the book "Understanding Digital Signal Processing" by R.G. Lyon and the series of publications from D.A. Lyon "The Discrete Fourier Transform".

# 5

## Dynamic Electrochemical Impedance spectroscopy: state of the art

[Da riferire] Impedance is defined as the transfer function between current input and voltage output of an electrical circuit that belong to the class of linear and time invariant system. As such the system must be stationary during the measurement, and the input-output relationship must be linear and causal, i.e. the complex-valued transfer function follows the Kramer-Kroning relationship. There are scenarios where the system is not stationary nor linear, for example because of inherent instability, while studying non-equilibrium reactions or while operating electrochemical devices for practical applications. In these setting it is still possible to obtain, both theoretically and experimentally, an "instantaneous" impedance. The idea was explored during the 70's from Creason, Smith, Bond and colleagues in a series of paper on the admittance of red-ox couples under constant or sweeping perturbations [?][?][?][?] using a multi-sine waveform as perturbation to excite specific frequencies in the electrochemical system and use the Short Time Fast Fourier Transform (STFFT) to compute amplitude and phase of voltage and current and obtain the impedance from their ratio. In the 90's, with the advent of faster computers, this methodology gained a new interest and development thanks to Popkirov, Darocicki, Házì and their colleagues [?][?][?][?][?]. During the first years of this century, the method was refined from both experimental [?][?][?] and theoretical [?] [?] sides from Sacci, Harrington, Slepški and colleagues and the name dynamic electrochemical impedance spectroscopy (DEIS) started to take over. In 2012 Breugelmans, Hubin and their colleagues extended the new contribution of Pintelon and Schoukens on the identification of non-stationary systems and the Best Linear Approximation to electrochemical systems, introducing an approach based again on the DFT of voltage and current signals followed by regression of the frequency spectra to extract, impedance, non-linearity, non-stationarities and noise; the method took the name of ORP-EIS or operando EIS [?]. These concepts were recently covered in a comprehensive review paper[?]. In parallel, also La Mantia and Battistel [?] introduced a method based on DFT and filtering for voltage and current signals to estimate the impedance at low frequency, in a range in which the standard

STFFT method is biased by the drift. As multi-sine perturbation, several waveforms were used, such as pseudo-random sequences, ternary binary sequences, chirps[?], sin function or pulses, as well as pseudo-log distributed multi-sine.

## Part II

# Methodologies



# 6

## Acquisition of non-stationary impedance

### Contents

---

|   |    |
|---|----|
| Multi-frequency data acquisition . . . . .                                  | 49 |
| Automation of the acquisition for batteries . . . . .                       | 50 |
| Automatic calculation of the impedance . . . . .                            | 53 |
| DEIStools: a Python application for dynamic impedance . . . . .             | 54 |
| Multi-sine design . . . . .   | 55 |
| Impedance estimation . . . . .  | 59 |
| Old part . . . . .  | 60 |
| Multi-sine design . . . . .   | 61 |
| Connecting cells in three-electrode configuration . . . . .                 | 63 |
| Electrochemical devices . . . . .   | 63 |
| Connecting the device and acquiring the signals: set-up version 1 . . . . . | 64 |
| Automatic cycling with . . . . .  | 64 |

---

### Multi-frequency data acquisition

The estimation of the impedance require the sampling of input and output signals from the system when an excitation signal is applied. For electrochemical systems, one uses an electrochemical workstation that contain all the hardware necessary to impose a desired voltage or current to the cell. In this work we exploit the possibility of an electrochemical workstation to recieve external signals and output the analog signals of voltage and current. This features is available for different brands, in my work I used a BioLogic device. This possibility has two advantages: generate an excitation signal of arbitrary complexity provided by dedicated high-end generator, and acquire the cell signals at very high frequency with dedicated device. This possibilities are not available using the softwar eprovided by the manifacturers. Usually no arbitrary signals can be used or they are very limited in the number of points and generation frequency, and secondly the maximum sampling frequency is low (5kHz at best). Fruthermore data can not be used for online caluclation using computation languages like Python. On the other hand the use of commercial electrochemical worksta-

tion lifts us from the work to develop custom electronic control suitable for high frequency and small currents.

## Description of the set-up

For this work we assembled multiple set-ups using BioLogic electrochemical workstations, Keysight waveform generator and PicoTech PicoScope acquisition devices. The components are connected together using the auxiliary input-output port of the workstation. The waveform generator to the input (that superimpose the signals through an analog circuit) and the scope receives the voltage and current signals for the synchronous sampling. The series and the model might vary experiment by experiment, therefore I will report the exact devices in the next part of the thesis where the results of discussion of multiple application of DEIS are reported. The brand, though, remain the same as well as the operating principles and software for their control that is the topic of the current chapter.

BioLogic workstations have for each channel an auxiliary 9-pin port for the input and output of analog signals. For the purpose of this project I was interested in only three: Input (Auxiliary In2), voltage monitor and current monitor. The company supplies adapters for the 9-pin to BNC connectors but for me was more practical to just build them myself. A reference for the construction is available in the appendix.

Appendix: Each channel of BioLogic workstation (not valid for cycler) has a 9-pin port adibits for input and output for the connection of external devices. The manual provides all the details on the pins positioning such that one can build their own cable. As material we gathered a 9-pin connector, BNC connector and coaxial cable. As instrumentation was needed only a solder with tin soldering wire and sharp scissors to cut and unsking the cable.

I needed to access the pins X, Y and Z, as in figure XX. I then used 3 cables, soldering the core to the proper pin and the shell together to the ground. Finally I connected the other end of the cable to the BNC connector and close the encapsulation of the 9-pin connector after testing all the terminal points with a multimeter. Figure XX shows the soldering on the 9-pin connector.

End appendix

## Automation of the acquisition for batteries

### Problem statement

In the simplest scenario, the acquisition of multi-frequency signals with the set-up explained above, requires only to use a programming language to manage the streaming of the signals from the oscilloscope to the computer and store them. The previous publication of the group exactly followed this idea. Specifically a MATLAB script was used (Github Battistell?). The MATLAB script was adapted from the examples provided by the manufacturer. For my project I made Python implementation beyond the simple script defining a practical object (a library) for a much compact code. The

details of the Python implementation, and the design behind it are given in the Appendix. The potentiostat is used only for the electric control of the cell while not applying any perturbation (0V chronoamperometry or 0A chronopotentiometry) while the waveform generator provides the multi-frequency small excitation as well as the quasi-cyclic voltammetry pattern. The arbitrary waveforms are loaded manually to the device via a .arb file transferred via USB drive from the computer. How the .arb file is build? This approach was the one I used for the first two applications (topic of the third and final part of the thesis) of the dynamic impedance for energy storage, also published as peer-review articles.

For the goal of the thesis of acquiring the dynamic impedance during the CCCV cycling of a battery the previously described approach is not enough. Two problems arise: the first is the huge amount of data streamed from the device to the computer to be saved into the RAM, limited to a few GB, and secondly the need to change the waveform for the excitation during constant current (chronopotentiometry) or constant voltage (chronoamperometry) steps. To overcome this problem and automation routine is needed, but before going into it I shall unpack the two issues one at the time. Regarding the management of the streamed signals the problem is to sample for a long time, in the scale of weeks or months, while acquiring at high frequency. Let's say that one chooses a moderate sampling frequency of 50kHz while sampling a system excited with a maximum frequency of 10kHz, it means 50kSa per second are stored, equivalent to 355 MSa per hour that we can translate to about 4.3 GB per channel per hour. Even using systems with huge memory, only a few hours of acquisition would be possible, not weeks. The alternative is to store into the hard drive the sampled signals before the RAM is filled up and without loss. One can decide a fixed amount of points for the storage or execute the saving at the end of a technique (chronopotentiometry or chronoamperometry). Before commenting which of the two approaches are more suitable for the project, I must discuss the second of the issues mentioned above. The multisine, its design will be thoroughly explained in a later chapter, is not just characterized by the frequency content but also its absolute and the relative amplitude of the sinusoidal components. The absolute amplitude is important for making the experiment itself, in the sense that for a chronoamperometry experiment the amplitude in volt of the excitation is the exact value applied on the cell. For a chronopotentiometry experiment instead, the signal in volt produced by the generator is converted to current passing through the measurement resistor. It is clear that the amplitude of the excitation must be changed when the running technique is a chronoamperometry or a chronopotentiometry. In addition, the relative amplitudes of the single sinusoidal components must be optimized (instead of being all equal) to the system. The method I prefer to use is to measure the impedance once experimentally and deduce its module to decide the relative amplitude of each sinusoidal component such that the output has a certain amplitude for a good signal to noise ratio. In other words, if one follows the formula

$$V_{output}(\omega_i) = |Z_{exp}(\omega_i)| \times I_{input}(\omega_i)$$

can deduce the necessary current to obtain a certain oscillation in volt for each sinusoidal component for the system under study. It is fundamental to note that the relative amplitude for a chronoamperometry experiment

would be the reciprocal of the one for a chronopotentiometry technique to maintain the same signal to noise ratio. For this reason one should generate two different multisine with the two series of relative amplitude and then generate them during the correct technique using a suitable total multisine amplitude to perturb the system enough. It is indeed an art that require trial and error and a lot of time spent on looking at the peaks of the Discrete Fourier Transform for input and output.

## Software solution

The work around for both the questions seems to be an automatic system that can, during the execution of the experiment, change the excitation in the waveform generator remotely accordingly to the technique in execution and save the signals from the scope when a technique is finished. This simple idea hides the main technical complication of this work: having a computer program that works with the generator and scope, and also monitors the execution of the sequence of techniques that forms an CCCV experiment. The software that BioLogic provides EC-Lab is not meant for software automation but can only send trigger analog signals to other device. It would solve the communication with the generator but not with the streaming software of the scope. Luckily, BioLogic do provide the API for the control of the instruments in multiple programming languages, including Python. The downside is that the API is not officially supported and it is very primitive. Especially the data has to be streamed from the machine and converted manually in the user code, similarly to the code for the scope. So I decided to write a library for the control of the BioLogic workstation in Python with some specific requirements:

- work in multi-threaded fashion to allow multiple channels from the same machine to work independently and each of them to communicate to the device without blocking execution;
- allow easy integration with other libraries to create flexible set-up;
- allow to construct the same experiment structure, i.e. sequence of techniques, of EC-Lab to compare results from both.
- implement software limits for voltage and current that consider the average value of the quantity to compensate the oscillation of the multisine.

## Design principle

The automation of the instruments compatible with multi-threading uses the design pattern of the worker object. A worker object executes operation inside a *while True* block on a dedicated thread, and terminates with a pause of 1 second or less (with the sleep command) during which the main thread is allowed to execute the code of another worker object. The multi-threading standard library of Python is capable of automatically manage all the objects without user indication in the code (compare to the other library like `asyncio`).

Worker object has a property with the name *running* that can be used

from other object to check their status. This idea is at the base of all the library used to synchronize the electrochemical workstation, waveform generator and scope. It is important to notice that given the modularity of the approach, it is possible to use different hardware to perform the experiment in the same manner, given the interface is similar (i.e. it has the same name of the methods that return the same objects).

Multi-threaded objects can share memory in the form of memory buffer to avoid the well known problem of concurrency. Since all the mathematical operation in the Python code uses the library Numpy and its array type for storing the data it made sense to me to have a circular buffer with the type of Numpy array to work with. Unfortunately the only existing implementation on public repositories (`NpCircularBuffer`) was not updated to the current version of Numpy, therefore I made and published my own simple implementation of a one-dimensional circular buffer with the name `nplibuffer` and used it across the library needed for this project.

## Automatic calculation of the impedance

The automation of the acquisition allow to record signals for battery cycling and mixed techniques but still has on other limitation regarding the data size. When considering the impedance of a battery, the desired frequency range might differ depending on the chemistry. In some cases 100Hz could be the maximum needed frequency for bigger batteries in pouch format, but when going to smaller sizes and laboratory scales it is generally needed to probe until higher frequency, up to 1MHz where the inductance of the connections cell to instrument became the predominant response (here I am not including solid state electrolytes that might need frequencies up to 7 MHz). For the application presented later, I determined an highest frequency of excitation of 100kHz (maintaining the lowest to 10mHz) that requires a sampling frequency of 500kHz or 1MHz (both worked in my tests using the following method, although according to the Nyquist limit 250kHz is enough). Such an high sampling rate would store very big data in the hard drive that soon will require expansion after weeks of measurement and experiment repetition. Furthermore the highest frequency would be repeated for a huge amount of times while we are actually interested of sampling long times to identify the lowest frequency. The upper part of the frequency band can be considered in a quasi-stationary condition and therefore doesn't require mathematical techniques to decouple with the main drift. The method used here follows this idea: calculating the impedance of the upper part of the frequency band (ex. above 10Hz) using the FFT-EIS method, apply a low-pass filter to remove these same frequencies and decimate the signal to a much lower rate (ex. 50Hz) to be stored for later estimation of the time-varying impedance (ex. with DMFA). Finally, the total spectra is reconstructed concatenating the impedance estimated with the two methods.

This is the first contribution of this work: measuring broad-band non-stationary impedance continuously during the cycling of the battery.

## DEIStools: a Python application for dynamic impedance

The previous sections introduced the ideas of automating the multi-sine switch, save acquired signals periodically and process the signals online. These tasks are performed for each of the active channel of a multichannel electrochemical workstation. The heart of the operation is a library with the name DEIStools that contains everything need to prepare the experiment, execute it, analyses the data and visualize the results. It builds upon the separate libraries that interface with the three devices of the set-up using the same *worker object* building block discussed before. DEIStools provides the object DEISchannel that automate the measurement. The user provide to the class initialization the objects for the Channel of the electrochemical workstation, the generator and the scope, already connected and initialized. For the online processing of the signals, another object is provided by DEIStools called PicoCalculator, that has the name suggest, takes the PicoScope object and extend its functionality to perform the calculations on a block of data of a specific length (one can think of the concept of windowing of signal processing). To continue into the idea of modularity, the calculation is performed by the object BlockCalculator that receives as arguments of its method a numerically converted copy of the signals (from the ADC values), and performs with them the FFT-EIS and downsampling . With this design, the processing can be personalized for new experiment without touching the rest of the code for automation. The calculation is, as well, performed on a dedicated thread while the PicoScope object keep receiving data from the device without interruption.

Finally, the sequence of multisine waveforms, their amplitude, sampling frequency and when to turn them on in the sequence of the experiment is also managed by a convenient object MultisineWave that the user passes to DEISchannel. The modularity is provided by the software design pattern of dependency injection. The object Channel of pyeclab, for the control of a workstation channel accept as attribute a function that is always execute at the end of a technique, that, for the case of DEISchannel, executes the saving of the downsampled signals and updates the multisine.

### Software limits

When a multisine is applied on top of the drift, it is difficult to determine when to stop the galvanostatic experiment. Generally batteries are cycled between an upper and lower voltage limit and the constant voltage step of the CCCV terminated on a lower limit for the current. The easiest approach is to add to the desired limit the amplitude of the oscillation, but this is not always known. In my approach, I implemented two options for average limits. One is included in the DEISchannel object and computes the average over a user-selected number of points from the sampling of the workstation (note: not the scope, so the signal is likely to contain strong aliasing). The other is performed by the PicoCalculator object that uses the value of the zero-frequency bin in the DFT already calculated for the processing of the data, sparing any further computation. In both cases, the user can specify as many software limits as desired, using the proper syntax.

## Multi-sine design

It is now time to dive into the details of the computer generation of multi-sine signals. It was already introduced that a multi-sine is the sum of N sinusoidal waves as in:

$$\sum_{i=1}^N A_i \sin(j2\pi ft + \phi_i)$$

where t is a vector of time with equally spaced units of  $f_{sampling}^{-1}$ . This creates the look-up table for the generator.

### Frequencies selection

The frequencies f must be chosen in a way that one period of the whole multi-sine contains integer numbers of oscillation to ovoid spectral leakage. The period is then defined by one oscillation of the sinus with lowest frequency  $T = \frac{1}{f_{min}}$ . Every other frequency i-th must satisfy the condition  $f_i = k \times f_{min}$ , where k is an integer. In this work we generate the desired frequencies from an harmonic series of integer to insure the above condition and the possibility to re-use the sequence for multi-sine with different  $f_{min}$ . With the term harmonic sequence I refer to  $h_i = \frac{f_i}{f_{min}}$ ; such that it always starts from 1. The sequence is generated as a logarithmic distribution with a number of point per decade around eight. Lower values gives spares spectra while high values give a denser one. Denser spectra are more beneficial for the data regression having more points to cast in the cost function, but the power of the signal increases. Eight points seems to me the sweet spots, according to my experience.

### Amplitude optimization

In a previous section, I introduced the idea of adapting the relative amplitudes of the sinusoidal components to obtain the best signal-to-noise ratio. When the amplitudes are all the same, it is said to have a "flat" multi-sine. To question is: how to decide the amplitudes? It can be achieved via analytical formulas or experimental extrapolation. The first case was used in Battistel and Hellmanns, with opposite results, making the amplitudes drop logarithmically with the increase of the frequency. In my work, I measured the non-stationary impedance for many different chemistry and geometries obtaining quite different results in sense of the module of the impedance. Hence, I prefer the approach of choosing the amplitudes based on previous experiment. One can just measure a classic stepped-sine impedance with any electrochemical workstation and use its module to calculate the desired input amplitude. Alternatively, and more effective for energy storage systems, is to measure the non-stationary impedance first using a flat multi-sine and then extract from the, often noisy, data the average value and use again its module.

## Phase optimization

When working with non-linear system, the process of identification should be carried with small excitation around the stationary point. Multi-sine waveforms can often time have large peak to peak total amplitude after optimizing the relative amplitudes derives by the superimposition of multiple sinusoidal component at the value of their peak. In most cases though, it can be reduced acting on the phase of each sinusoidal component in the total multisine. The quantity one is interested to reduce is the *crest factor* (CF) defined as

$$CF = \frac{|x_{max}|}{x_{rms}}$$

where  $x_{rms}$  is the root-mean-square and consequently the peak-to-average power factor (PAPR) equal to the square of the crest factor. The crest factor of a pure sinusoidal wave is  $\sqrt{2}$  that serves as a lower ideal boundary (it is matched only by a chirp waveform, a square wave though as a CF of 1).

The crest factor minimization consist of solving the optimization problem

$$\min_{\theta}$$

Multiple approaches has been proposed in the field and their characteristic is a trade-off between speed and accuracy (find the absolute minimum). The right method strongly depends on the type of problem and on the following characteristics: distribution of frequency (logarithmic or linear), number of points per decades, number of frequencies in the waveform and relative amplitude (flat, linear, logarithmic, arbitrary).

The first to deal with the problem was Schroeder in 1990 whom proposed the analytical formula that carries his name:

$$\varphi_m = \varphi_0 - 2\pi \sum_{n=0}^{m-1} (m-n) \frac{|a_m|^2}{\sum_{k=0}^{M-1} |a_k|^2}.$$

Since it is fast to calculate, it is often used as both reference value and initial parameters for a following iterative optimization. Newman and Ojarand took the work forward with analytical formulas but without significant advantages.

As an alternative, randomization of the phases offers an equal or better crest factor but the computational time increases significantly with the number of frequencies.

Iterative algorithms achieve much better results. They belong to two families. One is based on the "clipping" method of the DFT peaks of the multi sine until the crest factor reaches a constant value. The other consist in a mathematical optimization using metaheuristic approaches that perform better than derivative methods for such big parameters space (ex simulated annealing and genetic algorithm).

Recently Kallel et al. proposed a mixed method, though it gives better results than the analytical formula for small multisine of 3-4 decades.

In this work, the iterative-stochastic optimization was used in all the experiments presented later, although not the optimal it gives a sufficiently low CF for the explorative stage of this work.

## Multi-sine splitting

Waveform generators consist of electronic circuits made around a digital-to-analog converter (DAC). An integrated modern DAC chip has a buffer memory in which the waveform values are written and during the generation such memory is read in loop. Commercial devices have a buffer memory consisting of 12 to 32 kSa that is quite small for the excitations used in batteries that might span 6-7 decades (at least for the laboratory scale). A practical solution (used for example for the playback of audio files in any electronic device) is called direct digital synthesis (DDS) that creates a direct communication between a DAC and a micro-controller with sufficient memory. This option require to be proficient in the programming and setting of micro-controller, specifically synchronizing the parts to the same clock. In our laboratory we use instead a dedicated bench-top Arbitrary Waveform Generator (AWG) with two channels each with 64MSa; a huge upgrade to conventional integrated DACs. This amount of memory allow multi-sine waveforms containing at least 6 decades. It is, in fact, the standard device use in the set-ups for dynamic impedance available in the laboratory. Indeed, most of the experiments described later use one channel of the generator for the multi-sine perturbation.

To study batteries, though, my desire was to have seven or more decades in the multi-sine and being able to switch between two waveforms optimized specifically for a chronopotentiometry and a chronoamperometry. The solution I came up with is to divide a multi-sine waveform into two waveforms and use the ability of the generator to sum the signals of the two channels ("dual channel mode") at output. The two separate waves are much 'shorter' in 'length of samples' and allow to fit two types of multisines in the memory of the device. Let's consider a seven-decade multisine waveform from 10mHz to 100kHz, generated at 1MHz (the higher the frequency, the lower is the leakage that will be brought into the FFT of the signal. Using 10 times the value of the maximum frequency is giving us good results; some advice even to use 100 times. It might be also depending on the method the device uses for generation. Keysight devices have a proprietary 'TrueForm' technology to reduce jitter that might help with limiting the spectral leakage in the final signal). Generating it in one waveform correspond to 100 MSa (obtained as  $period \times f_{gen}$ ). Deviding (or splitting) the wave at the middle frequency of 100Hz creates two waves: one from 10mHz to, around, 100Hz (the frequency before in the list) generated at 1000Hz of length 100kSa and a second one from exactly 100Hz to 100kHz generated a 1mHz that, chosing a period of 1s, leads to a waveform of 100kSa. The two will take up only 200kSa of the generator memory to produce the same excitation.

In the example I used two arbitrary parameters: the 100Hz boundary frequency and the 1s period of the high band waveform. For my case 100Hz sits in the middle so this might be adjusted case by case with the same ra-

tionale. Regarding the period of the second wave, one might think of using 0.01 second to have one exact period of the lowest frequency. One must now consider that the frequencies of the two waves must follow the same rules described before to avoid intermodulation and such, being made from a sequence of harmonics. Logarithmic sequences chosen for intermodulation tend to be sparser on the low frequency part and denser later. If for both waveform one generates the frequencies start from the harmonic of 1, the measured impedance spectra would have a sparser points distribution in the decade from 100Hz and 1kHz where the high band multi-sine waveform starts. To get a uniform distribution of points, I generated the frequencies starting from 1 Hz and discarded the points until 100Hz (not included), since they are already present in the low band waveform. Then, the period of the waveform must be of 1Hz otherwise there will be spectral leakage in the final excitation (note that the frequencies are all integer multiples of 1Hz). The sum of the two smaller waveforms generated with this method have the exact distribution of a single-generated wave. Figure 6.1 shows the density of points when restarting the multisine from 100Hz, from 10 Hz and discarding the first decade and 1 Hz and discarding the first two decades. To summarize, for a CCCV experiment for batteries, on channel of the

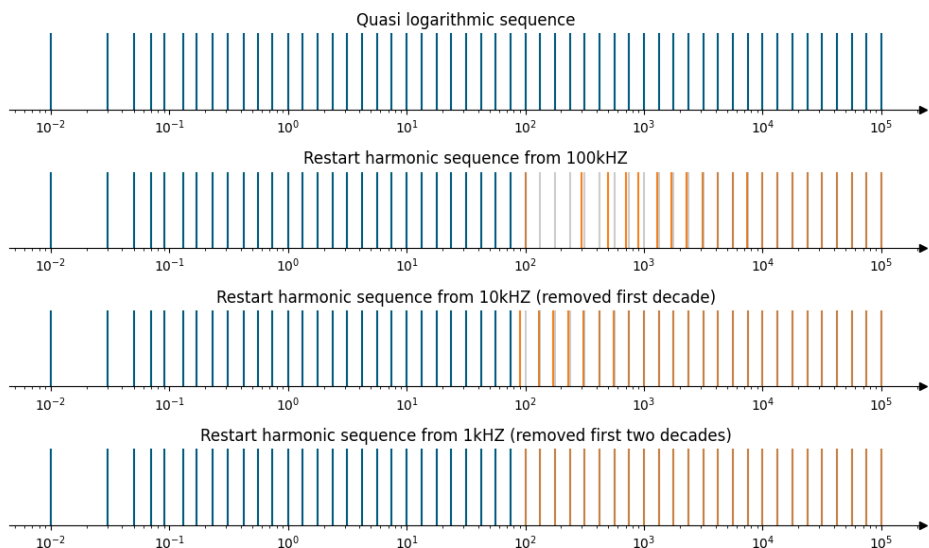


Figure 6.1: Enter Caption

generator would have loaded in memory two low band multisine waves, one optimized for chronoamperometry and the other from chronopotentiometry, and the other channel have loaded the two optimized high band multisine waves.

The automatic switch of the multisine during electrochemical experiments as described before can still be done by DEISchannel for the case of combined multisine waves passing during initialization the object MultisineWaveCombined, also provided in the package TrueFormAWG.

## Software

To streamline the design of multisines I created a Python library also for it, with the name Multisine. It provides the object Multisine that gen-

erates multisine, optionally optimize phases for minimal crest factor though iterative randomization and provides tools for visual spectral analysis. It is available as open source software at [XXX.github](https://XXX.github)

## Impedance estimation

In the experimental works presented in this thesis, we estimated the impedance using the methods of the sliding short-time Fourier transform and dynamic multifrequency analysis; the first only during the online signal processing. The STFFT method has not much tuning. The only user parameters are the length of the window and the windowing function type. The length is dictated by the resolution that one wants to achieve, so on the lowest frequency component of the excitation. The windowing function instead alters the input and output signals time series to put more or less importance to the central part of the signal rather than the borders (makes the impedance confined in time at the price of spectral power) to obtain the instantaneous impedance at the middle points. For the experiment presented here, I assumed that being the drift of the system much slower than the perturbation, the impedance would not vary much and no windowing function is necessary. For the Dynamic Multi-Frequency Analysis, one needs to chose a filter function with care. Here we used the symmetric Fermi-Dirac delta with bandwidth of 0.01 Hz and an order of 8. A previous publication of the group showed the effect of these two parameters on the final result. The most important is the bandwidth because it reflects on the number of spectra estimated and their separation in time. Battistel and al. showed in XX the shape of the filter function when trasnformed to the time domain and it is similar to a sinc function for its main lobe and small oscillation asymptotically to zero. The dynamic multifrequency analysis performs a multiplication in the frequency domain of the filter with the fourier spectra of the signal around one frequency, that correspond to a convolution of the time domain. Hence the time-domain transformed filter as a function shifted in time by a quantity equal to the reciprocal of the bandwidth. The windows should not be shorter than the period of the multisine and furthermore one should put care in the oscillating lobes that could bias the impedance estimation, as shown in Chukwu.

In both methods, one can strongly reduce the zero-frequency skirt in the Fourier space and the Gibbs effect by removing the baseline for current and voltage signals. I chose to use just a simple baseline removing because other classical methods did not work for me. Typically one can use sliding window averaging, spline or polynomial fitting or gaussian process regression to name the main one. In my experience non of these methods could effectively decouple the trend and the first few frequencies of the multisine that are overlapping. A complete Python library can be used to test these and more trend removal techniques, it is called Wotan. Hellemans and al. developed a method for de-trending signals with low frequency containing multi-sine but there is no available Python implementation to try out and the functional analysis used in the official is above my mathematical skills to implementing it myself.

## Old part

The estimation of the time-varying impedance require the system to be perturbed with a multi-sine waveform and record input and output synchronously. Most commercial potentiostats-galvanostats do not have the implementation for user-defined arbitrary waveform on the computer user interface to be transferred on the instrument hardware and when a workaround is possible (i.e. ...) the number of points of the multi-sine and the maximum frequency are limited. Usually the buffer memory for the digital-to-analog converter of FPGA boards is a value between 12 kSa and 32 kSa according to my experience browsing manufacturers catalogs, which translates to a multi-sine of ??? decades. Furthermore the maximum frequency of sampling, which defines the maximum recordable tone according to the Nyquist-Shannon theorem, is quite limited due to the difficulty of transferring big amount of data from the instrument to the computer. The maximum sampling frequency for a premium device might be in the order of 50 kHz. For most electrochemical systems the impedance is informative over 5 or more decades and to frequency up to 1MHz. On the other hand, commercial potentiostats-galvanostats have high precision electronics, with tested circuit boards that allow very small and high current and voltage ranges. The approach used in this work is to integrate a commercial arbitrary waveform generator and a high performance signal acquisition device to a potentiostat/galvanostat exploiting its input and output ports and avoiding the need of designing a high power circuit from scratch. In a nutshell, the set-up we used is composed of an arbitrary waveform generator which applies a custom waveform that define the experiment on the potentiostat though an auxiliary imput. The signal from the cell is recorded on the computer by the digital acquisition device though the auxiliary current and voltage ouput of the potentiostat which sends directly the anaolg signal of the cell. The data are later processed on the computer using custom software. In the following the parts of the set-up will be better explained, as well as the connection between the devices.



Model 33520B



Model 33522B

## Arbitrary waveform generator

As arbitrary waveform generators we have chosen the TrueForm 33500B series because of its elevate digital-to-analog converter memory buffer. Two models has been used, the 33520B and 33522B which differs only in the value of buffer memory, the first of 16MSa and the second of 64MSa, both per channel. The other important characteristic of these devices are

- high frequency generation capability of 20MHz, much higher then the electrochemical upper response limit (usully below 1MHz),
- two distinct channels with own memory and the possibility to store multiple waveforms,
- possibility to sum the waveform in the two channels (and output the total on channel 1),
- imrpoved signal integrity thanks to high generation fidelity with 0.03% of harmonic distortion, a jitter as low as 1 ps and proprietary *Trueform* generation technology compared to the Direct Digital Synthesis

Figure 6.2: Keysight Trueform arbitrary waveform generator units from the series 33500.

method; all contributes to reduce any source of intermodulation in the multisine.

(more on that <https://www.youtube.com/watch?v=HLPoSiorh30>)

Further details are reported in the witepapers supplied by the company Keysight though their website.

The user can set the parameters using the convenient front panel of the device, as shown in Figure 6.2 or sending commands via USB or Ethernet connection. The instrument can communicate with a computer through SCPI (Standard Commands for Programmable Instruments) language. I developed a small but convenient Python module to communicate with the instrument using the PyVISA package, Python implementation of VISA (Virtual Instrument Software Architecture). The module is available on my GitHub page (<https://github.com/federicosarpioni/TrueFormAWG>). The manufacturer also provides a collection of stand-alone software for the control of the instruments, the design of waveforms and automation of electrical tests, that I did not used for this work. An exception is the software Keysight connect to verify the connection with the instrument through USB or Ethernet sub-network and get their addresses for establishing the connection with the dedicated Python library mentioned before.

## Multi-sine design

### Running the multi-sine in the waveform generator

The waveform can be transferred via USB drive accessing the front panel or via SCPI communication.

### Digital acquisition device

The acquisition stage of the set-up must satisfy two requirements:

- Sampling at frequency of the order of MHz,
- Sample very long signals of hundreds of thousands of points.

Many solutions are available on the market to easily achieve these goals. They mainly fold into two categories base on their connection: USB or PCI. For this work we chose to use a USB device which satisfies all the requirements while being relatively inexpensive. USB devices are practical and portable and it is possible to connect many of them on the same computer. The devices chosen are from the PicoScope digital computer oscilloscope from Pico Technology. The devices can interface with a computer through the proprietary software PicoScope Software or the feature-rich software development kit available in multiple programming languages directly from the manufacturer GitHub page (<https://github.com/picotech>). Pico Technologies sells different series of devices with different capabilities. In this work we used

- PicoScope 4824A (4000A series) with 8 channels and a resolution of 12bit,
- PicoScope 4262 (4000 series) with 2 channels and a resolution of 16bit,

- PicoScope 5442D (5000 series) with 4 channels and a resolution of 16-15-14 or lower bit depending on the number of channels active.

For the concerns of this work, the main differences between the devicea are

- the number of channels,
- the resolution of the analog-to-digital converter expressed in bit (higher number is better, as discussed in ??)
- the maximum sampling frequency (which is always fare above the needs in electrochemistry),
- the cutting frequency of an internal filter low-pass filter.

The peculiar characteristics of these devices is the *streaming mode* for transferring continuous acquisition of signals without loss even when the signal is longer than the device memory (other modes are available such as block mode and ???). The software development kit (SDK) from the manufacturer provides an interface to the USB drivers to conveniently include the streaming of data into the user program. The streaming mode works as follow: the user defines in their program a memory segment and a function to execute some actions on the data which are bidden to the software and when some new data is ready, the USB drive automatically writes the new numbers in the memory segment and calls the function (which is commonly referred to as callback function). In the callback the data in the memory segment should be processed, saved or evaluated in some way because will be overwritten in the next call anyway. The routine runs in a infinite **while** loop. A common approach, and also the suggestion from the manual, is to have another memory segment in the user program, let's call it *signal storage* for clarity despite being save on the RAM volatile memory and not in the permanent disk, large as much as the signal to sample where to copy the new data at each execution of the callback. The manual from the manufacturer gives a lot of information on the streaming mode and how to set it up. Code examples are also available for each supported programming language.

The data streamed are the numbers coming from the digitization step and they need to be converted before using them. The conversion factor depends on the resolution of the devices used (see ??).

The most straightforward to handle the streaming data is to keep in memory all the data coming from the devices and then save the data to storage. This is the approach used also for this work at the beginning. The limitation is the actual RAM memory installed in the computer in use. A standard office computer with 16 GB of RAM might be sufficient to store the complete voltage and current signals for short measurements. The duration of such experiment would depend on the aquisition frequency. The amount of points that can be usually stored in 16GB is 900.000.000 per channel which correspond to ?? GB . The memory occupied by the operating system and other application has to be taken into account. For example, when acquiring at 5MHz with the PicoScope the acquisition lasts 180 seconds while at 5KHz 50 hours. The first case should apply for studying electrode reactions during voltage sweep technique as for the study of hydrogen evolution on catalysts while the second for the study of battery

degradation in galvanostatic mode. 50 hours is still a short time when compared to Li-ion batteries that it in the order of month. To measure the impedance for such long time one might decide to periodically store data into the computer hard-drive freeing up the memory or acquiring the signals not for every cycle. This ideas will be further development in a later paragraph.

## Connecting cells in three-electrode configuration

Collecting the time-varying impedance of both positive and negative electrode of a three-electrode cells together requires some considerations. The potentiostats/galvanostats have usually only two auxiliary analog outputs: voltage versus reference and current. Furthermore, in any technique, the device controls the voltage difference between working and reference terminal. It effects either chrono-amperometric techniques because the counter as traditional for electrochemistry is only there to complete the circuit and chrono-potentiometric were despite the controlled counter being the same in the entire cell, it is not always possible to control the full cell voltage as it is not output in analog signal. Biologic devices are capable of changing the voltage control from working electrode vs reference to working vs counter through the hardware configuration section of the software EC-Lab. Unfortunatly this is not implemented in the EC-Lab SDK version ?? and one must come up with alternative, creative solutions. The easiest workaround is to employ two channels of the potentiostat, both in two electrode configuration with on to controll the techniques between working and counter electrode and the other between working and reference electrode to record the voltage drop in the half cell in OCV technique. Using just one channel of the instrument in three-electrode configuration and measure the voltage between working and counter (the full cell volage) with the digital aquisition device doesn't allow the controll of the full cell voltage, which is crucial for batteries, and connecting the instrument in two electrode configuraion connecting working and counter and recordng the voltage drop between working and reference is not a good practice because the imput impedace of the PicoScope is just of 10 M $\Omega$ , one order of magniuted less than a potentiostat, that would cause a big bias current flowing on the referenece drifting it out of the quasi-thermodynamic equilibrium that would have instead.

## Electrochemical devices

For these work we decided to use BioLogic potentiostats/galvanostats from the Premium class which can work easily with external connection using the EC-Lab software (from version ??? or EC-Lab express all versions). The devices used for this work are:

- SP-300 two channels,
- VSP-3 six channels,

fully equiped with Frequency Response Analyzer for measring the impedance up to 1MHz. The voltage range span between -12 and 12V, the total current across the channels is of 500mA, many current ranges are availabel

and the analog to digital converter resolution is of 16 bit. These devices are configured with the EC-Lab and EC-Lab Express software. A software Development Kit for EC-Lab is also available in different programming languages albeit not officially supported by the manufacturer. In addition, for less demanding circumstance, a BioLogic battery cycler ??? was used

## Connecting the device and acquiring the signals: set-up version 1

In the previous section, it was discussed how it is possible to generate and acquire multi-frequency signals. Now it is time to dig into the combination of these device for create a set-up suitable for the measurement of impedance in non-stationary conditions. The central point of such set-up is the potentiostat/galvanostat that provides all the electronics and implementation of electrochemical techniques. Some of the commercial devices have the ability to receive and record external signals or output directly the analog signals for voltage and current though coaxial connector.

### Automatic cycling with

# 7

## Analysis of impedance

### Contents

---

|  |    |
|--|----|
| Parametric models . . . . .                              | 65 |
| Simultaneous fitting . . . . .                           | 66 |
| Determination of the system degrees of freedom . . . . . | 67 |
| Determining transfer function structure . . . . .        | 67 |

---

### Parametric models

Once the impedance is measured, one can attempt to identify its dynamic fitting a physical or non-physical mathematical model (parametric). The work presented later in this work use one type or the other. The physical models where all taken from the literature. We used a model for ion adsorbtion on nanoparticle to analyse the measurement of electrical double layer capacitors and we adapted a model for intercalation with porous electrode theory both developed inside the group in the previous years. The core measurement of this work was made on lithium-ion cells, that is not the classic analytical cell with reference electrode commonly employed by electrochemists. The absence of the reference electrode makes cumbersome to develop a physically derived model so we decided to take the route of black-box model. Compared to the time-domain characterization where plenty of black-box models exist for any type of systems (ARMA, ARIMA, NARMAX, ecc.), the frequency-domain characterization lacks such variety and standardization, especially for time-varying systems. The approach in our group is to estimate the instantaneous impedance at quasi-stationary points using the dynamic multi-frequency analysis, hence treating the system as linear and time-invariant. Therefore the approach is to fit a generic rational function of order  $n$  inferring the correct structure of the transfer function of the system though statistical methods.

## Physical model

## Transfer function model

## Simultaneous fitting

The approach of fitting for dynamic impedance is similar to what is commonly done for static impedance, but there is the challenge that for a non-stationary experiment the dynamic of the system can change with the activation or deactivation of chemical processes with time, voltage or temperature. For example, a battery would change its state of charge during a galvanostatic technique and the system response might change at different potential, and with its cycling history. The common approach, sometimes called batch fitting, would be of fitting one spectra of the time using the optimized parameters of the previous spectra for the following. The problem is that some parameter of the model would be close to zero in some part of the dataset and potentially very big in others. Solving optimization problems with small and redundant parameters might lead to local solutions. Furthermore, when more than one parameter is of this type, the solver might converge to different minimum for each spectra even when the optimized parameters of the previous spectra are used as starting points. This issue can be addressed minimizing the entire dataset at ones and introducing a regularization term in the objective function as firstly introduced by Battistel et al. The objective function become:

equation?

Intuitively, one can consider a term that minimizes the distance between data points and model while another term keeps the parameters slowly evolving across the dataset. The penalty term avoids sudden variation of parameters that arises in those areas of the dataset where there is unavoidable overparametrization. Recently Cuckwu extended the concept of penalized objective function implementing modern methods to solve high dimensional optimization problem as used in the field of Machine Learning. An improvement in computation time for big dataset has been obtained combining the efficient methods for calculating derivatives called "automatic gradient" or automatic differentiation and the solver ADAM. Both can be find in the open source package JAX that uses the Python pre-compiling from the jit library to perform the calculation in multiple threads, processors or even distributed computing (including GPUs). JAX is supported for optimization-specific problems in the open source package Optax. Cuckwu implementation is open source but compatible up to Python 3.9 and only with JAXopt, the previous project from which Optax derived (not in development anymore). Dr. Nicoló Pianta updated Chucwu's code base to modern version and added a convenient object representation for the model function, similar to the well-established python library for non linear fitting nlfit. For each experiment of the Applications part I will specify which library was used to analyze the impedance.

## Fitting error

We estimate the standard deviation from the Jacobian of the objective function. The error allows to verify in most of the cases the accuracy of the model and which parameters are not significant in the estimation.

## Determination of the system degrees of freedom

When fitting physical models, the user decides *a priori* the degrees of freedom of the system through the number and types of approximation and the equation that chose to keep. The process of model regression gives to the scientist a confirmation that the model can represent the nature of the system under the operating condition or not. On negative result one keeps modifying the model until satisfied. On the other hand, when working with black-box model the scientist makes the opposite: identifies the degrees of freedom of the system and then look for a proper gray-box or white-box model of the same structure to understand the physics of the system. This data driven approach relies on the fact that the frequency response function is a numerical realization of the real transfer function of the system inside the frequency band of the experiment. From dynamic system theory it is known that the number of parameters of the transfer function is equal to the number of variables in the state space model, directly connected to the differential equations that define the system. For batteries, that works as two-electrode devices, the response of the single electrode is superimposed making even harder to define a general physical model. Usually the model are largely over-parametrized. Knowing the correct transfer function, leads scientists to chose proper approximation when developing physical model or can be used for prediction or classification of the system in control engineering. It immediately comes to mind the possibility of using it for smart control of the battery in battery management systems.

## Determining transfer function structure

The identification of the transfer function structure is the process of finding the order of the nominator and denominator of the polynomial rational function through statistical approach. In this work I ...



## Part III

# Results and discussions



# 8

## Coin cells

From the impedance response of the battery and given an appropriate model, one can infer the internal workings of the system for control and prediction. Classical impedance spectroscopy is widely employed to estimate the state of charge (SoC) of individual cells or modules, and to indirectly extract information such as internal temperature or detect the occurrence of side reactions, such as lithium plating. More broadly, the internal resistance of the cell is strongly associated with its state of health (SoH). <- maybe this should go in the introduction or method section and instead here go directly to the point of the experiment! The reader is already aware of the reasons.

In this chapter, I present the measurement of dynamic impedance of batteries during operation, continuously during the cycling lifetime. The aim is to demonstrate the advantages of impedance measurements under operating conditions compared to the classical stationary approach, in order to promote further research in this direction particularly in addressing the challenges of hardware implementation (for research or on-board control electronics) and the development of dedicated software solutions for the estimation and analysis. The acquired spectra are analyzed using standard methods, including distribution of relaxation times (DRT), transfer function parametrization, and statistical approaches.

For the experiments, I choose to work with a commercial rechargeable Lithium-ion battery. The constraint was the total deliverable current of the electrochemical workstation at my disposition, equal to 500mA, that means 90mAh for each of the 6 channels if all are running simultaneously. Furthermore, for an immediate evaluation of the methodology the cycling life should not be too long (weeks is preferable than months). Assembling cells in-house was an option but it impacted reproducibility. The decision lent on the Panasonic ML2020 coin cell with the following characteristics:

- Maximum theoretical capacity 45mAh;
- Positive electrode of Lithium Manganese oxide;
- negative electrode of alloy of lithium and aluminum;
- Electrolyte of ??? with no specified lithium salt.

The battery is meant for use as buffer for low power electronics and have a very limited self-discharge. The manufacturer advises to recharge the battery with a current of 100uA and the suggested operational limits are between 1 and 3 V.

## Method

The experiment here conducted was the measurement of dynamic impedance during a constant current - constant voltage (CCCV) testing profile, typical for testing of batteries performance and degradation in laboratory. To analyse the impact of the multisine perturbation on the cell, the same protocol was performed without any additional perturbation to the cycling drifts. To compare the impedance under operation and the stationary case, another set of measurements was performed in which the test protocol was interrupted, the cell rested and classic impedance acquired. All the experiments were conducted at room temperature.

The data were analyzed ??? Fitting of transfer function, DRT, long short-time memory???

## Cycling test

Voltage limit, current limits, c-rate, room temperature For the classical testing of battery using the constant current -constant voltage technique, I used the voltage limits suggested by the manufacturer of 1-3V and a current of 4,5mA, corresponding to a C-rate of C/10. After testing the capacity at C/20, 10 5 and 3 it was clear that the C/10 rate is the fastest that could possibly extract all, or very close, the theoretical maximum charge of 45mAh. During the potentiostat step, the voltage is kept to a value of 3V with a lower current limit of 1mA,corresponding to C/45. I collected a dataset from 12 identical cells of the type ML2020 Panasonic syyclend them with this protocol in a BioLogic battery cycler at room temperature.

## Operando acquisition of stating impedance

To obtain the impedance of the cells at different open circuit potential the same cycling protocol described in section above was here used with the addition of an interruption after 10% of the total charge is flown in the cell (corresponding to 4.5mA). When this charge limit is reached the system is held at open circuit for 1 hour for relaxation and the classic impedance measured. The range is from 20kHz to 10mHz.

## Real time acquisition of dynamic impedance

For the measurement of the dynamic impedance, the electrochemical workstation was set to produce the same CCCV protocol as described above. The multisine perturbation used here is from 10mHz to 100kHz, divided in two waveforms generated from two channels of the waveform generator. The waveform covering the lower band of the spectra is from 10 mHz to 87 Hz created with a time step of 1e-3s(equivalent to 1000 Hz) and a period of 100s. The harmonics comprising the frequency sequence are the ones obtained

without intermodulation, with 8 points per decade. The higher band of the spectra consisted of a range multisine from 100Hz to 100 kHz created with a time step of 1e-6 (1MHz) and a period of 10ms. In both cases the phases were independently minimized via randomization repeated 200 times, keeping the lower value.

For the sampling of the voltage and current signals from the cell a picoscope of the series 4000 (two channels) was used. The acquisition frequency was 500Hz, twice the Nyquist frequency of the signals. For the online computation, a window of 100s was used, equal to the period of the multisine, the DFT performed to compute the impedance of the frequency band from 1Hz to 100kHz and the signals low pass filter with a symmetric Fermi-Dirac filter with bandwidth 0.9 Hz and order 25 centered around 0Hz. The filtered signal was then resampled at 50Hz for storing.

The remaining part of the spectra from 10mHz to 0.8Hz was estimated offline using the Dynamic Multi-frequency Analysis with again a symmetric Fermi-Dirac filter centered at each frequency to analyze. The bandwidth is of 0.01Hz, the order of 8. After performing the analysis, both voltage and current signals were detrended using a simple linear baseline removal to reduce the effect of the drift.

## Analysis of impedance data

- Fitting of transfer function
- Correlation analysis of the coefficient
- long short-memory neural network
- DRT

## Results

From the regular cycling of the 12 identical coin cells I computed the total charge during discharging per cycle. The results, reported in figure...

## Discussion

### Identification of battery state

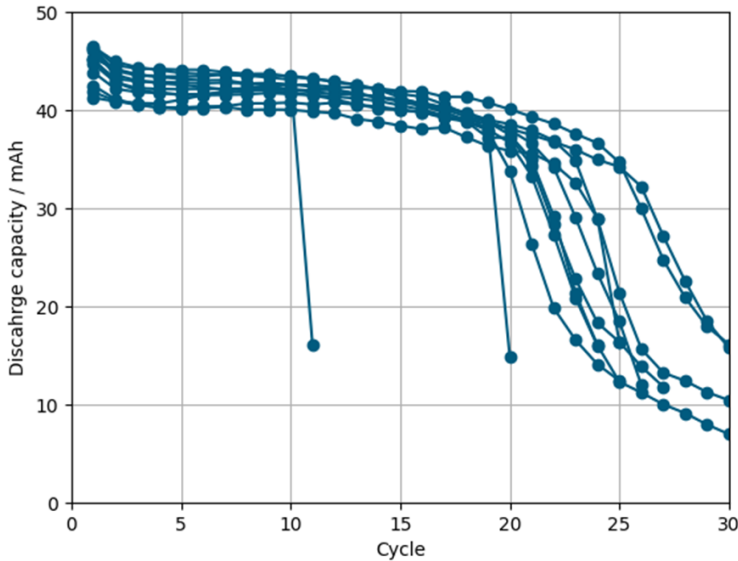
In this section it I described the work on the characterization of commercial coin cells though their life-time from their time-varying response. For this project I used a complete “battery”. In this introduction I would like to point out some terminology differences used in this chapter, following the discussion of para-

## Choice of the cell

With the intent of demonstrate the relationship between the time-varying impedance of a battery during standard operation and state of health, I decided to rely on commercial cells whit the assumption of a more consistent aging behavior compared to hand-made cells. Looking at the consumer market for Li-ion batteries one quickly relies that the capacity (or maximum charge) of this type of cells start from around 1Ah and goes up. The instrument at my disposal (BioLogic potentiost/galvanostat of the premium series) are capable of delivering a maximum of 500mA in total among the active channels. On the instrument with 6 channels that I intended to use for measuring the cells in parallel it means a maximum current per channel of 90mA. The only available rechargeable batteries that satisfies the maximum current limitation when cycled at 1C that I could find where the Panasonic ML2020 45 coin cell. Thier characteristics are reported in the table ???

These cells are base on MnO<sub>2</sub> and Li/Al alloy in a glycol based electrolyte. Manganese oxide is one of the first material used for the intercalation of lithium. It is cheap despite not the best in performance. Its drawbacks are : i) Lower energy density compared to more modern cathode materials; ii) Limited cycling stability, which can lead to capacity fade over time; iii) Lower operating voltage compared to other cathode materials, resulting in lower overall cell voltage; iv) Potential for manganese dissolution, especially at elevated temperatures, which can negatively impact battery performance.

On the negative electrode of such cells there is metallic lithium alloyed with aluminum. Lithium alloys quite well with aluminum (give some proof!!) giving less chances of dendrite formation. The electrolyte is a not precisely specified salt in ??? solvent that possess a low conductivity, probably to reduce cell self-discharge, which is a characteristic underlined in their marketing allowing for a maximum current of 4,5 mA (equivalent to C/10) to extract the full 45mAh capacity of the cell. Such a limitation reveled to be significantly useful for this project. In fact the low current in the system produces a system close to linearity facilitating the separation of the component of the multisine perturbation from the main drift. Furthermore this cells posses a scarce cyclability at this c-rate (C/10) with a degradation of the capacity below 80% of its original value in just 25 cycles, more or less; means circa 3 weeks of instrument time. Indeed these cells are meant as buffer for electronics components that use very little power. The raccomandare charging current from the manufacturer is C/200. For this project was a good platform to develop the software to control the instrumentation over a sufficiently long time-scale, testing and evaluating the stability of the algorithm while being able to spot di errors end implement the solutions in a matter of days.



## Performance test of the cell

Put the test at lower and higher c-rates

The tests were performed in a battery cycler .....

I was initially concerned by the possibility that the long term exposition of the cell to a multisine perturbation could accelerate aging. From a theoretical perspective the oscillation of the multisine is small enough to produce a negligible power and such a negligible heat generation at the interface of the electrode. To prove this point, 12 coin cells were tested through a constant-current-constant-voltage protocol with a current of 4,5mA, a voltage window between 1 and 3V and a termination of the constant voltage phase when the current reaches 1mA. The discharge capacities of the cells is reported in Figure.

## Static impedance evaluation

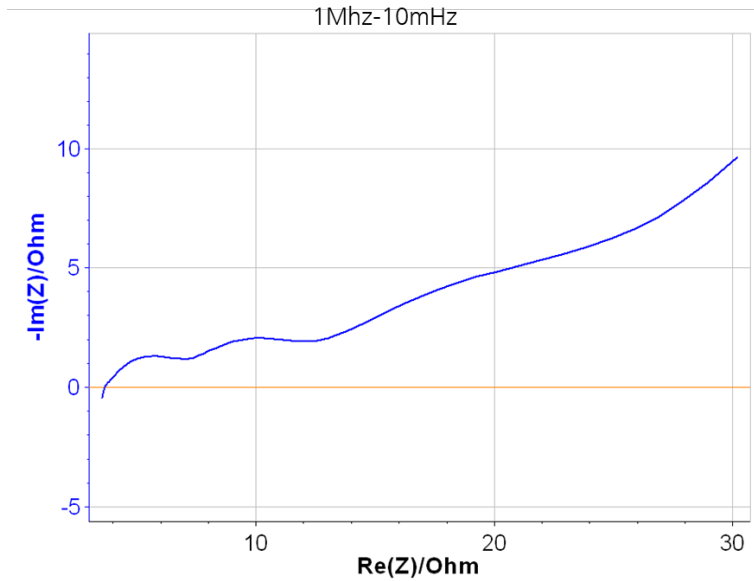
The static impedance for a new battery at the production voltage of 2.8V is reported in the figure.

Plot the static impedance at different states of health and comment the time required to perform it.

## Time-varying impedance acquisition

Following, I performed a series of experiment using the multisine perturbation imposed during the constant-current-constant-voltage experiment maintaining the same experimental parameters. In this case the limits where chucked on the avarage value of the voltage or current over 30 seconds to compensate its oscillation; a control loop in the software was included for this task.

For this project, the experiment contemplate the combination of both a voltage and current controlled techniques therefore two multi-sine waveforms were prepared to be used during the two techniques. Both were composed of the same amount of sine waves of equal frequencies but the amplitude was designed differently to garante always an output signal with



enough intensity for each frequency. The phases where chosen via iteration of random values to reach a low crest factor. The consideration for creating multi-sine are discussed in section ?????. The lowest frequency in the multisine is of 10mHz while the highest of 1kHz. The waveforms were generated with a frequency of 5kHz and sampled with the digital acquisition device PicoScope 4000 or PicoScope 5000. The two series of devices have different amount of channels and more importantly different precision of the analog-to-digital converter (16 bits and 14 bits) although no effect on the quality of the extracted impedance was found.

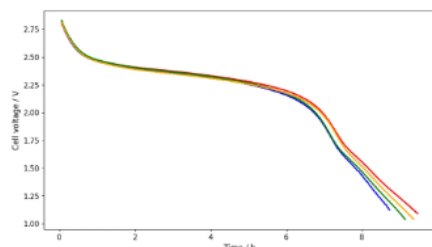
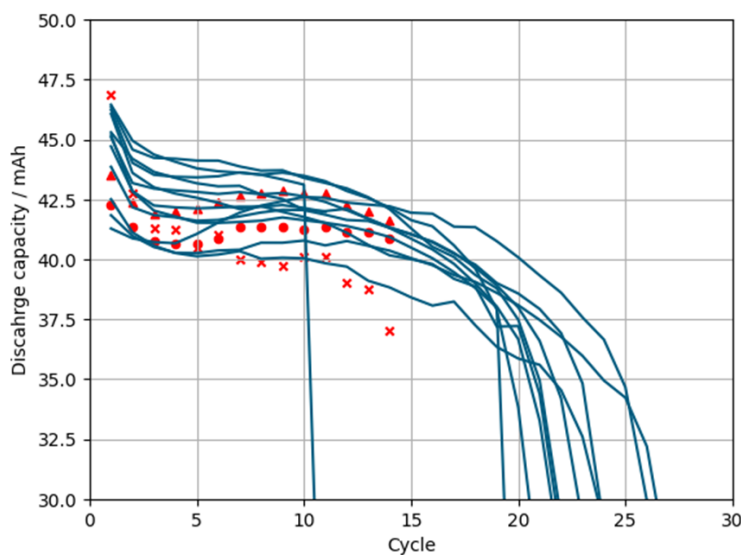
The two types of multi-sine, for the galvanostatic and potentiostatic experiment were both loaded on the memory of one channel of the arbitrary waveform generator. A control loop in the Python application is responsible of monitoring the running technique on the potentiostat and switch accordingly to the opportune multi-sine waveform on the generator.

The multi-frequency current and voltage signals were recorded and streamed to the memory of the Python application which saves them in separate folders per techniques. The time-varying impedance was then estimated independently from the multi-frequency signals of each technique using the Dynamic Multi-Frequency Analysis following the removal of the baseline in the non-constant (on the median) signal. The filter used for the analysis was a Symmetrical Fermi-Dirac Function with a bandwidth of 0,01Hz and n-value of 8.

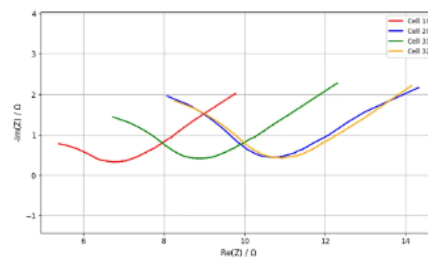
The discharge capacities for the cells under continuous multi-sine perturbation are reported with the previous set in Figure XX; it can be concluded that no significant acceleration of the degradation is related to the use of multi-sine.

Now a qualitative evaluation of the time-varying impedance estimated from the Dynamic Multi-Frequency Analysis will be given. First, I analyzed the shape of the first discharge curve and the impedance at same depth of discharge. The comparison is reported in figure.

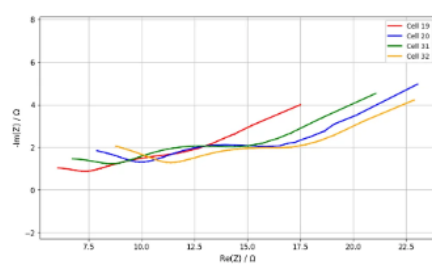
The cells exhibit similar capacity and equal voltage profile for the first half of the discharge. The last part of the discharge varies a little bit in its over-potential, probably due to the increased and uncontrolled rough-



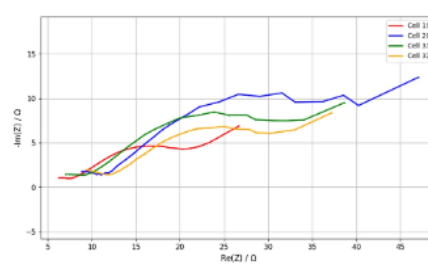
Discharge profile of cycle 1



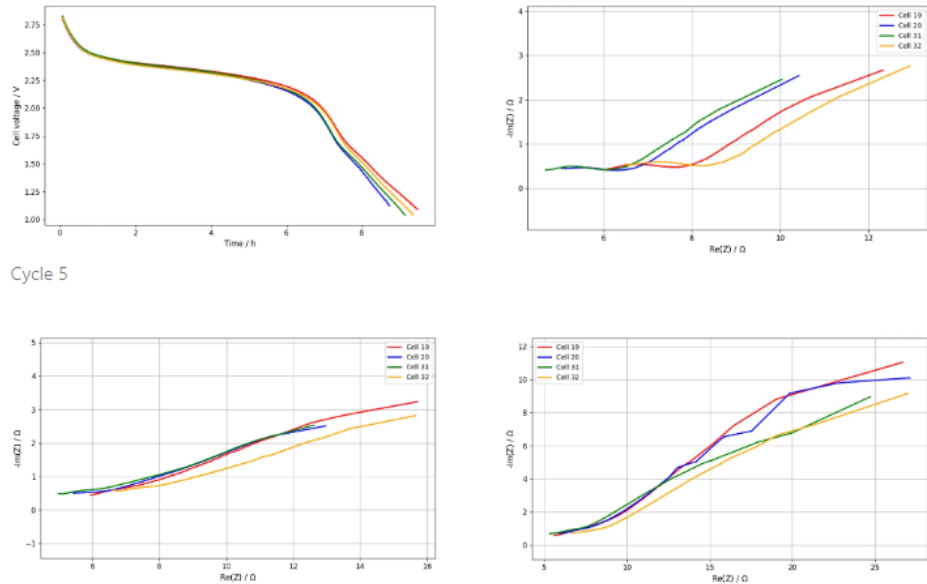
Beginning



Middle



End

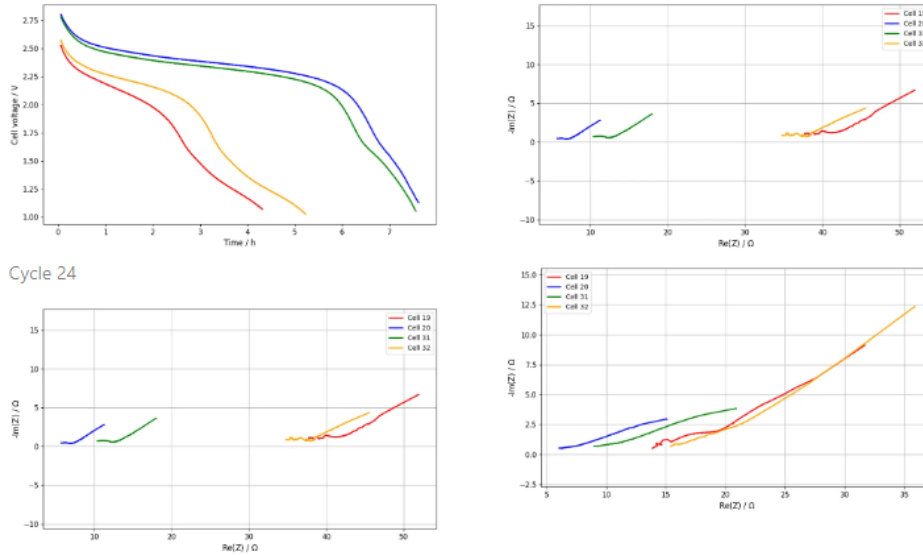


ness of the surface of the negative electrode during alloying. Considering the potential of alluminium and lithium alloying at 100mV vs Li/Li<sup>+</sup> thermodynamically, with such high overvoltage I expect the potential of the negative electrode to go easily below zero and cause a parallel lithium deposition reaction. I believe this is also the cause of such fast lost of capacity, for the low cycling efficiency for the dissolution of lithium deposit smaller than critical radius, and events of short circuit. Figure ??? also shows the impedance of the cells at different depths of charges, circa at the beginning, in the middle and at the end of the discharge. Here a first observation come, the impedance of the cells at the beginning are different of around 20-30% while the voltage profile looks identical. This is a first advantage of the impedance of showing characteristics that are invisible at the low frequency scale (means direct current) but might have a significant impact on the performances. It is interesting to notice the blue and yellow lines to be very similar from the beginning to the end, while the red curve showing always a smaller impedance value. It is not surprising to se the highest discharge capacity (visible as longer time to discharge) for the cell with the lowest impedance (red line).

The shape and magnituse of the impedance for the four cells reveal a different response for the consequent cycles. In the Figure XXX it are reported

The time-varying impedance of the cells conserve a similar a similar trend until the aging start to accelerate faster. Here we also assist to a larger discrepancy between the cells in terms of both discharge capacity and impedance. See Figure XX.

The time-varying impedance of a system is a particularly big dataset that can be seen as two dimentional, as a function of time, or three dimensional as a function of charge and cycles. The latter is in my opinion the most informative being the cycling of a battery similar to a seasonal time series. The voltage and impedance of a cell as a function of the charge represent the state of charge while their dependency with the cycle number represent the state of health. Both informations are much informative to acquire and it is exactly the scope of this project. Nontheless such a rich



information (considering also that the impedance is complex) is impossible to fully display on paper as 2D immages. In this section, some snapshots of the full movie, to ripropose the picture-movie analogy from the introducion, are provided to the reader after a filtering of the author. This is a intrinsic problem of data visualization that belong to any science. ?????

During the data analysis process, interactive figures where fundamental to find interesting variation on the system impedance, but still in a qualitative way, just base on the eyeballing. A way to codify the information in a lower dimensional is needed to demonstrate the relationship between impedance and the states of the batteries, both of charge and of health. This is the topic of next section.

## regression of rational polynomial

Despite begin so challenging to measure the impedance of a system, especially in non-stationary condition, it is only half of the job. To make all the work worth, one must extract information about the system under study.

A transfer function, as is the impedance, is in its analytical form a rational polynomial as shown in the introduction. After estimating the impedance spectrum of a system over a set of frequencies from an experiment, it comes natural to want to deduct the transfer function that output such results to be used as model of the system and simulate it behavior under different operating conditions than the experiment. For this work we combined some ideas from statistics and system theory to find in a robust approach to find such function among the many possible. The first idea is to have a generalized model of additive terms, i.e. polynomial, as from the Generalized Additive Models but non linear and especially both rational and of incremental power. This translates in a model of such a form:

$$f(x) = \frac{a_0 + a_1x + a_2x^2 + \dots + a_kx^k}{b_0 + b_1x + b_2x^2 + \dots + b_kx^k} \quad (8.1)$$

This is identical to the definition of transfer function. It is convenient to fix  $b_0$  to 1 to have always a finite value. The second idea come from In-

formation theory and it is about the choice of an opportune  $k$  which means to have a criteria to decide when to stop adding term to the polynomial. In fact, a fitting gets always “better”, or the residues of the regression are smaller, with the increase of the number of parameters. On the other hand the new parameters have no physical significance or do not univocal define the system. In this case we talk about overparametrization. The problem of estimating the original information from a signal with uncertainty is at the core of a branch of statistics and Computer science called Information Theory. The amount of information, translated in common means as degree of freedom of a system, is converted to a quantity called Entropy of information. Minimizing this quantity brings to the correct number degrees of freedom for a model to describe the data. This concept was formalized by Akaike and further developed in the years.

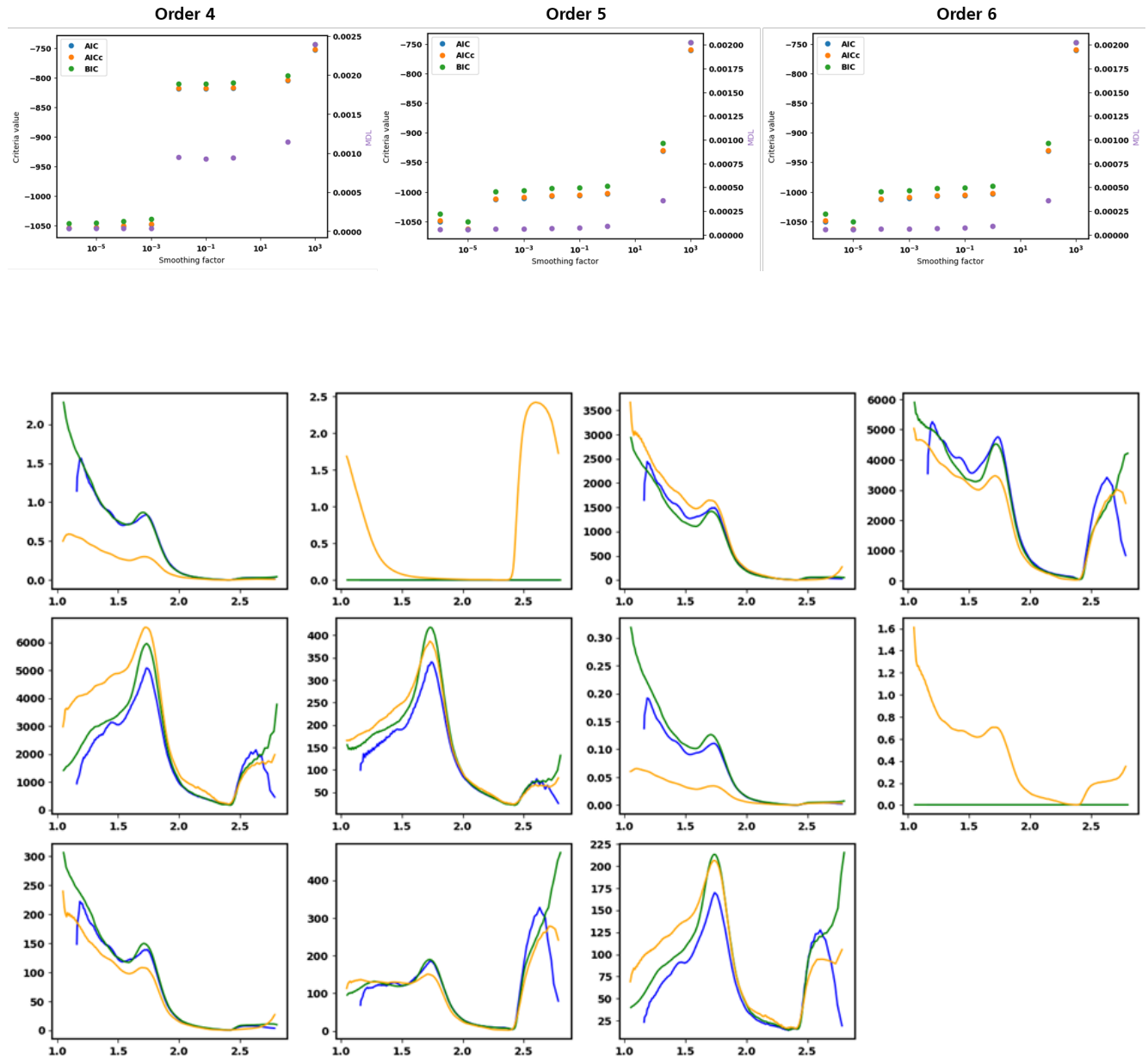
When searching for the correct transfer function model for the case of time-varying systems it is also expected that the coefficients ( $a$  and  $b$ ) of the rational function continuously change during the evolution of the system physiacal chacartesitics without any sudden jump or going to zero. This scenario can very when the model is overparametrized in certain parts of the dataset (for example at the beginning or at the end of the experiment). In fact the parameters space of the fitting procedure becaome rougher with many close minima. The solution might not anymore be unique. Thi is clear when fitting the single impedance spectra from a time-varying experiment one after the other. To ensure smoothness and continuity of the fitting parameters, a penalty factor can be added to the object function of the minimization. For this work we used a penalty on the second derivative of the parameters and this means adding one non-free paraemeter on the function. The choice of this parameter has of course a great influence on shape of the costa function hyper-surface and so the minimization procedure. A value too big don't allow the parameters to vary until exactly fitting them while a value too small make the penalty negligible. The objective function to minimize in now the sum of the residues for the fit of all the spectra in the dataset analysed (i.e. the time-varying impedance of one discharge) plus the penalty factor. The problem defined this way has a very high dimensionality and could not be solved with standard solver for its uge memory consuption. For this projecy I use once again the library pymultipleis that take advantage of JAX virtual mapping to split the problem in smaller problems and efficiently parallelize it on the machinne. Furthermore the autodifferentiation capabilities reduce the compution time.

The working principles of the library are described extensivelly in the introduction.

The fitting of the model where conducted on the admittance using the modulus as weighting factor. This helps the convergence to the absolute minimum giving less importance to the lower frequency that carry higher uncertainty. To decide over the correct model and penalty factor value for an opportune model, I compared the different information criterium values of multiple optimization run in which I screened the rational function of increasing order  $k$  and eight smoothing factors for each, one value per decade from 1e-6 to 1e4. I repeated the regression for each of the four cells and the results are summarized in figure XX.

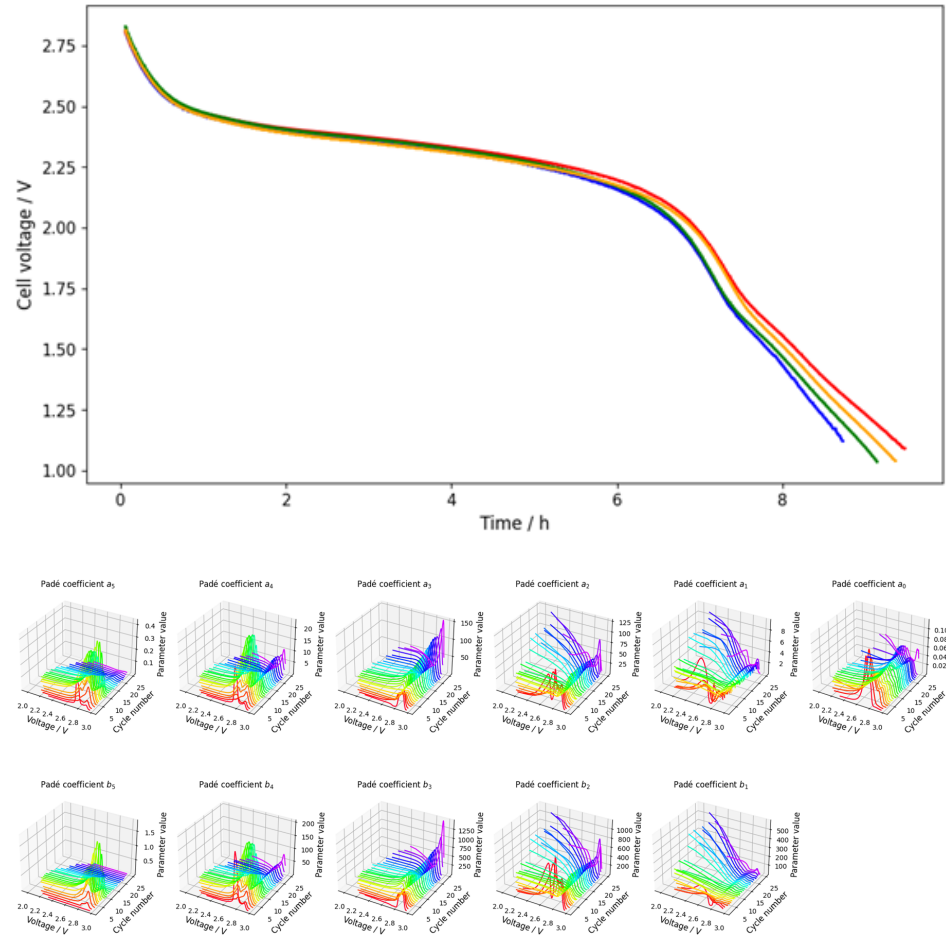
From the previous figure it is clear that some of the parameters follow the exact same trend. Those are in fact correlated and should not me considered in the count of the degrees of freedom.

Criteria tested: AIC, AICc, BIC, MDL



The figure shows how the coefficients of the rational polynomial for  $k=5$  evolves during the first discharge of the cell. Each of them have 2 or 3 distinct peaks centered at 2.6V, 1.7V and 1.3V. This values correspond to the change in steepness of the voltage profile. colorboxBurntOrangeThis is more clear analysis the differential voltage curve.

Once identified the proper model, the time-varying impedance for the life time of the battery was fitted producing the result in figure XX. From the picture it is clear the evolution of the parameter with the state of health and state of charge. This parameterization though ration polynomial regression allowed to visualize the time-varying impedance from one cell at one glance. The complex-valued impedance is transformed in real valued parameters.



### Associating measurement values with battery state

The goal of this project is to demonstrate a relation between the impedance and battery state, ideally to use the data at one point of the cycling for the forecasting the rest. One of the most important information any user needs to have is the end of life of the device. It is not only practical for the user but represent a great economical value for the second life expectancy of a battery module.

# 9

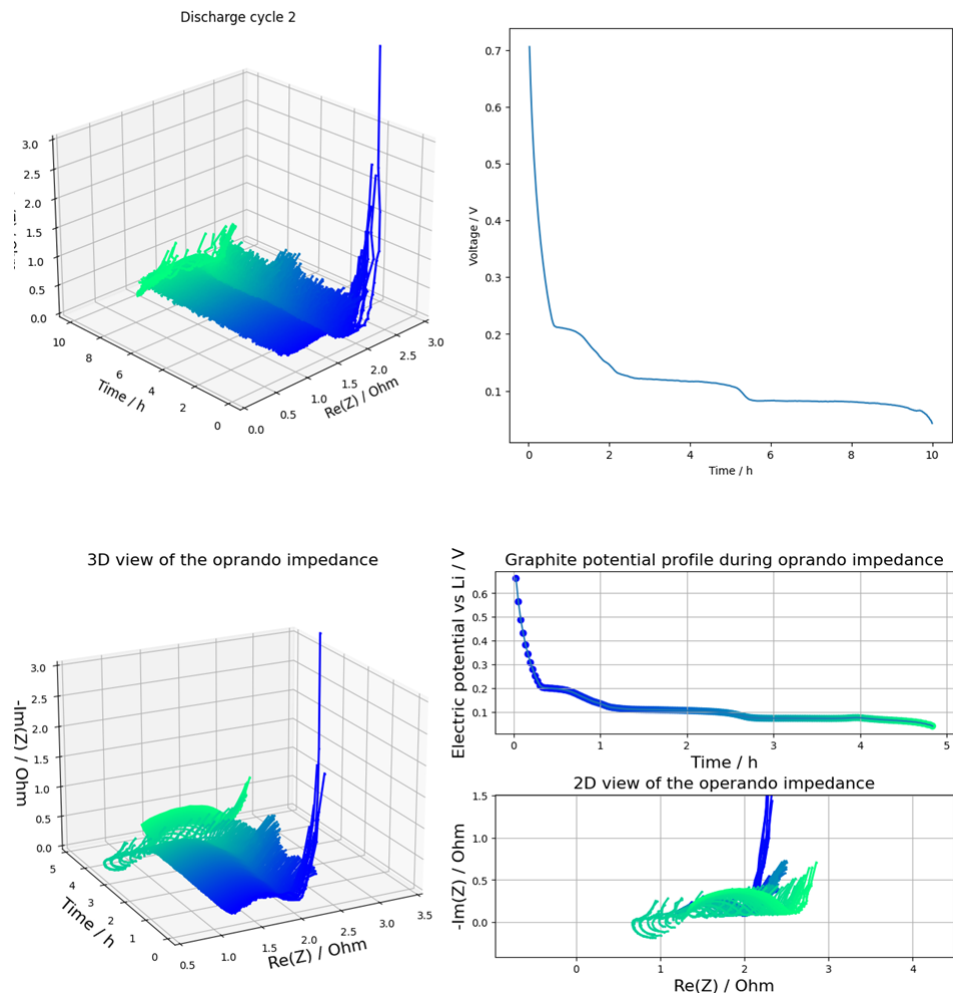
## Identify lithium plating on graphite

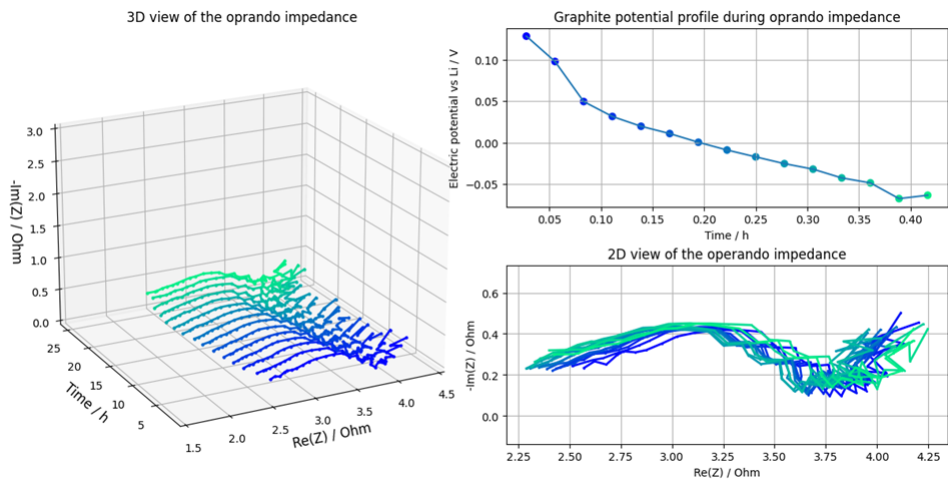
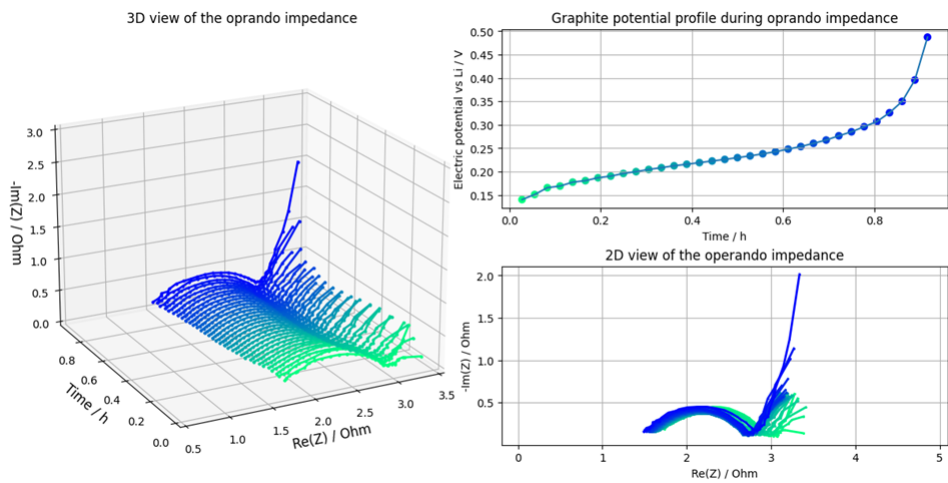
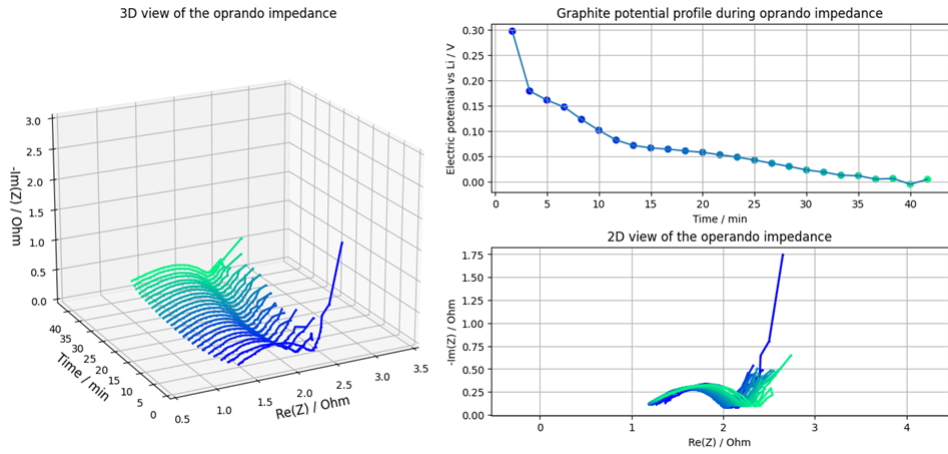
With the experience gained working on the projects described in the previous two sections, I was curious on the possibility of identify lithium plating in situ during reduction of the graphite though time-varying impedance. This is a huge topic, especially in the last years where company achieved (es. StoreDot) extreme fast charging. Fast charging, while enabling a greater diffusion of electric vehicles for the convience of it, should be used sparingly. As described in the introduction, charging with high current densities pushes the potential of the negative electrode much lower than its thermodynamic values to a point where lithium reduction is possible. Fast charging a battery every cycle inevitably reduced the life of the device. It is interesting though to know what happens after one fast charge cycle to the graphite electrode and if the impedance can retrieve some information. The set-up used is similar to the one used for the project regarding silicon carbonitride and the mechanisms of sodium intercalation; I assemble a three electrode half cell in pouch format with natural graphite electrode and microscopic electrodeposited electrode, discharge the cell at 1C without any potential limitation but rather time limitation (i.e. charge) and then performed consecutive non-stationary impedance experiment in galvanostatic mode with increasing current density.

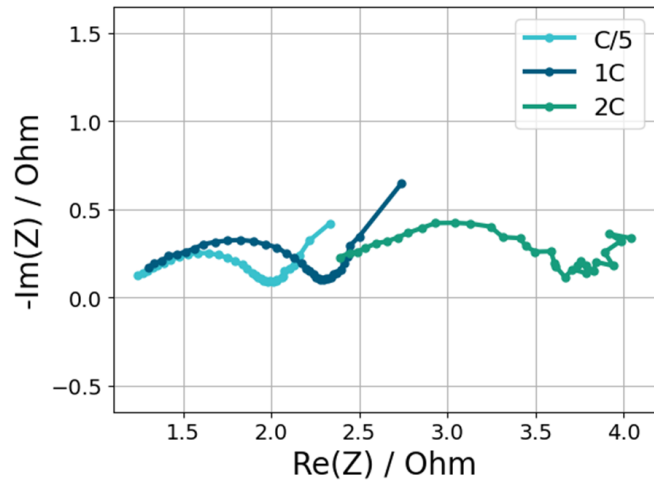
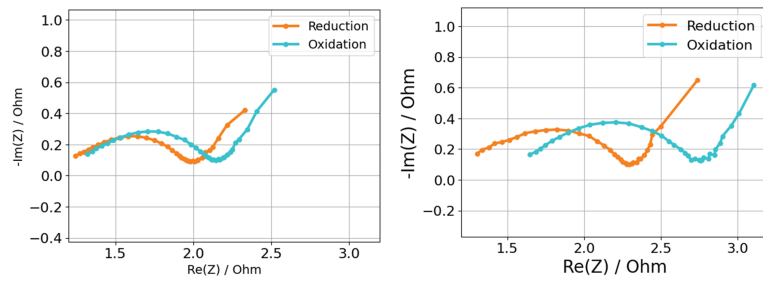
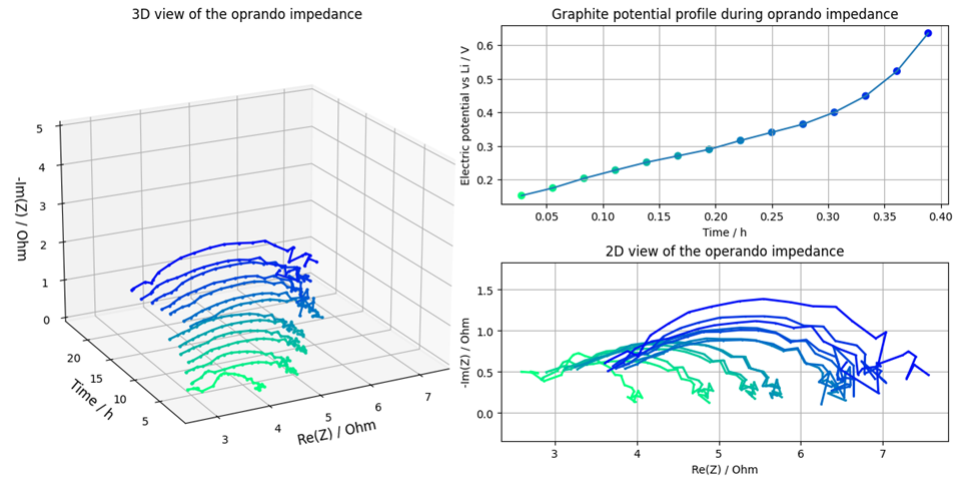
### Cell assembling

For this project the working electrode was a graphite slurry of SBR and water doctor bladed on copper foil. The counter electrode was a square of lithium foil 22x22x?? mm (99.?? %, Sigma Aldrich). An insulate copper wire current collector with diameter of 130um was produced with the same method described in the section before and the cell assemble using two glasfiber separator with the reference copper wire between them, placed in such a way to have the exposed copper area in the center of the electrode area. 300 uL of electrolytic solution LiPF6 in EC:DMC 1M with 2% of VC was poured in the cell and the device underwent 2 cycle of underpressurization of 10 mbar to remove gasses from the pores while allowing the permeation of the liquid. The cell was sealed with a coffee bag under a pressure of 10 mbar. Transform in pascal

### Time-varying impedance measurements







# 10

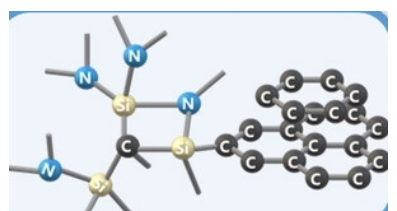
## Discriminating sodium storage mechanisms

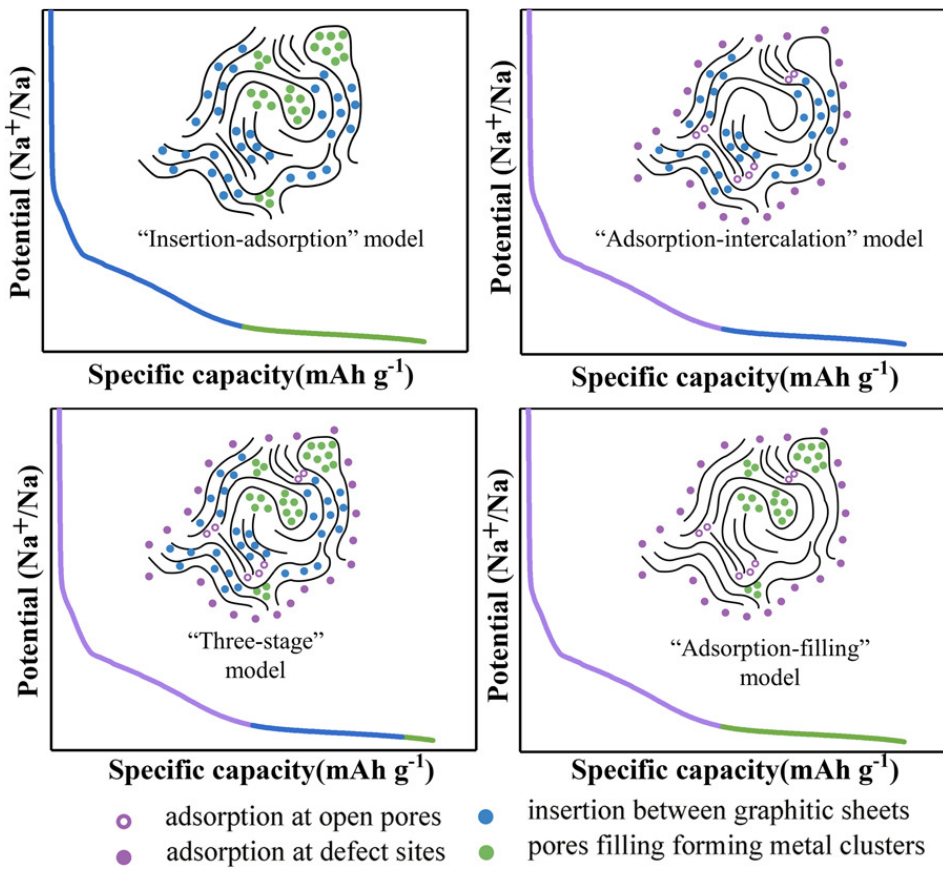
This project is about using the information from the time-varying impedance to infer the mechanisms of Na storage in porous silicon carbonitride as candidate material for the negative electrode of non-aqueous Na-ion batteries. The material was developed and patented at the inorganic chemistry department of the Technical University of Darmstadt as an alternative to the most known hard carbon. This class of partially distorted and highly porous materials are especially indicated for the storage of Na cation, as it is bigger than Li. Graphite, in fact has not enough interlayer space to accommodate Na cation. Many mechanisms for the Na cation storage into disordered structure have been proposed and it is likely that they happen all in parallel. The goal of this project was to connect the shape of the impedance with specific mechanisms and take advantage of the operando condition to get information on the potential windows these mechanisms take place.

The material used for the project was synthesized and the electrode produced at the University of Darmstadt by Marco Melzi d'Eril.

### Silicon carbonitride

Silicon carbonitride belongs to the category of polymer derived ceramic material which are obtained from the pyrolysis of preceramic polymers which are characterized by the heterogeneous covalent bond of silicon, boron, carbon, nitrogen and oxygen giving to the final material excellent chemical, thermal and mechanical properties among them hardness. The pyrolysis procedure gives a high control on the structure and morphology of the final product allowing to increase the porosity. The structure of silicon carbonitride is reported in the figure. The preceramic polymers precursor can be even manufactured as complex three-dimensional structure by additive techniques and pyrolyzed in a second step. The presence of both carbon-carbon and silicon-nitrogen bond give to the material the properties of electron conductivity, hardness and has a lower binding energy of the physisorption process for the Na cation compared to carbon (ref Sodium/potassium metal anodes, Xian Chen 2020). This material is in comparison with hard carbon, also obtained by pyrolysis of carbonaceous precursors in inert atmosphere, which exhibits good mechanical properties

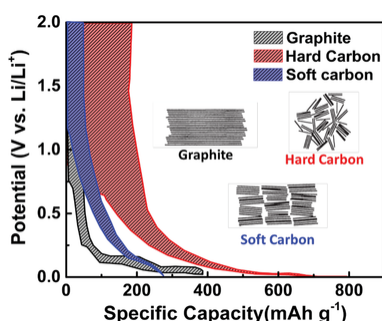


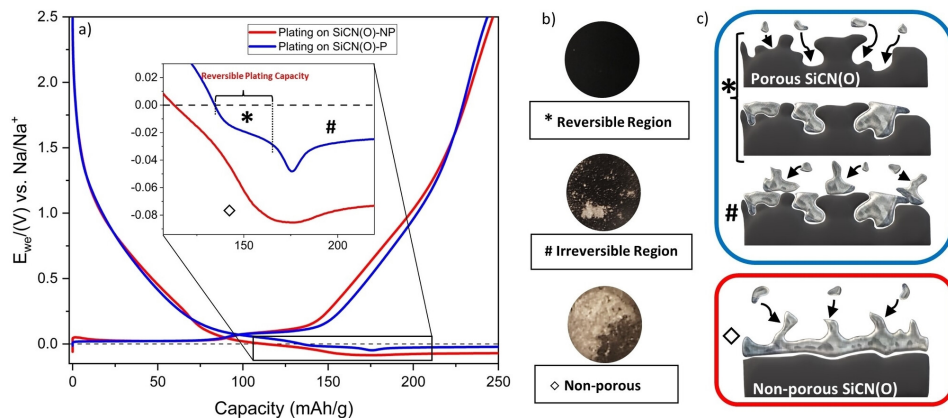


and electrical conduction. This class of material exhibits low density and high microporosity make them excellent candidates for the storage of cation. Hard carbons are widely used as negative electrodes in lithium and sodium ion batteries while the silicon carbonitride was demonstrated to give comparable capacity (ref Carbon-rich SiCN ceramics as high capacity/high stability anode material for lithium-ion batteries, Reinold et al. 2013 and Sic et al. SiCN Ceramics as Electrode Materials for Sodium/Sodium Ion Cells – Insights from <sup>23</sup>Na In-Situ Solid-State NMR 2022). The research is still ongoing on the micro scale structuring, doping and functionalization of these materials to increase the storage capacity (ref Enhancing the performance of hard carbon for sodium-ion batteries by coating with silicon nitride/oxy carbide nanoparticles, Hang Cheng et al 2021, Understanding of the sodium storage mechanism in hard carbon anodes, Chen et al. 2022)

### Storage mechanisms

Multiple mechanisms are responsible for the storage of cation in the micro-porosity of the materials. Figure XX shows the different in the material potential vs Li during reduction of the electrodes. It is clear the absents of plateau which are associated with a phase change of a crystalline ordered structure, absent for the case of disordered carbon. The most accredited storage mechanisms are adsorption, insertion and metal electrodeposition, as schematized in the Figure. It is still an open question which of this processes contribute the most and at which potential, and important information to design materials with higher capacity. Multiple theories are taken into account to far as reported in Figure. Study such characteristics





can only be done in operando condition with in situ techniques. Researched used different methodology for the identification of the position of the cation in the strucutre such as Nuclear Magnetic Resonance and Raman Spectroscopy.

Silicon carbonitride, for the presence of Si-N bonding should a particularly good binding energy with atomic sodium, favorating the electrodeposition in the pore of the material. Marco Melzi et al demonstrated an increase of capacity when allowing the lower voltage limit to negative values, i.e. allowing electroceposition of Na to happen with high efficiency. Reducing the micro-porosity during the synthesis step removes the gain in performance. The goal of the project here describe was to find evidences of metal plating through the impedance during reduction and help inferring the mechanism.

### Cell housing for three electrodes and optimization

The measurement reported in Figure XX is a galvanostatic cyclation performed on a two-electrode half-cell with metalli sodium as counter electrode.

Descrivi la cella e le componenti.

While this cell is fine for the screening of material properties in term of capacity and its retention, it is not suitable for electrochemistry investigation and more advance techniques like the Electrochemical Impedance Spectroscopy. This is especially true for the case of sodium half-cells were the sodium metal - electrolyte interface has an high impedance, up to two orders of magnitude than the silicon carbonitride electrode. For analyzing the impedance of the working electrode only a reference electrode has to be designed. For this work we started experimenting with a simple thin metallic sodium strip, positioned in the middle of the cell stack. To maintain the cell geomerty from the original pubblication a T-shaped three electrode was obtain from a Swagelock gas junction at the workshop of the University of Darmstadt. A section of the cell is reported in Figure XX. The results were at first interesting but we were not sure about the intruction of artifacts due to the size and thickness of the strip of sodium as reference electrode, comparable with the size of the electrodes itself. The pressure applied to the stack, in presence of glass fiber separator was high enough to easilly deform the sodium counter electrode. We later tried to use a microscopic reference electrode which should avoid the presence of artifacts according to the simulations. The details on it manfuacturing will be discussed in

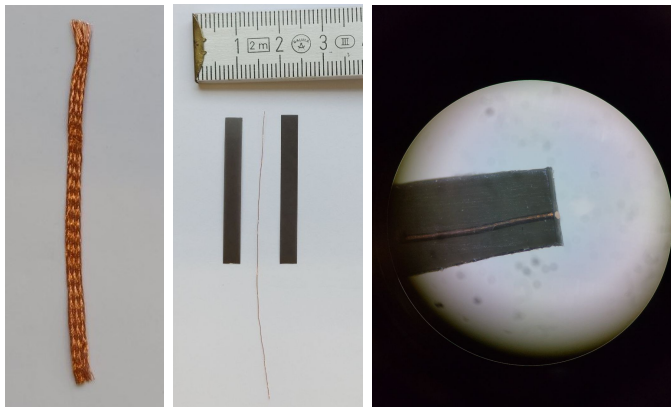
| Nname  | Type of cell  | Electrodes | Type of reference electrode                                  |
|--------|---------------|------------|--|
| Cell05 | IFAM Swagelok | SiCNO/Na   | Strip of sodium metal  |
| Cell10 | DTU Swagelok  | SiCNO/Na   | Strip of sodium metal  |
| Cell13 | DTU Swagelok  | SiCNO/Na   | Strip of sodium metal  |
| Cell35 | DTU Swagelok  | SiCNO/Na   | Sodium electrodeposited on insulated copper wire (no piston) |
| Cell36 | Pouch cell    | SiCNO/Na   | Sodium electrodeposited on insulated copper wire (no piston) |
| Cell38 | Pouch cell    | SiCNO/Na   | Strip of sodium metal  |
| Cell39 | Pouch cell    | SiCNO/Na   | Sodium electrodeposited on insulated copper wire (no piston) |
| Cell40 | Pouch cell    | Na/Na      | Sodium electrodeposited on insulated copper wire (no piston) |

depth in the next section. This electrode is an insulated copper wire with only a section exposed (i.e. a disk of copper) on which sodium was in situ electrodeposited. Giving the concentration of the electrolyte of 1M constant as approximation during the cell evolution, its potential should be constant. The use of microscopic reference electrode for the relative measurement of electrode potential in batteries has gained a lot of interest in the last year. As explained in the introduction, alloying lithium with other metals, especially the noble ones, produce a stable reference electrode. Unfortunately sodium does not alloy with gold or aluminum, but only with tin. On the other hand sodium electrodeposits quite well on copper, in fact I got potential stability for months as will be reported later. The microscopic wire electrode was difficult to introduce in the T-shaped cell. For a simple assembling, the wire was screwed into a stainless-steel piston. Assembling such cells was difficult and gave inconsistent results and frequent short circuits. Finally I decided to move to a different geometry which I believe is much easier to assemble, leave more freedom on design and should guarantee a better insulation: the pouch cell. The final design is schematized in Figure XX.

Moving from a macroscopic to microscopic reference electrode was a choice based on the ideas that a microscopic reference might introduce artifacts in the impedance. As shown in the following section about the solid-electrolyte conductive interphase, an inductive loop was observed and the origin of such feature is often associated to geometrical considerations of the electrode positioning.

### Microscopic reference electrode of sodium

While the concept of microscopic reference electrodes is getting accepted for lithium redox couple in non-aqueous solutions, the same is not true for the case of sodium as described in chapter XXX. For this project we aimed to design a simple microscopic electrode using ready available materials in every laboratory or workshop. The reference material is metallic sodium electrodeposited in situ on the exposed face of an insulated copper wire. The wire here behaves only as current collector and mechanically strong substrate for the deposition of sodium. The entire length of the wire was insulated using two thermoplastic polymer strips, usually employed for the



sealing of pouch cells. The copper wire, with a diameter of 130 $\mu$ m, come from an inexpensive solder tip cleaner.

The insulation of the wire was done putting the wire between two strips of polymeric strip longitudinal to the heating strip of an ultrasonic sealer for coffee bags. The Excess polymer were removed with a scalpel and a section of the wire exposed like shown in Figure XX. It takes a bit of practice to cut the section parallel to the axis and get approximately a circular section. Without checking on the optical microscope, one might end up with elliptical section resulted from non perpendicular cut and hence a much higher surface area.

For the electrodeposition the wire was connected to the working pole of a potentiostat using a disk of metallic lithium as counter (12 mm diameter) in a two-electrode configuration. The procedure was conducted with a two steps technique, first 10 minutes of potentiostatic set at -100mV and then 3 hours in galvanostatic with -50 $\mu$ A of current. It followed an open circuit technique. The reference electrode produced with such techniques were stable under parasitic current of the potentiostat for 6 months.

Mettere le figure dell'OCV del reference

## Time-varying impedance

For this application I used the set-up Version 3 as discussed in the experimental section. The main drift consisted only of a galvanostatic reduction and oxidation with potential limitation without any rest or potentiostatic steps, to match the protocol used in a previous publication. The current was set to C/20 in respect to the theoretical capacity calculated as ???? in the potential windows of 0V to 2.5V vs Na. The multi-sine was generated with frequency components from 10mHz to 1kHz with 8 points per decades and remove frequencies that produce intermodulation. The amplitude was kept flat to arbitrary 1 V (see discussion for a comment on this choice) and crest factor optimized by random iteration of the phases. After loading the multi-sine on the waveform generator an amplitude of 80mV was set on the instrument. The multi-frequency signal was collected with a sampling frequency of 5kHz and the time-varying impedance estimated through a Dynamic Multi-Frequency Analysis using a Symmetric Fermi-Dirac filter with 0.01Hz of bandwidth and n of 8.

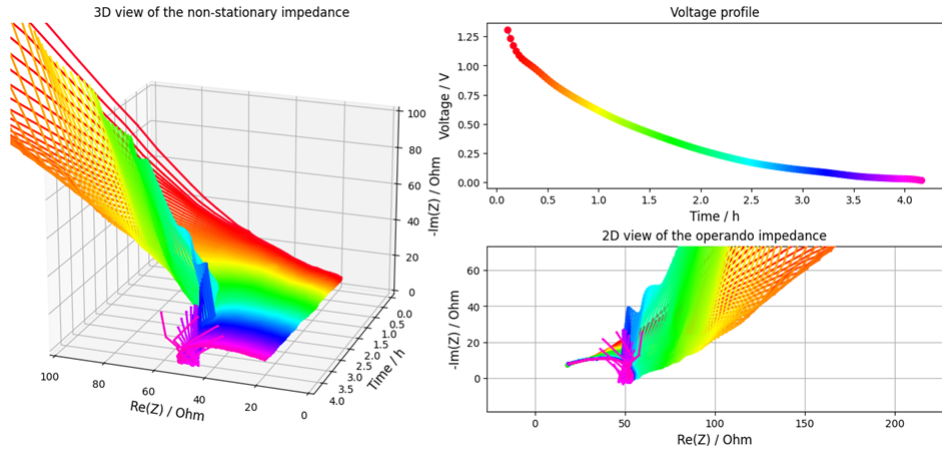


Figure 10.1: Cell 10 first discharge after formation.

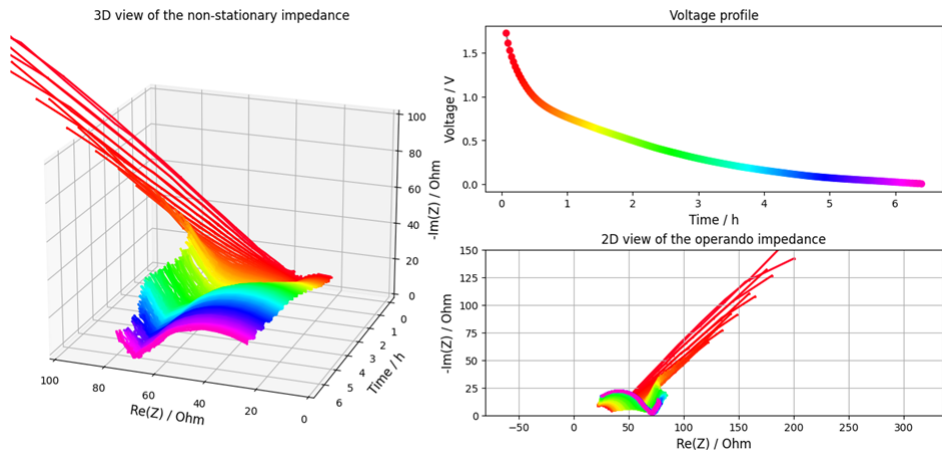


Figure 10.2: Cell 35 first discharge after formation.

Sodium electrodeposition on sodium substrate

Time-Varying impedance during SEI formation

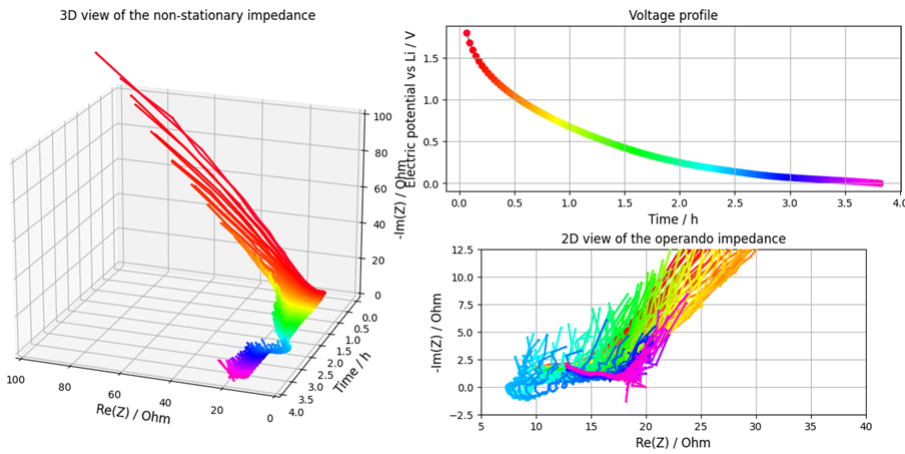


Figure 10.3: Cell 36 first discharge after formation.

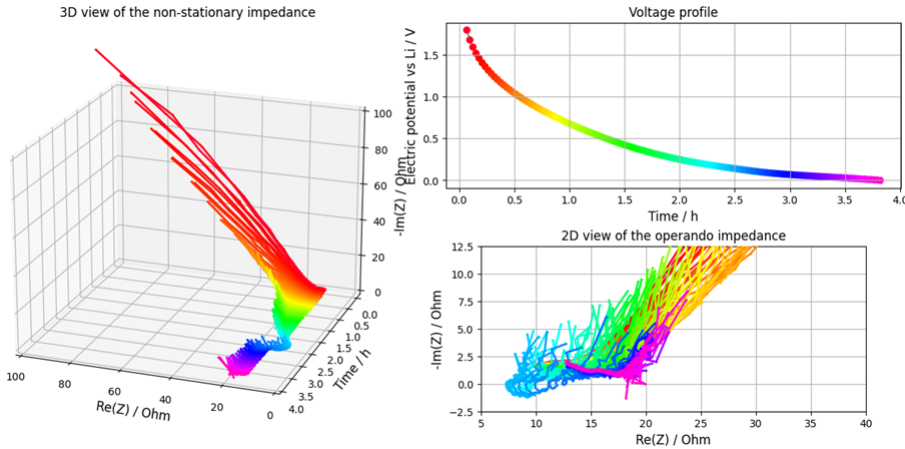


Figure 10.4: Cell 38 first discharge after formation.

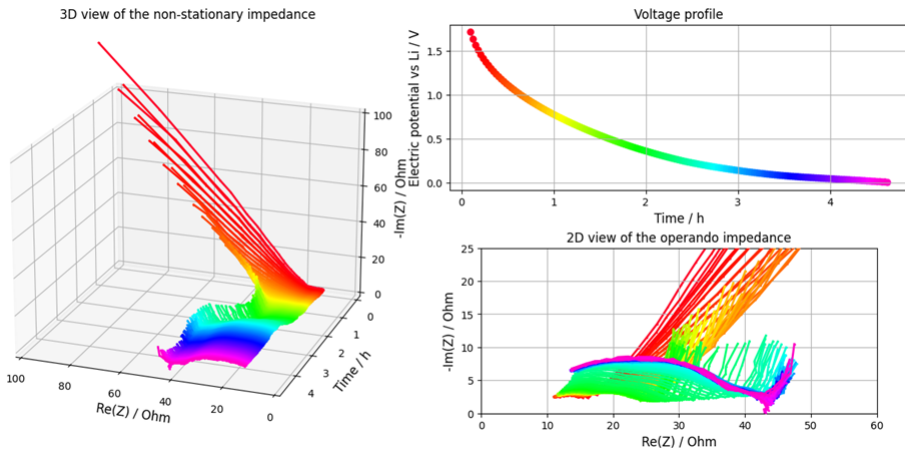
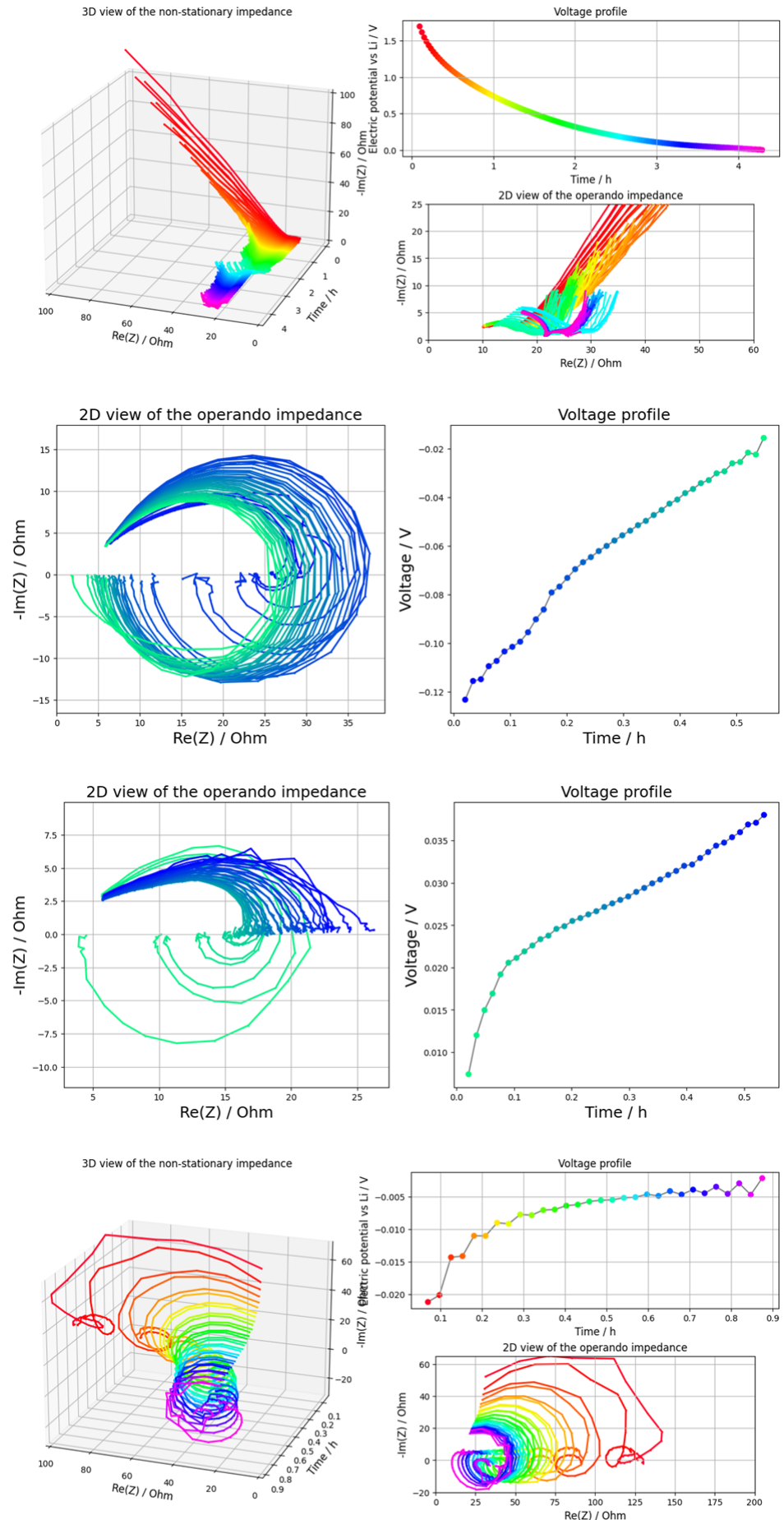


Figure 10.5: Cell 39 first discharge after formation.



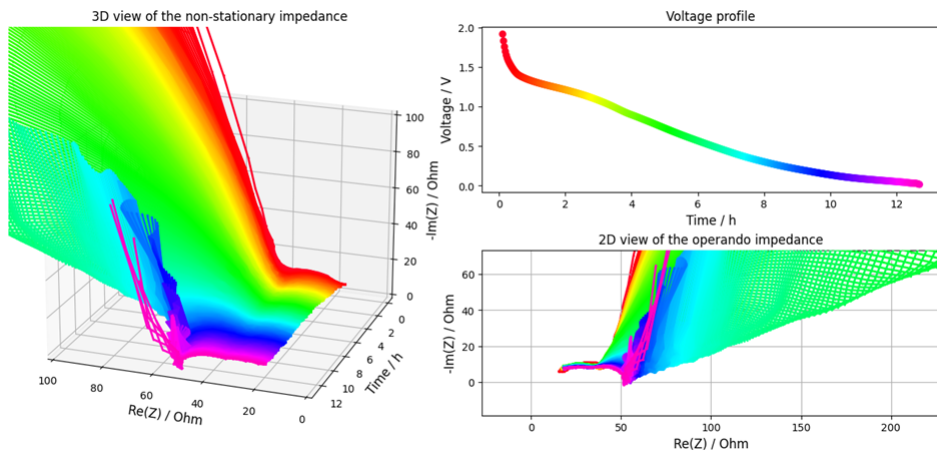
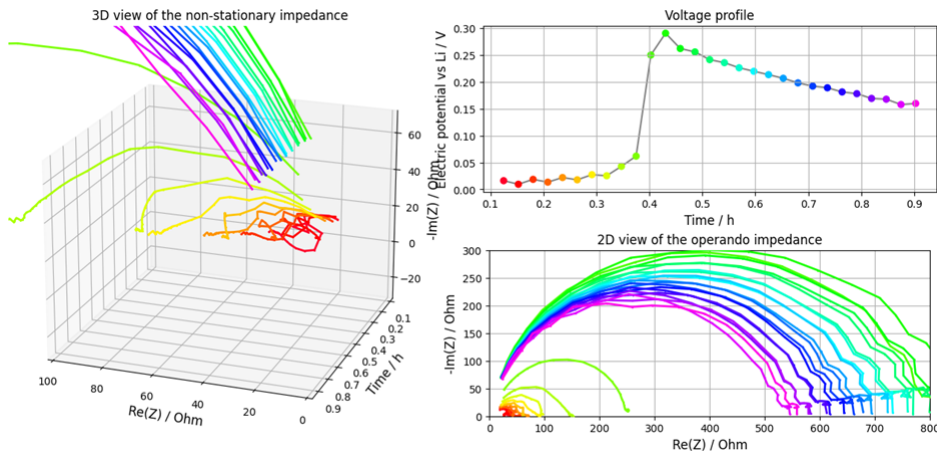


Figure 10.6: Cell 10 formation.

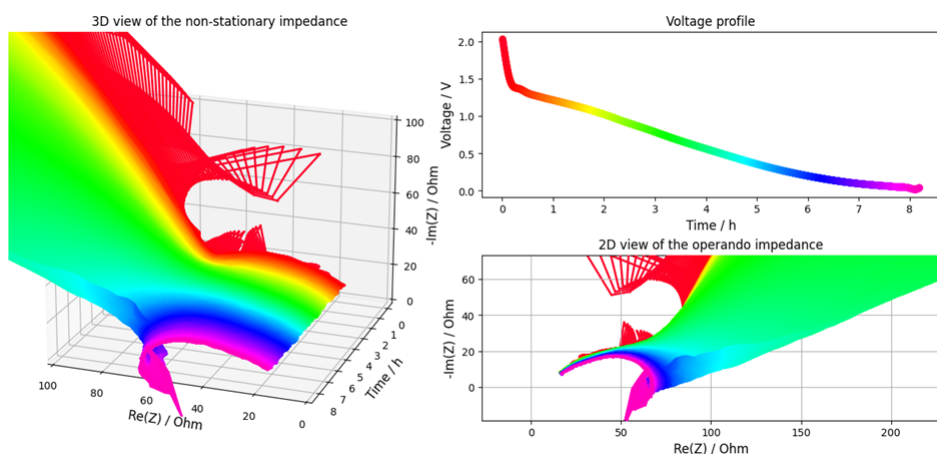


Figure 10.7: Cell 13 formation.

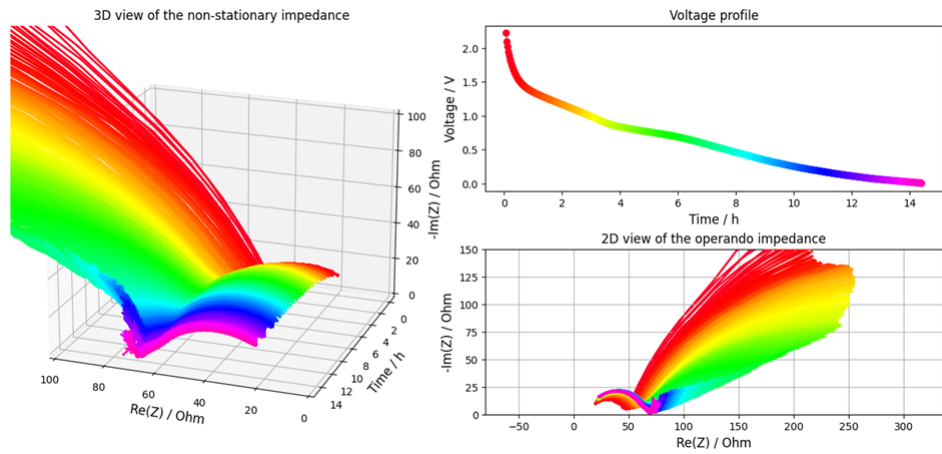


Figure 10.8: Cell 35 formation.

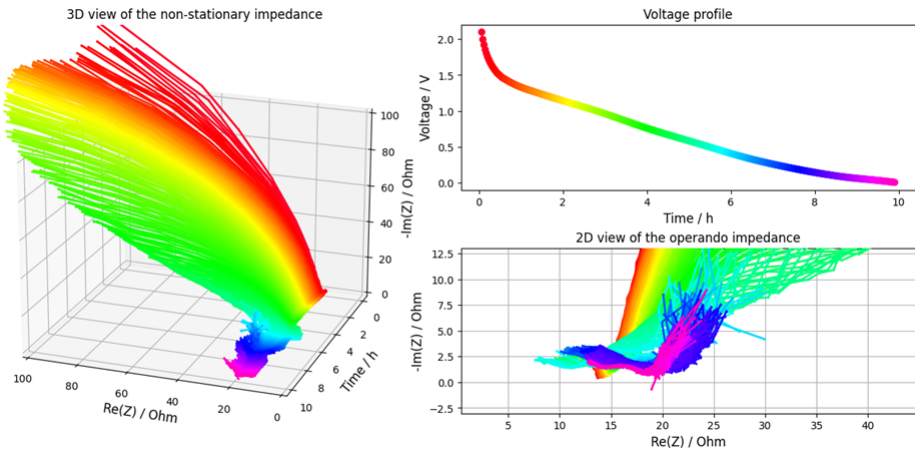


Figure 10.9: Cell 36 formation.

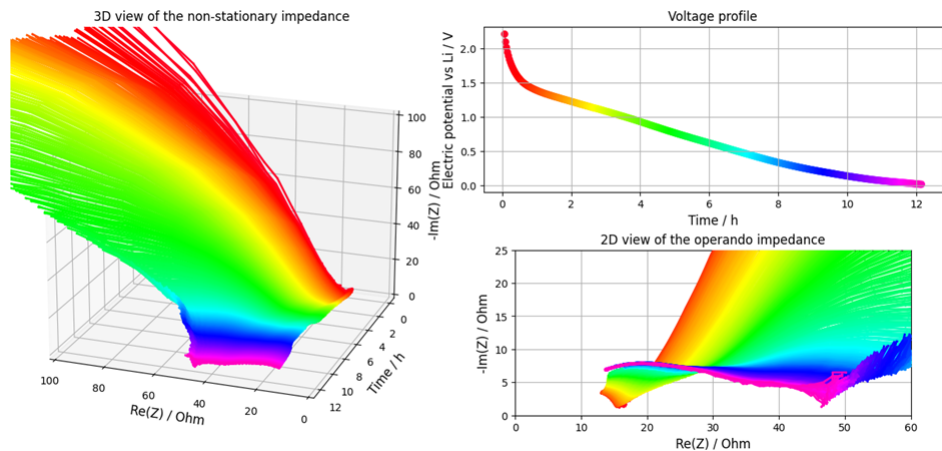


Figure 10.10: Cell 38 formation.

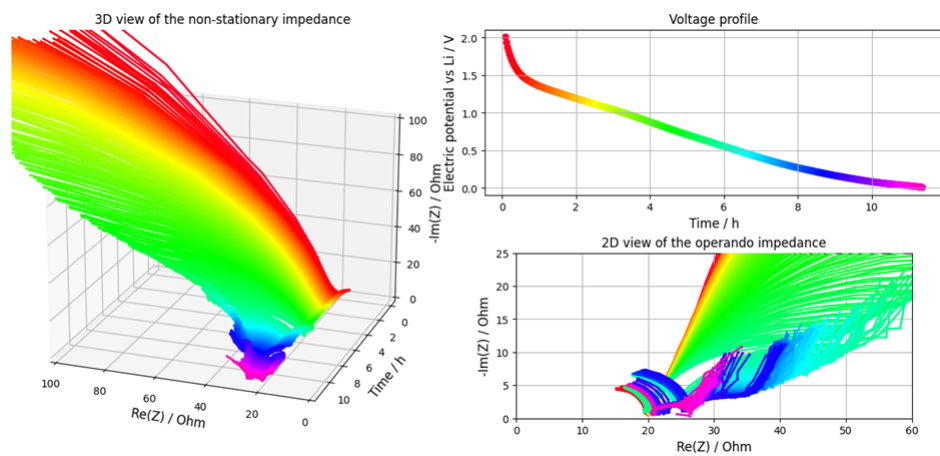


Figure 10.11: Cell 39 formation.



# 11

## Studying intercalation

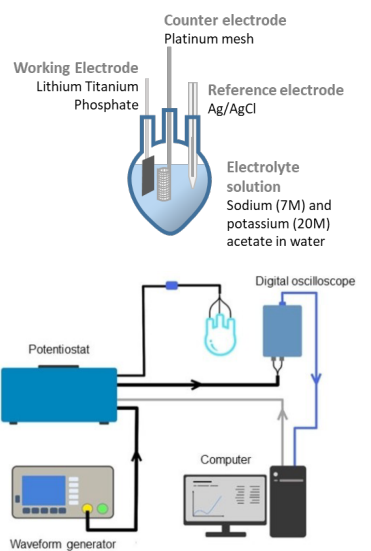
The project discussed in this section deals with the characterization of the processes at a single electrode. The most efficient method for storing energy is through ion intercalation between atomic layers of an inorganic material. Here we used Lithium titanium phosphate as active material as negative electrode for aqueous sodium-ion batteries. As for the previous project, the material was produced by Dr. Nicolò Pianta in the research framework of next generation sodium-ion batteries in the group of Profesor Riccardo Ruffo in the University of Milano Bicocca. The non-stationary impedance of the electrode was estimated during constant current and voltage-sweep drifts. The difference between the two is analyzed as well as a physical interpretation. The results of this project led to the publication to a peer-reviewed article [??].

### Materials and cell assembly

The project discussed in this section deals with the characterization of the processes at a single electrode. The most efficient method for storing energy is through ion intercalation between atomic layers of an inorganic material. Here we used Lithium titanium phosphate as active material as negative electrode for aqueous sodium-ion batteries. As for the previous project, the material was produced by Dr. Nicolò Pianta in the research framework of next generation sodium-ion batteries in the group of Profesor Riccardo Ruffo in the University of Milano Bicocca. The non-stationary impedance of the electrode was estimated during constant current and voltage-sweep drifts. The difference between the two is analyzed as well as a physical interpretation. The results of this project led to the publication to a peer-reviewed article [??].

### Measurement set-up

For this project we used the set-up Version 1 (see page ???) connecting the cell with the potentiostat as a three electrode measurement. In fact, in this case we were only interested in the impedance of one electrode. The connections of cells and devices are reported in figure???. We used the same multi-sine of the previous project (see page ???) with a frequency band between 100mHz and 10kHz, sine components amplitude extracted from an EIS experiment and phases selected randomly to minimize the



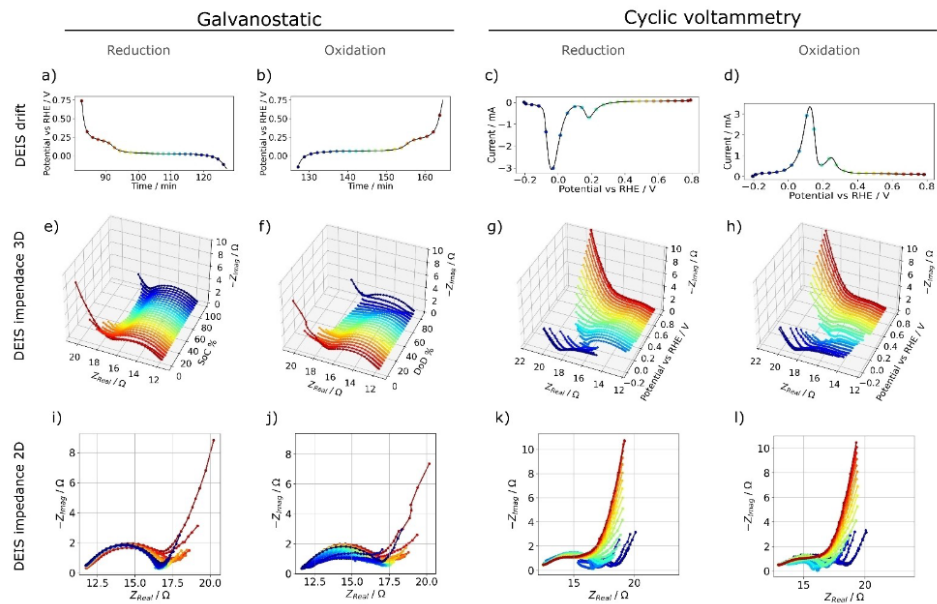
crest factor (the design of multi-sine perturbation is described in ???). The difference here, is the choice of the drift. We superimposed the multi-sine to a cyclic-voltammetry experiment and a galvanostatic experiment. For the former technique we used a scan rate of 0.8 mV/s that correspond of a period of about two hours for a direct comparison of the latter technique in which we used a current of 138mA/g equivalent to a 1C current rate. The multi-frequency current and voltage signals were sampled at a frequency of 50kHz and store in the storage of the computer. The total amount of points was ??? which contains an integer number of mult sine periods.

### Physical model for intercalation

The electrode under study in this project is made of an active material for ion intercalation and presents a macroscopic porosity. To model its impedance we selected an intercalation model and applied to the Levi's theory of porous electrodes. The intercalation

### Results and discussions

We estimated the impedance from the multi-frequency voltage and current signals through a Dynamic Multi-Frequency Analysis. We set a bandwidth of 0.1 Hz of the symmetric Fermi-Dirac filter with an  $n$  value of 8. A first qualitative analysis of the result of the experiment gives already quite a hint on the previous of intercalation systems. The time-varying impedance during galvanostatic and voltammetry experiments is reported in figure???.



It is firstly interesting to see how different they look. The impedance remains of a similar shape

The second curious observation is the asymmetry when inverting the current sign. This characteristic was not observed in the previous project where the double-layer capacitor was tested. It suggests an asymmetry in intercalating and deintercalating ions and the energy necessary to adsorb or desorb them. Continue with the argumentation

## Comment

The previous two sections describe two measurement on distinct energy storage devices with the scope of demonstrating the utility of non-stationary impedance for the study of such category of devices and justify the further development. In fact, the technical aspect for the estimation of the impedance are non-trivial. Multi-sine design, signal generation, signal sampling, cell geometry and reference electrode chemistry and placement are too be all carefully considered at the same time. There is a need to understand the physics of the system to deduct the parameter for the measurement. Knowledge of the electronics of potentiostat is fundamental as well as numerical computation and automation via software (i.e. coding). The observation from the results of this two projects were very promising. The following development is the measurement of non-stationary impedance of batteries and its use for the identification of aging. This is the reason why no in-depth study of the electrochemistry of porous activate carbon and carbon-coated lithium titanium phosphate was continued. Nevertheless I hope that this preliminary work might inspire scientist interested in mechanistic understanding of such system of replicate our methodology.



# 12

## Studying non-Faradic reaction in symmetric cell

Electrochemical double-layer capacitors are a class of energy storage devices characterized by high power and low energy density. The process of storing energy is based on adsorption of ions, a non-Faradic process, which gives the characteristic fast kinetics at the expense of capacity; they also exhibit high self discharge. The capacity is due to the electrode/electrolyte surface area, therefore materials with high porosity are particularly indicated. In this section, it is reported a work on self standing activated carbon electrodes in three-electrode cell. The presence of the reference electrode allows to separate the time-varying impedance of positive and negative electrodes during the operation of the device. The electrodes were produced by Dr. Nicolò Pianta in the group of Prof. Riccardo Ruffo at the University of Milano-Bicocca. He brought the electrodes in Bremen during his visiting period where we worked in close collaboration on the establishments of the measurement apparatus and software. The results of this project are published as peer-reviewed journal [??] and the data to a public repository [doi: 10.6084/m9.figshare.21082168].

### Materials and cell assembling

The porous carbon electrodes were produced according to this publication [M. Tribbia, N. Pianta, G. Brugnetti, R. Lorenzi, R. Ruffo, A new double layer supercapacitor made by free-standing activated carbon membranes and highly concentrated potassium acetate solutions, *Electrochim. Acta* 364 (2020), 137323]. The device stores energy in form of adsorption of potassium and fluorine ions why???. The electrode was cut as disks of a diameter of 12mm. A solution of 10mM of KF was used as electrolyte, soaked into two glass filter separator to complete the cell stack; the pH of the solution is 10.7. The stack was introduced in a T-shaped cell with a Polyether ether ketone (PEEK) body which posses excellent mechanical properties and is resistant to chemicals (aqueous or organic) and compressed between two stainless-steel cylinders. The third entrance of the body was left for the reference electrode, described in the following.

## Reference electrode and position in the stack

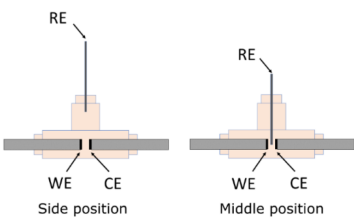
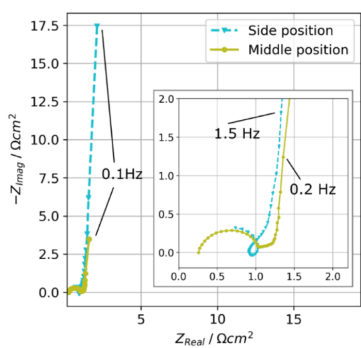


Figure 12.1: Text of the caption



The geometry of the cell and pH of the electrolytic solution pose a challenge on the choice of the reference electrode. The most common reference electrode for aqueous solutions is AgCl/Ag but its glass encapsulation is too big to be used in a compact systems. A miniaturized electrode must be used for this task which could behave as pseudo-reference electrode in the KF solution. We had to search an element and it halogen that is not soluble in KF solution with a pH of 10.7. The only solution that we found was the red-ox couple PbF<sub>2</sub>/Pb which produced a stable voltage of 191mV vs RHE. The thermodynamic properties of the materials where deducted from the Porubet diagram at the pH of the solution. It was practical to produce the PbF<sub>2</sub> in situ after the introduction of a wire of Pb between the two glass fiber separators. Furthermore we investigate the effect of the position of the reference in the measurement. In fact someone would argue that a commercial AgCl/Ag electrode could be used in this geometry by putting a lot of electrolyte in the body until the level of the liquid would be high enough to accomodate the electrode. We called this a “side position”, where the electrode is posed on the side of the electrodes stack. A schematic is reported in figure ???. A classic EIS measurement immediately shows the insurgent of an artifact due to the position of the reference. The result of the experiment is reported in figure ???.

I would like to note that also later in the manuscript a wire will be used as reference electrode current collector, but here the entire length of the Pb wire has PbF<sub>2</sub> deposited making the electrode surface area quite extensive (while later the wire will be isolated on its length). Nonetheless, the artifacts in the form of a loop in the middle-to-high frequencies are suppress for most of the cases (yes, not completely; cfr. later) when the reference is in the middle of the cell stack.

## Physical model

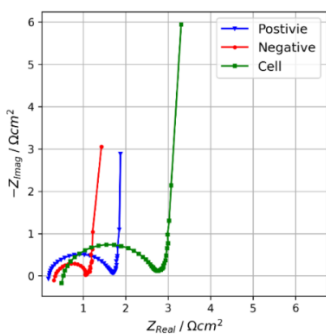
### Results and discussions

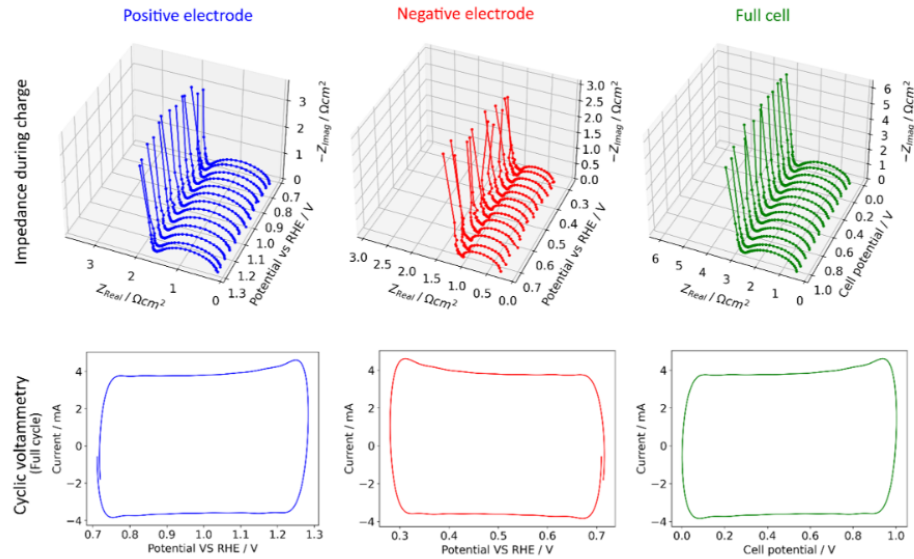
We used the Dynamic Multi-Frequency Analysis to estimate the time-varying impedance from 4 consecutive cycles of cyclic voltammetry. !!! parameters used in the DMFA!!! The impedance of the second cycles is reported in figure ???

The impedance of on half-cell does not change significantly during the cycle although one can notice some noise in the lowest frequencies for the negative half cell. In the report of the results we omitted the impedance point for the lowest frequency (namely 100 mHz) because it is too much effected by the skirt of the zero frequency and the estimation of the impedance was usefulness; so the figure report the impedance in the interval between 300mHz and 10kHz. In fact, the lowest frequency has to be chosen in relation with the velocity of the dynamic of the system. For examples in this case the system evolves in a bandwidth from 0 to 200mHz.

Looking at the shape and magnitude of the impedance for the two half-cells in figure ???, it is very interesting to notice the difference of the two interfaces.

Despite the electrodes being chemically identical, the impedance of the two is quite different. We attributed this evidence to the difference in elec-





trode potential, hence the quantity and quality of adsorbed molecules as well as the history of the electrode. The figure show the impedance in the discharge state, where the full cell is almost at 0 V and so the electrical potential of the two interfaces would be the same (around 700mV vs RHE). At the interface, adsorbed molecules can be charged or neutral. In the assumption that both electrodes have the same surface area (being prepared in the same way), we deduce that the nature of adsorbants is different. On the positive electrode in fact, some oxygen anion and oxygen molecule might be still adsorbed at the interface after they are formed in the region between 0.7 and 1 V of the full cell voltage. The presence of elecetrochemical inactive species at the interface would slow down the adsorbtion process of the ions, increasing the interface impedance

From the voltage-time profile of a capacitor one can calculate the average capacitance  $C = \frac{\Delta Q}{\Delta V}$ . We found a value of 42 F/g for the positive electrode and 54 F/g for the negative one.

Finish the discussion here → take from the paper

## Quantitative interpretation of the impedance

We also analyzed the time-varying impedance through a physical model with the aim of identifying the variation of physical parameter with the time evolution of the system.

Graphical analysis of the Bode plots?

## Remarks

One might argue that the difference in the electrode impedance is not due solely by the history of the electrodes but also the preparation itself. The latter could be identified characterizing more electrodes with the same method. Here the scope of the project was to demonstrate the use of multi-sine non-stationary impedance spectroscopy for characterizing energy storage devices in three-electrode configuration, with less attention on the chemistry. The results where such promising to make us curios of characterizing energy storage devices using non-stationary impedance during galvanostatic

drifts, a technique much more appropriate to study such systems. This is the topic of next section.